University of Stavanger

Faculty of Science and Technology

MASTER'S THESIS

Study program/ Specialization: Petroleum Engineering - Drilling Technology	Spring semester, 2015 Restricted access
Writer: Magne Hurum	…… (Writer's signature)

Faculty supervisor: Mesfin A. Belayneh

External supervisor: Ola M. Vestavik

Thesis title:

Extended Reach Drilling using RDM – Heavy Over Light solution.
Stability and control of the well annulus fluid.

Credits (ECTS): 30

Key words: Reelwell ERD RDM Heavy Over Light solution Barite Sag NMR Viscoelasticity Wellplan	Pages: 98 + enclosure: 21 + attachment: 1 experimental DVD Stavanger, 15.06.2015

Abstract

The oil and gas industry has large benefit from cost reductions and increased efficiency. One of the segments that is most affected by these factors is the drilling industry. There are large costs related to rig rates, equipment and manpower. One solution to these challenges is extended reach drilling (ERD). By using fewer rigs where each is capable of reaching further, there is a large potential for cost reductions. One of the companies that delivers ERD technology is Reelwell, located in Stavanger, Norway. The company has developed their own extended reach drilling technology named the Reelwell Drilling Method (RDM).

One of the features of the Reelwell Drilling Method (RDM) is the Heavy Over Light (HOL) solution. The concept is comprised of using two drilling fluids with different densities on the inside and the outside of the drill string. This creates an increased buoyancy force on the drill string, making it possible to drill further due to the reduced torque and drag effects. The fluid on the outside of the drill string must be able to keep the weight material in suspension to avoid operational problems and loss of well control.

The thesis presents an experimental study of weight particle sagging in horizontal sections. The focus has been on both dynamic and static sag in oil-based mud (OBM), with both standardized and non-standardized experiments such as NMR, viscoelasticity and rig testing. A modern (BaraECD) and a standard (OBDF01) oil-based drilling fluid were tested. The BaraECD showed preferred properties having high ES values and low density variations in dynamic sag scenarios. The measurements showed that there is a potential of static and dynamic sag in a horizontal well section. Wellplan simulations and buoyancy calculations showed that sag is not expected to be a problem for the pipe buoyancy when using the HOL solution. The results indicate that sag rather can be beneficial by increasing drill string buoyancy and thereby reduce torque and drag effects.

Acknowledgements

First of all I would like to thank Professor Mesfin Belayneh, my faculty supervisor at the University of Stavanger. His support and academic guidance has been outstanding through the whole process of writing the thesis.

I would like to thank my external supervisor CTO Ola M. Vestavik and technical advisor COO Harald Syse, for giving me the chance to write the thesis for their company. We have had several interesting discussions both through meetings and in relation to laboratory experiments.

Halliburton has provided both the components and recipes used to prepare the drilling fluids used in this project. I would like to thank Hege Anita Handeland Nielsen, Team Leader - Baroid Lab, Halliburton, for giving me the chance to use their laboratory when conducting the conventional testing. I would also like to thank the laboratory and drilling fluid engineers for interesting discussions around drilling fluid behavior.

Last, I would like to thank my dear parents for supporting me through all my years of studying.

Stavanger, June 2015

Magne Hurum

Table of contents

List of figures

List of tables

Abbreviations

BHT	Bottom Hole Temperature
CSG	Casing
DDS	Dual Drill String
DP	Drill Pipe
ECD	Equivalent Circulating Density
ERD	Extended Reach Drilling
ES	Electrical Stability
FCU	Flow Control Unit
HOL	Heavy Over Light
HPHT	High Pressure High Temperature
IPV	Inner Pipe Valve
LSRYP	Low Shear Rate Yield Point
LVER	Linear Viscoelastic Range
NCS	Nowegian Continental Shelf
NMR	Nuclear Magnetic Resonance
NRV	Non Return Valve
OBM	Oil-Based Mud
OH	Open Hole
OWR	Oil Water Ratio
POOH	Pull Out Of Hole
PSD	Particle Size Distribution
PV	Plastic Viscosity
RDM	Reelwell Drilling Method
RPM	Revolutions Per Minute
SG	Specific Gravity
TDA	Top Drive Adapter
VSST	Viscometer Sag Shoe Test
WBM	Water-Based Mud
WPS	Water Phase Salinity
YP	Yield Point
BHT	Bottom Hole Temperature

1 Introduction

The thesis presents an experimental study of particle sagging in horizontal sections of the Reelwell, RDM - Heavy Over Light drilling method. The thesis will focus on dynamic and static sag with both standardized and non-standardized experiments.

1.1 Background

Today's oil industry is of great need of cost reductions and increased efficiency to be able to continue the exploration and production of new fields and improve recovery from already developed fields. One of the major cost drivers in the industry today is drilling. In the drilling segment of the oil industry, there are enormous costs related to rig rates, equipment and manpower. To be able to reduce these costs, we must find better and/or more automated solutions. By using extended reach drilling (ERD), some of the cost challenges can be solved. The main limiting factors when it comes to ERD are torque and drag, proper hole cleaning and managing downhole pressure. To be able to reach further than before, these challenges must be solved in an efficient manner. A company that has come up with a solution is Reelwell ^{TM}. They started in 2004 their work for an increased efficiency in the oil industry by introducing their own technology, which has the potential of reducing both the number of rigs, the quantity of equipment and the need for manpower. The main goal of the company is to be able to drill a well of 20 kilometers MD, using the Reelwell Drilling Method (RDM). RDM uses a dual conduit drill string, which pumps drilling fluid through the outer conduit and transports the returning drilling fluid and cuttings through the inner conduit. This solution makes it possible to use two drilling fluids in the hole at the same time. The heavy phase controls the pressure and maintains buoyancy, while the light phase provides cooling of the bit, efficient cuttings transport and lubrication of the bottom hole assembly (BHA). The two phases is therefore named the passive and the active fluid by their properties. The technology of using two fluids is named Heavy Over Light (HOL) solution. More details about the Reelwell technology will be presented in chapter 2.

1.2 Problem formulation

To use the HOL solution, we need two fluids with different properties. In this thesis, the focus will be on the properties of the passive fluid. The passive fluid must be able to keep the solids in suspension to avoid uneven specific gravity in the fluid column and further lost well control. The passive fluid will be agitated by the drill string during drilling, but will also be standing static, when there is a stop in drilling or there is a need to pull out of hole (POOH).
The thesis will focus on both dynamic and static sagging in an oil-based mud (OBM). To create a scenario as close to real life as possible we have contacted Halliburton Brazil to get the formulation of the drilling fluid that most likely will be used during a HOL operation in Brazil in 2016. The drilling fluid will be mixed and tested by the author at Halliburton Fluids Laboratory in Tananger, Norway. There will be mixed two different fluids with different properties to show some differences in results and possible scenarios when drilling the actual well. In addition to the actual testing of the fluids in various standardized and non-standardized experiments, there will be performed simulations of torque and drag effects.

1.3 Objectives

The objectives of this thesis are the following:

- Perform theoretical studies for prediction of downhole fluid sagging
- Characterize the fluid behavior
- Perform sagging trials using standardized and non-standardized experiments
- Perform WellPlan simulations on torque and drag
- Consider the severity of particle sag in horizontal well sections

Reelwell came up with an additional area of interest during the work with this thesis. This is not part of the main focus of the thesis, but is an interesting sidetrack for the overall understanding of the fluid interaction;

- Perform vertical HOL experiments to study fluid interface
- Consider solutions to recondition fluids during HOL operation

2 Reelwell Technology

Reelwell was founded in 2004 by Dr. Eng. Ola Michael Vestavik. Reelwell was established to develop and provide the Reelwell Drilling Method (RDM). They have received numerous awards such as the ONS Innovator Award in 2010, and the OTC Spotlight On New Technology Award for five years in a row between 2009 and 2013. These awards have been given for different technological solutions they have come up with during their ten years in the industry. The main office is located in Stavanger and they are currently employing 17 people.

The RDM is a new drilling method that has been developed to meet today's demands for efficiency and extended reach wells. RDM is based on using a dual drill string (DDS) to form a dual conduit for fluids in a closed-loop circulation system. The drilling fluid is being transported down to the bit through the outer conduit while the returning fluid and cuttings are transported up through the inner conduit. This makes the greatest part of the drilling fluid in the annulus static, while the smallest part is active and in continuous circulation to clean the well. Using the inner string for cuttings transport has shown to cause less grinding of the cuttings and reducing the time needed to transport the cuttings out of the well. Since we have one passive and one active part of the drilling fluid, it is possible to use two different drilling fluids at the same time.

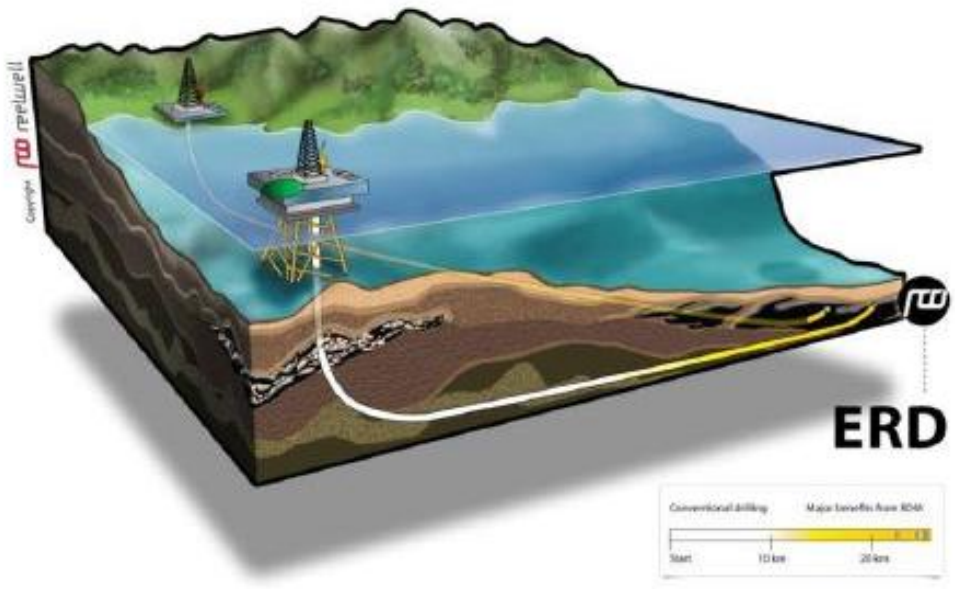

Figure 2-1: ERD. [F1]

2.1 Reelwell equipment

The RDM technology can be used on a conventional drill rig using special made components as shown in figure 2-2. These are presented in the following subchapter's.

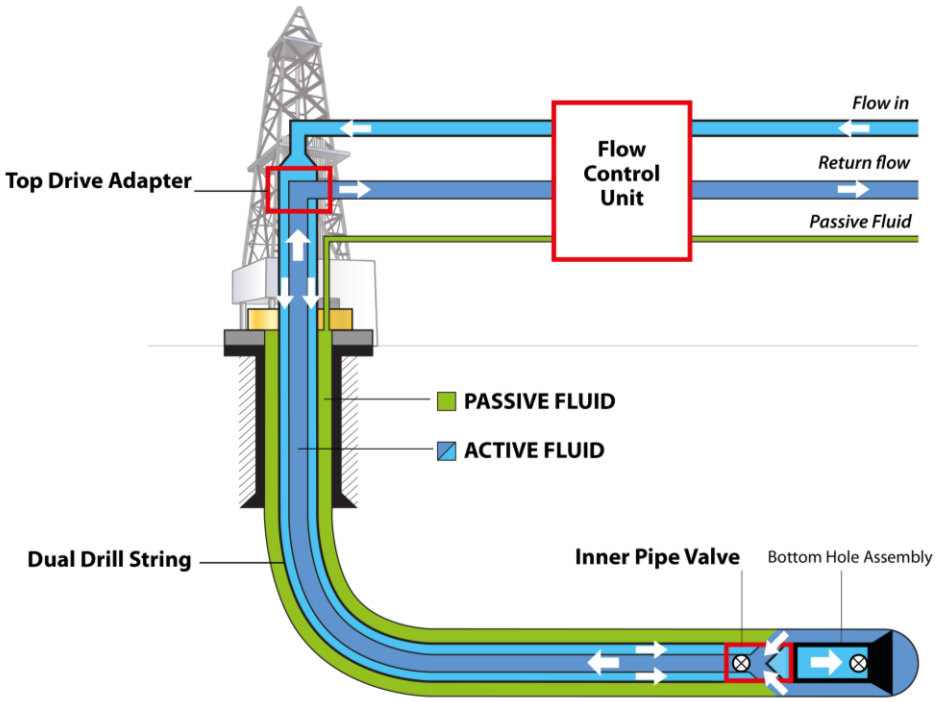

Figure 2-2: Illustration of the RDM. [F1]

2.1.1 Dual Drill String (DDS)

The DDS is the main difference between the RDM and conventional drilling. The DDS is currently delivered in 5 7/8 " and 6 5/8 " steel or aluminum drill pipes adapted with inner pipes with stab-in connectors. These pipes are handled on the rig in the same manner as conventional drill pipes [R2].

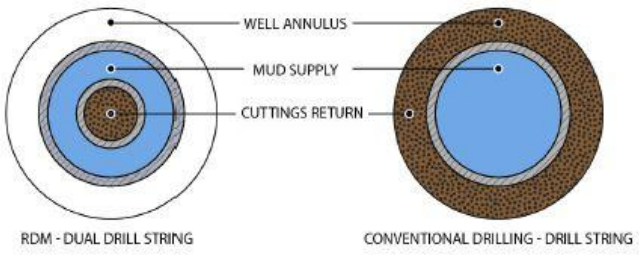

Figure 2-3: Illustration of a dual drill string and a conventional drill string. [F1]

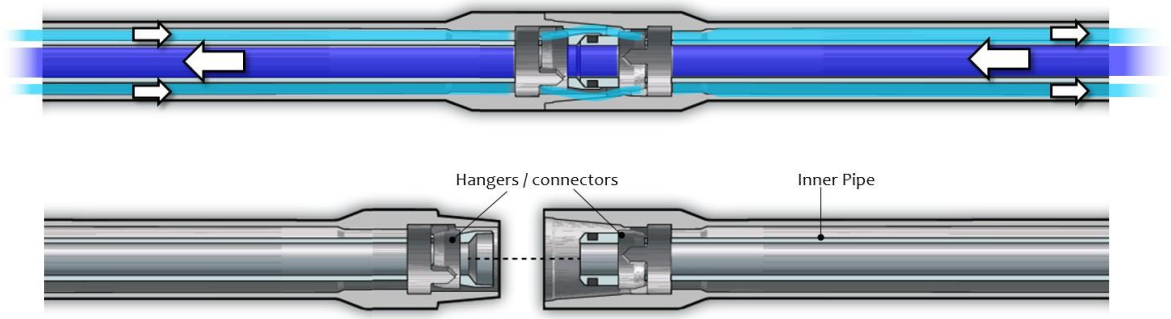

Figure 2-4: Illustration of the DDS connection. [F1]

2.1.2 Top Drive Adapter (TDA)

The top drive adapter, is a swivel adapter between the rig`s top drive and the DDS. The TDA is connected to the surface flow control unit through a second standpipe and mud hose [R2].

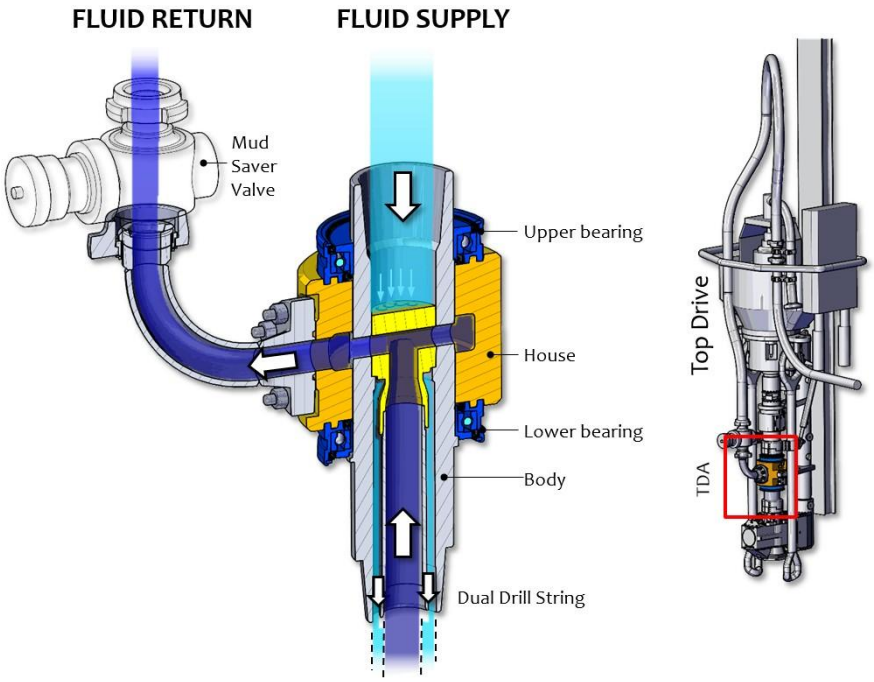

Figure 2-5: Illustration of the TDA. [F1]

2.1.3 Inner Pipe Valve & Non Return Valve (IPV & NRV)

The IPV isolates the DDS from the well during connections [R2].

Open:

- The pumps are started
- The IPV and NRV opens
- Return flow is initiated

Closed:

- The pumps are shut down
- The IPV and NRV isolates the well pressure

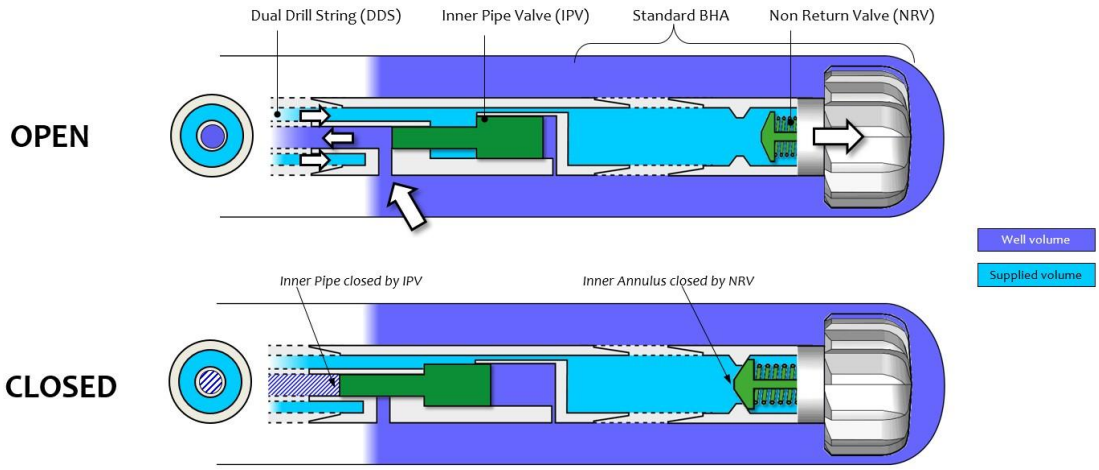

Figure 2-6: Illustration of open and closed IPV & NRV. [F1]

2.1.4 Flow Control Unit (FCU)

The FCU is a control valve arrangement equipped with pressure and flow sensors, and is used to control the whole system`s flow and pressure [R2].

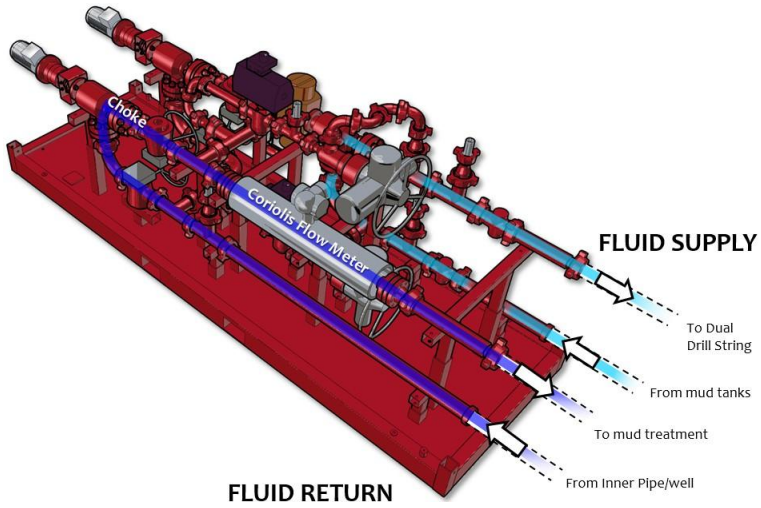

Figure 2-7 Illustration of the FCU. [F1]

2.2 Heavy Over Light (HOL)

The HOL solution is one of the main features of the RDM. A “hook” shaped wellbore is drilled to allow the usage of two fluids with different densities in the wellbore. The “hook” shaped well path creates a fluid trap in the horizontal section, to maintain the position of the fluids and to prevent u-tubing. In the HOL scenario, a heavy fluid lies stagnant in the annulus, while a light fluid is pumped through the outer conduit of the DDS and out through the drill bit nozzles. The light drilling fluid and the cuttings are transported back into the DDS through some holes located at the IPV on top of the BHA. As the drilling continues, heavy fluid is pumped into the well annulus at surface to secure the correct fluid interface position and wellbore stability. One purpose of the HOL concept is to allow for drill string buoyancy. This will significantly reduce the friction between the drill string and the wellbore. This will again reduce the force of torque and drag. The HOL concept creates buoyancy by using the difference in fluid density on the inside and the outside of the drill string. When using aluminum drill pipes, the buoyancy effect is very large, mainly because aluminum has only 1/3 of the density of steel [R1].

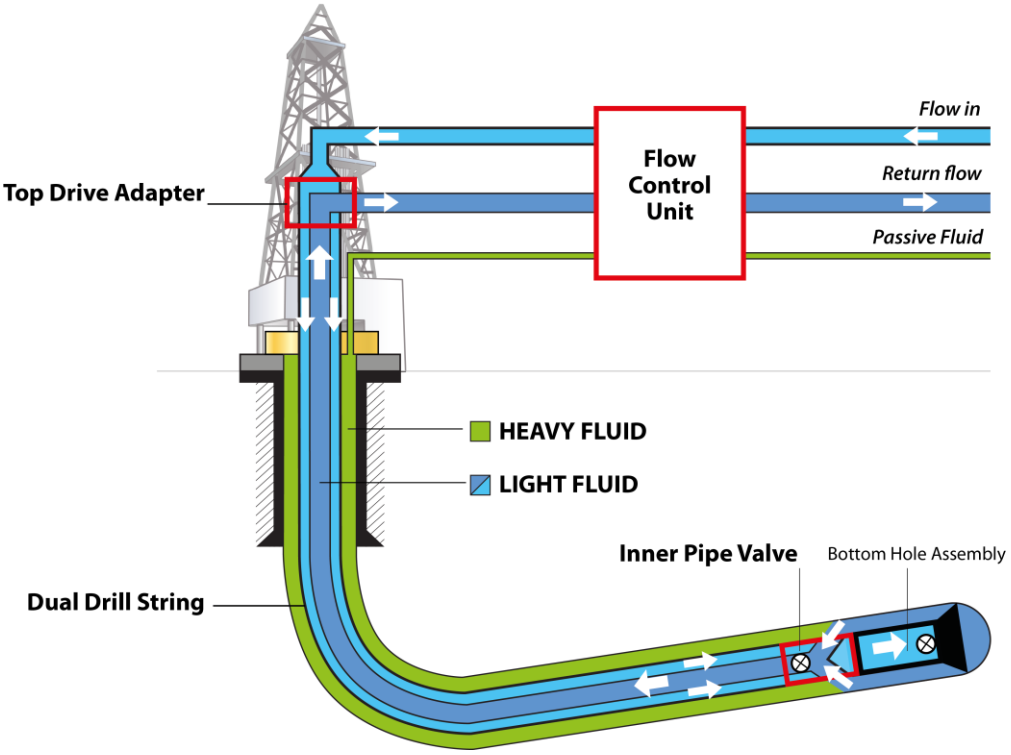

Figure 2-8: Illustration of the HOL principle. [F1]

Graphs displaying the effects on torque (figure 2-9) and drag (figure 2-10) in an example well, when using the buoyancy effect:

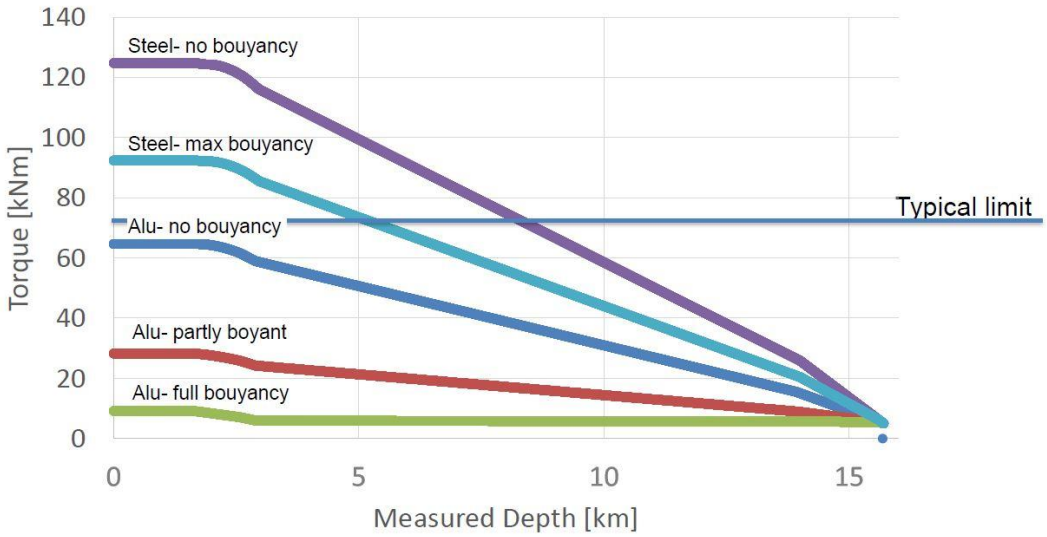

Figure 2-9: Graph displaying the buoyancy effect on torque. [F1]

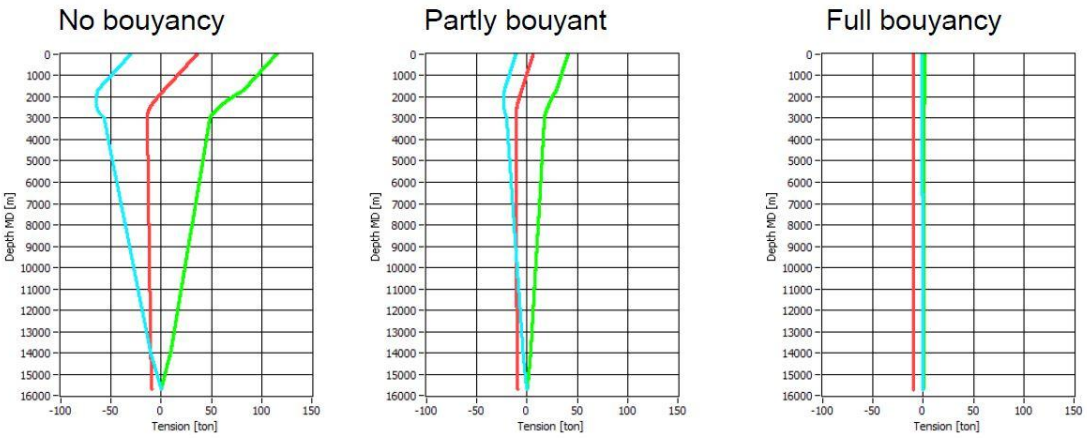

	Well annulus fluid density [sg]	Active fluid density [sg]
No buoyancy	1.2	1.2
Partly buoyancy	1.56	1.2
Full buoyancy	1.75	1.15

Figure 2-10: Graph displaying the buoyancy effect on drag. [F1]

3 Theory

This chapter presents theories that are directly or indirectly related to weight particle sagging in oil-based drilling fluids. The theory behind the standardized static and dynamic sag tests will also be presented.

3.1 Barite sag

Barite is a dense mineral with specific gravity of typically 4.20 – 4.30 g/cm^3. The name barite is derived from the Greek word for "heavy" and the mineral has been found both in Europe, America and Asia. The world's major producers are China, India and USA. The mineral comprises of barium sulfate ($BaSO_4$), and is the most important weighting agent in the drilling fluid industry today. Barite sag occurs when the weight material and/ or solids in the drilling fluid starts to settle in the wellbore. This can further lead to operational issues that can affect both safety and economics. It may cause various technical problems such as lost well-control, stuck pipe, reduced wellbore stability and lost circulation. In high pressure deviated wells, the torque and drag is high compared to the situation in a vertical well. Therefore, oil-based drilling fluids are used to reduce the friction factor. Especially in the case of ERD, it is of high importance to keep the friction factor as low as possible. Sag is a more severe problem in synthetic- or oil-based drilling fluids than in water based drilling fluids [T1]. First, OBMs are generally more viscous than WBMs, and efforts are made to reduce viscosity by minimizing the same additives that is used for suspending barite. Second, invert-emulsion drilling fluids do not develop gel strength in the same manner as WBMs [T2]. Another reason is that the base fluid in an OBM is a low-density mineral oil, while it is possible to use high-density brine as the base fluid in a WBM. Therefore it is necessary to add considerably amounts of weight material to get the desired specific gravity in an OBM.

Many factors are affecting sag in the invert-emulsion drilling fluids. This includes both operational parameters and fluid properties. Among the fluid properties affecting barite sag we have rheology, density, solids content, particle size and particle size distribution (PSD). In addition, we also have the interfacial chemistry of the dispersed solids and the aqueous phases. In 1996, Bern et al. [T3] wrote a paper that described the influence of different drilling variables on barite sag. Many tests were performed using a laboratory flow loop to

evaluate the influence and role of key drilling parameters on barite sag. They found out that angles of 60 - 75 ^{o} and low annular flow velocities gave the highest sag potential. By combining field observations with test results, four areas of importance to minimize sag have been addressed: well planning, mud properties and testing, operational practices, and wellsite monitoring procedures [T3].

3.2 Micronized weight particles

As the industry has developed towards a more high pressure – high temperature (HPHT) regime with deeper, longer and more demanding wells; it is of great importance to have fluids that can handle these extreme conditions. By using micronized weight particles, the gravitational force on each particle will be reduced, and it will be easier to keep the particles in suspension. This reduces the need for a viscosifyer that maintains the high viscosity of a fluid. The reduced viscosity will directly reduce the ECD and enables the well pressure to be kept within the narrow operating window. The barite particles are milled down to a smaller particle size, while being treated in an enhanced mineral oil. This procedure makes the particles get an effective oil wet surface. This further makes it possible to produce a stable OBM with high solids content and high density, while keeping the viscosity at a minimum.
Halliburton`s drilling fluid BaraECD was mixed and tested during the work with this thesis. This fluid contains micronized weight particles and was initially developed to be used on difficult wells in the Gulf of Mexico, but has been further developed to be used in other parts of the world such as the Norwegian Continental Shelf (NCS).

3.3 Hindered and Boycott settling kinetics

In 1920, Boycott observed that blood corpuscles in narrow tubes settled faster if the tubes were inclined rather than standing vertical. The kinetics of a vertical situation and a 45 ^{o} inclined situation is illustrated in figure 3-1 and figure 3-2. In both situations there are suspended particles that are substantially denser than the suspending fluid. As time goes by, the particles settle vertically due to the gravitational force at a rate v_0. Figure 3-1 shows three regimes of particle sedimentation in a vertical tube, this is known as "hindered" settling. The concentration of particles will increase from top to bottom.

The top layer, called the clarification regime has some few remaining particles that settle mostly individually ("free settling") and the particles will have close to no influence on each other. Stokes law will therefore apply here (see equation 3).

The next layer is called the "hindered settling regime" and has a lower rate of settling than in the clarification regime. This is due to the higher concentration of particles, making the particles crowd and interfere with the settling of individual particles. However, there may be formed clusters of several particles, making the settling faster due to the increased size and weight.

The bottom layer is called the "compaction regime" and is characterized by the accumulation of particles that support each other mechanically. Excess fluid is expelled very slowly upwards as the bed compacts [T4].

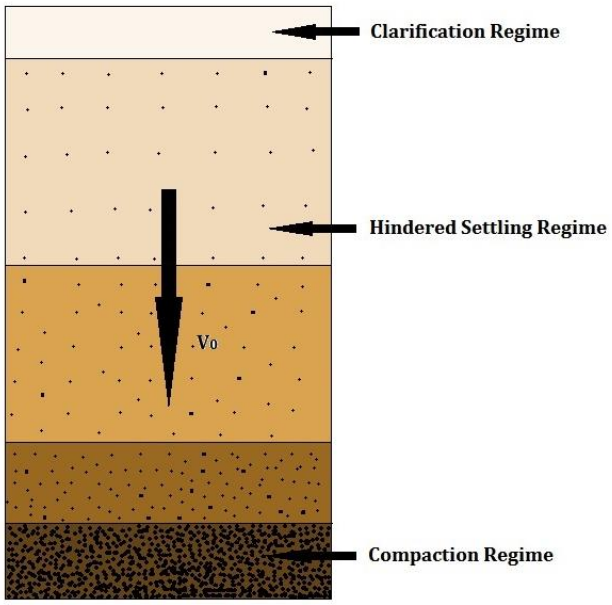

Figure 3-1: Hindered settling. [F2]

In the inclined situation illustrated in fig 3-2, we can see that the kinetics change. The particles still settle vertically, but the travel distance is significantly reduced. Sediment beds are formed on the low side of the tube, when the particles settle. These particles further forms clusters and accumulate on the bottom of the tube. The clarified layer on the other hand, moves upwards to the high side of the tube. Since the low-density clarified layer naturally migrates upwards as the particle settling proceeds, this will have an accelerating effect on the overall settling kinetics.

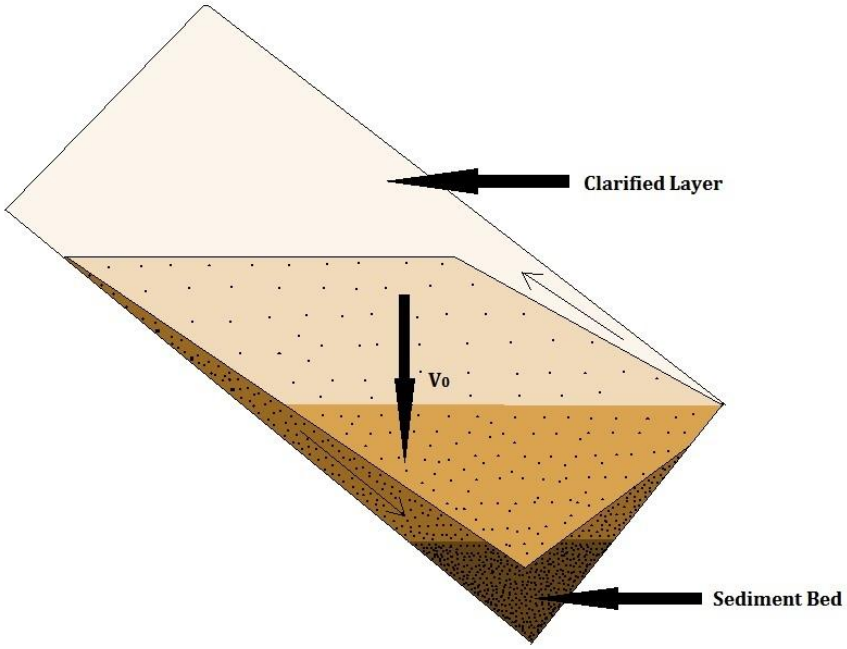

Figure 3-2: Boycott settling. [F2]

3.4 Stokes law

In 1851, Gabriel Stokes derived an expression that described the drag force exerted by a viscous fluid on a small spherical particle. This drag force is expressed by [T5]:

$$F_d = 6\pi r \mu v_t \tag{1}$$

Where:

r = Radius of the sphere

μ = Viscosity of the fluid

v_t = Terminal settling velocity

If we further consider a sphere that is under the influence of gravity, we have the following expression for the gravitational force:

$$F_g = (\rho_p - \rho_f) g \frac{4}{3} \pi r^3 \tag{2}$$

Where:

ρ_p = Particle density

ρ_f = Fluid density

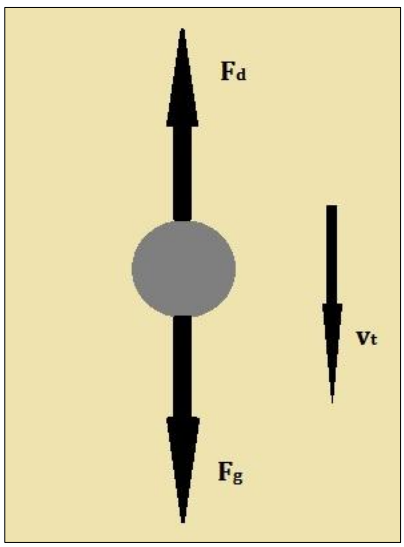

Figure 3-3: Spherical particle in a viscous fluid. [F2]

When the particle reaches a constant velocity, the drag force and gravitational force must be in balance (see figure 3-3). Setting $F_d = F_g$ gives the following:

$$v_t = \frac{2r^2 g(\rho_p - \rho_f)}{9\mu} \tag{3}$$

This is a simplified model to describe particle settling since it only takes one single particle into consideration. In addition, it does not take into account important factors such as temperature effects and particle – particle interaction [T5].

3.5 Gravity

The HOL solution is based on utilizing Newton`s theory of gravity. In modern language, the theory states the following: "Every point mass attracts every single other point mass by a force pointing along the line intersecting both points. The force is proportional to the product of the two masses and inversely proportional to the square of the distance between them" [T6]. Utilizing this theory, the gravitational pull on the heavy fluid will be greater than it will be on the light fluid. The heavy fluid will therefore position itself beneath the light fluid as fast as possible. The positioning of the two fluids requires therefore a sufficient difference in density.

3.6 Buoyancy

Buoyancy is defined as the upward force on an object exerted by the surrounding liquid or gas. The force of buoyancy opposes the force of gravity. The effective (submerged) weight of a wellbore tubular is calculated by multiplying the weight in air with the buoyancy factor (β). Note that the following equations 4 and 5 are valid for both vertical and deviated boreholes [T17].

The following equation is used if the density of the fluid on the inside and the outside of a tubular is the same;

$$\beta = 1 - \frac{\rho_{fluid}}{\rho_{pipe}} \tag{4}$$

Where:

β = Buoyancy factor

ρ_{fluid} = Density of surrounding fluid

ρ_{pipe} = Density of pipe material

If there is a difference in density on the inside and outside of the tubular, the buoyancy factor is found by [T17];

$$\beta = 1 - \frac{\rho_o r_o^2 - \rho_i r_i^2}{\rho_{pipe}(r_o^2 - r_i^2)} \tag{5}$$

Where:

ρ_o = Density of outer fluid

r_o = Inner radius of casing or wellbore (outer tubular)

ρ_i = Density of inner fluid

r_i = Inner radius of drillpipe (inner tubular)

3.7 Rotational force

When a drill string rotates it creates a rotational force by its angular velocity. The fluid deformation will be greatest at the wall of the drill pipe and will then be reduced as we move away from the pipe (see figure 3-4). This effect will be studied closer in the experiment chapter of this thesis, where we can see the effect of agitation of the drilling fluid by the drill string. The shear rate and angular velocity is given by the following [T7]:

$$\gamma = \frac{\omega r_{DP}}{r_W - r_{DP}} \tag{6}$$

Where:

ω = Angular velocity

r_{DP} = Radius, drill pipe

r_W = Radius, wellbore

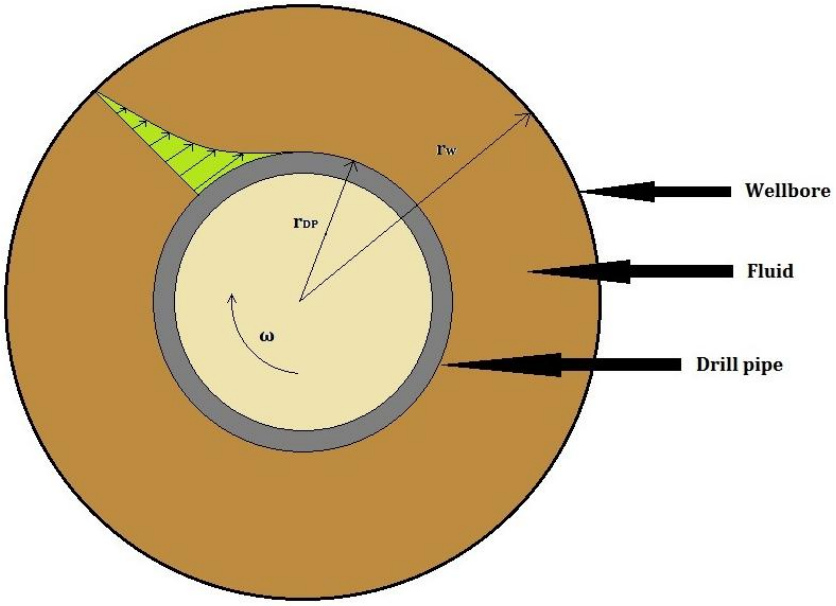

Figure 3-4: Cross section of a rotating drillpipe in a wellbore. [F2]

3.8 Density

Mud weight or mud density is defined as the mass of a given mud sample divided by its volume. Mud weight is largely dependent upon the quantity of solids that is present in the liquid phase, either in solution or suspended by the particles of the liquid phase. The density of the mud (ρ_m) is given by:

$$\rho_m = \frac{M_W + M_S}{V_W + V_S} \tag{7}$$

Where:

M_W = Mass of water (or oil)

M_S = Mass of solids

V_W = Volume of water (or oil)

V_S = Volume of solids

3.9 Rheology

Rheology is defined as the study of deformation and flow of fluids. One of the properties within the study of fluid deformation is viscosity. Viscosity is a property, which controls the magnitude of the shear stress that develops as one layer of fluid slides over another. It is a measure of the friction between layers of the fluid and provides a scale for describing the thickness of a given fluid. Viscosity is largely dependent on temperature, while a liquid`s viscosity is reduced by increasing temperature the opposite is the case for gas.

Gel Strength is a measure of the ability of a fluid to develop and retain a gel structure. It is analogues to shear strength, and defines the ability of a drilling fluid to hold solids in suspension. It also gives an indication of the thixotropic properties of a drilling fluid and, consequently, the thickness of a quiescent drilling fluid. Thixotropic refers to the ability of a suspension of fluid such as a drilling fluid to develop a semi-solid structure when at rest, and to become a liquid state when set in motion [T8].

Rheology models are categorized as Newtonian and non-Newtonian. A Newtonian fluid has a directly proportional relationship between shear stress and shear rate. This is the case for water, glycerin, oil and light hydrocarbons. Therefore, this fluid system can be described by the following one-parameter equation [T9]:

$$\tau = \mu\,\gamma \tag{8}$$

Where:

τ = Shear stress [lbf/ft^2]

μ = Viscosity [cP]

γ = Shear rate [1/s]

A non-Newtonian fluid can be a slurry, paste, gel, polymer solution etc. and can on a generally basis be classified as [T9]:

- *Thixotropic*: Apparent viscosity decreases with duration of a given stress
- *Rheopectic*: Apparent viscosity increases with duration of a given stress
- *Shear thinning*: Apparent viscosity decreases with increased stress
- *Shear thickening*: Apparent viscosity increases with increased stress

When we are describing a non-Newtonian fluid, we need a model that has two or three parameters. The most common models are the two-parameter models Bingham plastic and Power law in addition to the three-parameter model Herschel-Bulkley (see figure 3-5).

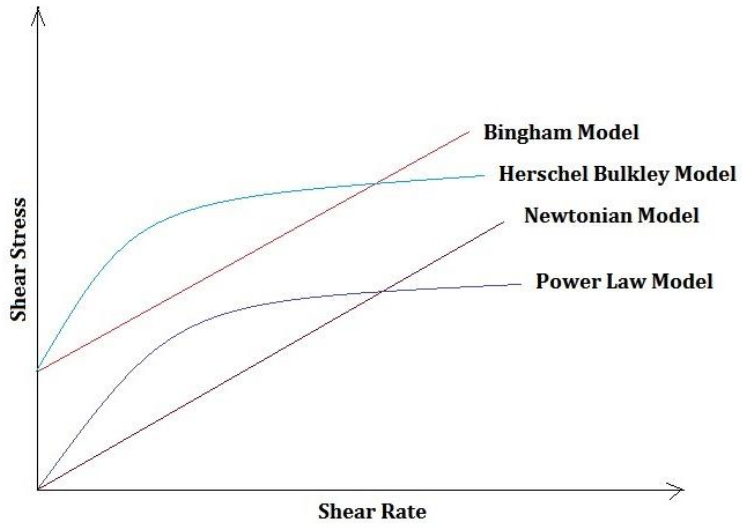

Figure 3-5: Rheology models. [F2]

3.9.1 Bingham plastic model

The Bingham plastic model describes a fluid that has a linear relationship between shear rate and shear stress. In addition it describes the fluid to require a certain yield stress to be set into flow. The model can be described by the following mathematical expression [T9]:

$$\tau = \mu_p \gamma + YP \tag{9}$$

Where:
τ = Shear stress [lbf/ft^2]
μ_p = Plastic Viscosity [cP]
γ = Shear rate [s^{-1}]
YP = Yield Point [lbf/100 ft^2]

Plastic Viscosity (PV) is the slope of the line in the Bingham model. The PV is a measure of fluid-fluid, fluid-particle and particle-particle friction. A low PV value indicates that we have a low-viscosity drilling fluid exiting the bit and therefore are capable of drilling rapidly. A high PV value on the other hand is most likely caused by a viscous base fluid and by excess of colloidal solids. PV is calculated using the following equation [T9]:

$$PV = \theta_{600} - \theta_{300} \tag{10}$$

The Yield Point (YP) part of the friction is due to an electrostatic force of attraction or repulsion between charges or ions within the drilling fluid system. The drilling fluid needs to have high enough YP in order to carry the cuttings out of the hole. The YP value can be determined using the following equations [T9]:

$$YP = \theta_{300} - PV \tag{11}$$

$$YP = 2\theta_{300} - \theta_{600} \tag{12}$$

Where:
θ_x = Fann* dial reading for the RPM, x.

* For more information, see the work method for the Fann viscometer in Appendix A.

3.9.2 Power law model

The Power law describes a fluid that decreases in viscosity as the shear rate increases. This type of fluid is known as pseudoplastic or shear thinning. The model describes fluids such as water-based polymer drilling fluids. The Power law for fluids is described mathematically as [T9]:

$$\tau = k\gamma^n \tag{13}$$

Where:

τ = Shear stress [lbf/ft^2]

k = The consistency index. Represents the average viscosity of a drilling fluid for its overall shear rate. [lbfs^n/100ft^2]

n = The flow behavior index, where pseudoplastic fluids has a value of: <1, Newtonian fluids: =1 and dilatant fluids: >1.

These can be found using the following equations [T9]:

$$k = \frac{R_{300}}{511^n} = \frac{R_{600}}{1022^n} \tag{14}$$

$$n = 3.321 * \log\left(\frac{R_{600}}{R_{300}}\right) \tag{15}$$

3.9.3 Herschel-Bulkley model

The Herschel-Bulkley model also describes pseudoplastic fluids, but takes the yield point into consideration, and is therefore the preferred model when it comes to describing drilling fluids. The constants k and n are the same as for the Powel Law, but has the additional yield point (τ_y) included. This model gives especially a better description of the lower shear rates. For low shear rates k is related to the viscosity of the fluid. For higher shear rates k is a measure of the solid content of the fluid. The lower the value of n, the more shear thinning the fluid is [T10]. The model is described by the following mathematical expression [T9]:

$$\tau = \tau_y + ky^n \tag{16}$$

Where τ_y can be set equal to the 3 RPM reading (simplified H-B) [16].

3.10 Viscoelasticity

Viscoelasticity is the property of materials that exhibit both viscous and elastic characteristics when undergoing deformation [T11]. The elastic portion of a viscoelastic material stores energy when deformed and do not dissipate energy. The viscous portion will when it is deformed dissipate energy as heat. Viscoelastic materials display time-dependent behavior when a stress or a strain is applied. Viscoelastic properties are temperature dependent [T12]. Steady-shear viscosity has provided useful rheological properties of drilling fluids under large deformation or shear flow. However, several phenomena cannot be described by the viscous property alone. Many processes related to drilling fluids are governed by viscoelastic properties. Drilling fluids are commonly not strongly viscoelastic. Therefore, out of the linear viscoelastic range, in nonlinear viscoelastic range, the viscous property is dominant. To obtain the viscoelastic properties of a drilling fluid in the linear viscoelastic range, test methods involved in small deformation are commonly employed. These tests are called dynamic tests, which can be divided into two major categories: transient and oscillatory. The two most common transient methods are creep-recovery and relaxation tests. The common oscillatory tests used to investigate the viscoelastic properties of materials are amplitude sweep, frequency sweep, oscillatory time sweep, and temperature sweep test [T11]. The basic principle behind the test method is to letting the fluid be exposed to periodic oscillations. The two-plate model can be used as an illustration, see figure 3-6. The sample is placed between a stationary plate and an oscillating plate. The oscillating plate is moving back and forth, causing sharing of the sample. Dynamic mechanical analysis applies a sinusoidal force, and the storage modulus can be described as an in-phase component, and the loss modulus as an out of phase component [T12]. The phase angle (δ) between the deformation and the response is shown in figure 3-7. The phase shift angle is a measure of the energy dissipation of the material.

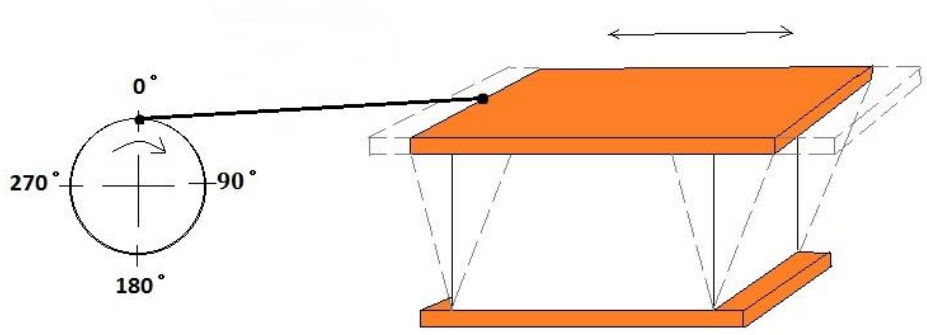

Figure 3-6: Illustration of periodic oscillations on a two plate model. [F4]

The applied shear strain is defined as:

$$\gamma(t) = \gamma_0 \sin(\omega t) \tag{17}$$

The measured shear stress:

$$\tau(t) = \tau_0 \sin(\omega t + \delta) \tag{18}$$

For a purely viscous fluid, the phase angle will be equal to 90 °. For a purely elastic material, the phase angle will be equal to 0 °. The phase angle for a viscoelastic material will be between 0 ° and 90 °. The shear stress can be written in term of strain as [T11]:

$$\tau(t) = \tau_0[\sin(\omega t)\, cos\delta + \cos(\omega t)\, sin\delta] \tag{19}$$

$$\tau(t) = \gamma_0 \left[\left(\frac{\tau_0}{\gamma_0} cos\delta\right) \sin(\omega t) + \left(\frac{\tau_0}{\gamma_0} sin\delta\right) \cos(\omega t)\right] \tag{20}$$

$$\tau(t) = \gamma_0[G' \sin(\omega t) + G'' \cos(\omega t)] \tag{21}$$

$$G' = \frac{\tau_0}{\gamma_0} cos\delta \quad and \quad G'' = \frac{\tau_0}{\gamma_0} sin\delta \tag{22}$$

The phase angle will further be given by:

$$\delta = tan^{-1}(G''/G') \tag{23}$$

The storage modulus or elastic modulus (G´), measures the energy stored per cycle, while the viscous modulus (G´´) measures the energy lost per cycle of sinusoidal deformation [T12].

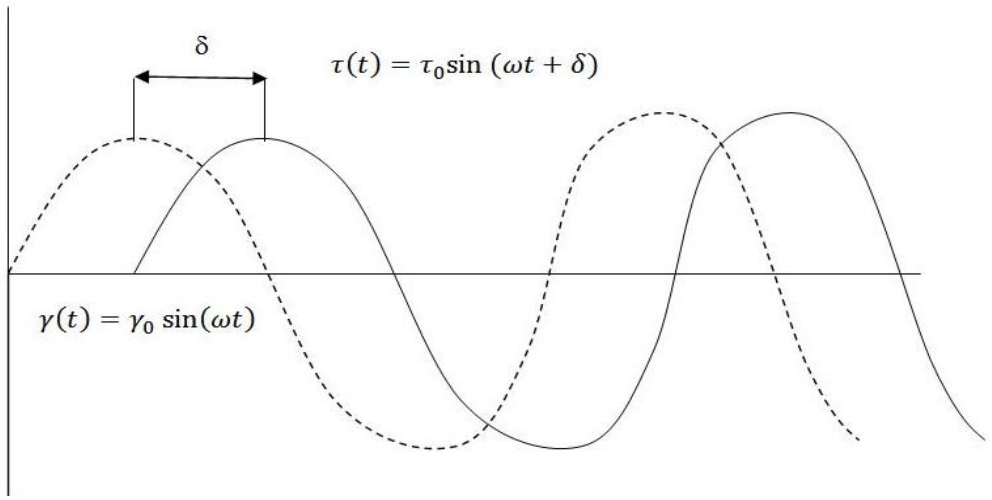

Figure 3-7: Viscoelasticity, phase angle. [F4]

3.10.1 Oscillatory amplitude sweep test

In an amplitude sweep test, the amplitude of the oscillation is ramped while the frequency is held constant. Under small strain, the sample will be deformed viscoelastically. The strain is increased to a critical point when the structure of the sample is irreversibly deformed. This will be seen, as the fluid will develop from a linear viscoelastic response to a nonlinear viscoelastic response. This test is normally the first test conducted on a sample to determine the linear viscoelastic range (LVER) and the range of strain (or stress) where the values of G` and G`` are constant. The test is also used to detect structural stability, strength and dynamic yield point of drilling fluids [T11].

3.10.2 Oscillatory frequency sweep test

In a frequency sweep test, the frequency of the oscillation is ramped while the amplitude is held constant. The speed of the deformation of the sample is changed and the response of the linear viscoelastic range is monitored. This test is used to detect time-dependent properties such as quantifying zero shear viscosity and structural strength at rest. The shape of the G` and G`` curves are characteristics of the material type [T11].

3.10.3 Oscillatory time sweep test

The oscillatory time sweep test directly provides information about how a material changes with time. Information such as dispersion settling, structure development, gelling time and gelling speed can be obtained. In these types of tests, the sample needs to be pre-sheared, in this case to simulate a circulating well. The oscillatory time sweep test is started right after the rotation (pre-shear) stops. During this sweep test, the amplitude, frequency and temperature are held constant while the properties are monitored over time. When the rotation is stopped, the sample will start to build structure that is monitored as an increase in elastic modulus. In this case this is the gel structure of the drilling fluid that forms rapidly after the circulation has stopped. This gel structure will keep the cuttings and solids in suspension in a real drilling operation, and is the reason why we want to study this behavior. A good gel structure should build strength rapidly, be stable with time and easy to break when circulation starts [T11].

3.10.4 Oscillatory temperature sweep test

In an oscillatory temperature sweep test, the amplitude and frequency are held constant while the temperature is ramped. This test is used to see the temperature dependence of the structure of the sample. Higher temperatures are often encountered along the wellbore, therefore it is of great significance to see how the drilling fluid behaves as the temperature is increased. Changes in temperature can affect the performance of the drilling fluid thus affecting the gel strength that keeps cuttings and solids in suspension. The temperature can be set to increase or decrease in this kind of test. If the temperature is decreasing it is possible to find the freezing point of the drilling fluid, and this can be of great importance when drilling in an arctic area, where the seabed temperature is very low. The oscillatory temperature sweep test can also be used to detect the formation of wax, hydrate and other phenomena related to the change in temperature. This test method gives a much better prediction and understanding of these phenomena than steady shear methods. Since the deformation is very small, the structure of the sample does not change significantly. The test will therefore not prevent or accelerate these phenomena [T11].

3.11 Electrical Stability (ES)

There are three basic criteria for preparing a stable emulsion. Firstly you need sufficient mechanical shearing to reduce water to small, uniform-size droplets, then an emulsifying agent in an amount that is sufficient to isolate the water droplets and prevent them from coalescing. You also need low-viscosity oil as the external phase.
Mechanical shearing of a mixture of oil, water and emulsifier breaks up water into smaller droplets that are stabilized and prevented from coalescing by a molecular film around each droplet. This film is an interface between the oil and water in which the emulsifying agent is concentrated. The function of the emulsifier is to reduce the interfacial tension, the natural tendency of water droplets to coalesce. By concentrating the emulsifier at the molecular interface between oil and water droplets, the interfacial tension is reduced. Water droplets, which have been reduced to minute size by applying mechanical energy, will not reform into bigger droplets if sufficient emulsifier has been used. In a well mixed and sheared emulsion, the droplet size will be about 1 μm [T1, T13].
A Fann ES tester is used to measure the electrical stability in the laboratory. See appendix A for a detailed work method.

3.12 Static sag

Static sag measurements are done to ensure a homogenous column of drilling fluid when the fluid is not in motion.

350 ml of a sample is being aged in a static ageing cell for a given amount of hours. The most typical amount of hours is 16, 72, 168, 336, 672 and 1344. This is to give an impression of the fluid stability over many different timeframes.
The top fluid layer, which in the OBM case is brine and/or base oil, will be measured as the free fluid (see figure 3-8). The next 50 ml down the cell is the top layer of mud. Then the next part of the mud will be removed from the cell until there is about 50 ml mud left in the cell. These 50 ml is reported as the bottom layer. The density contrast between the top and bottom of the main body of the fluid is used to calculate the Sag Factor and Sag Index of the fluid. Ideally the Sag Factor and the Sag Index should remain 0.5, which indicates a homogenous mud body. The Sag Factor describes the density contrast within the main body of fluid that

underlies any free fluid but does not relate the density and homogeneity of this fluid to the original fluid density. The Sag Index describes the degree of fluid separation by relating the density of the fluid at the base of the segregated fluid column to the original fluid density. This parameter does not describe the homogeneity of the fluid mass that underlies the Free Fluid layer. The Free Fluid, Sag Factor and Sag Index should therefore be used together to describe the relative condition of the segregated fluid [H1].

Formulas:

$$Free\ Fluid\ [\%] = \frac{Free\ Fluid\ [ml]}{350\ ml} * 100 \tag{24}$$

$$Sag\ Factor = \frac{Bottom\ Layer\ Density}{Top\ Layer\ Density + Bottom\ Layer\ Density} \tag{25}$$

$$Sag\ Index = \frac{Bottom\ Layer\ Density}{2 * Mud\ Density} \tag{26}$$

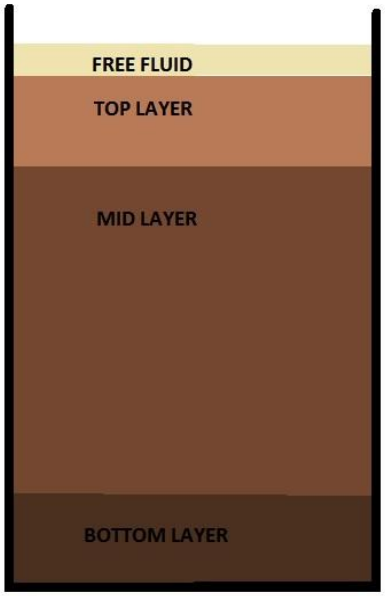

Figure 3-8: Static sag. [F2]

See Appendix A for a detailed description of the work method.

3.13 Dynamic sag

Dynamic sag measurements are as the name states ways of exploring the way particles settle in a drilling fluid, while the fluid is in motion.

The Viscometer Sag Shoe Test (VSST) is a well site and laboratory test that measures weight material sag tendencies of drilling fluids under dynamic conditions. The VSST uses a standard rotational viscometer like the Fann 35 as a mixer and a thermoplastic insert (sag shoe) that is designed to concentrate sagged weight material in the bottom of a viscometer thermo cup (see figure 3-9).

Equipment setup:

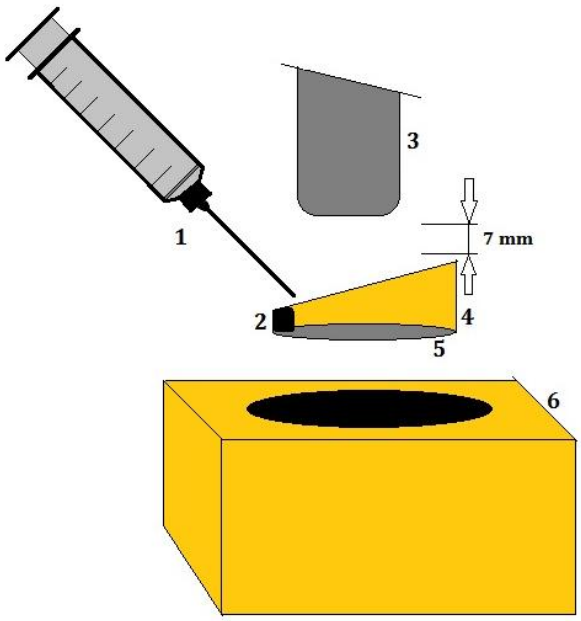

Figure 3-9: Dynamic sag equipment. [F2]

Key:

1. Syringe
2. Collection well
3. Viscometer sleeve
4. VSST Sag Shoe
5. Metal backing-plate
6. Thermo cup

The sag tendency is determined by the density increase of the samples extracted from the collection well, over a 30 min period at a certain temperature and rate of shear (usually 50 ˚C and 100 RPM).

Weight material bed pickup can be run in addition to characterize bed removal by higher shear levels. These results can be used to suggest opportunities for bed removal in the field prior to tripping out of the hole.

Formulas [H1]:

$$B_{VSST} = 0.834(m_{F2} - m_{F1}) \quad (27)$$

Where:

B_{VSST} = is the amount of weight-material sag, expressed in pounds-mass per gallon;

m_{F1} = is the initial mass of 10 ml drilling fluid (plus the syringe), expressed in grams;

m_{F2} = is the mass of 10 ml drilling fluid (plus the syringe) taken from the Sag Shoe following 30 min shear at 100 RPM, expressed in grams.

$$R_{BPU} = \frac{83.4(m_{F2} - m_{F3})}{B_{VSST}} \quad (28)$$

Where:

R_{BPU} = is the calculated bed pickup measurement ratio, expressed as a percentage;

B_{VSST} = is the amount of weight-material sag, expressed in pounds-mass per gallon;

m_{F2} = is the mass of 10 ml drilling fluid (plus the syringe) taken from the Sag Shoe following 30 min shear at 100 RPM, expressed in grams;

m_{F3} = is the mass of 10 ml drilling fluid (plus the syringe) taken from the Sag Shoe following 20 min shear at 600 RPM, expressed in grams.

Figure 3-10: Sag shoe. [P1]

Figure 3-11: Sag shoe (2). [P1]

3.14 NMR

Nuclear Magnetic Resonance (NMR) measurements can be used to determine the hydrogen content and distribution in a given fluid. This is done by detection of the nuclei spin of the hydrogen atoms in the fluid caused by absorption of electromagnetic waves from a strong magnetic field [T1]. By looking at the signal that is reflected during the test, it is possible to differentiate between the liquid and solid part of the fluid. Since the solid particles do not reflect the signal, this part of the sample can be seen as a weak signal. As time goes by, there can be seen an increasing, smooth signal upwards in the sample because we have a pure liquid at the top and an increasing gradient of solids downwards in the sample (see figure 3-12). In 2006, Rismanto and Van der Zwaag [T13] showed that NMR has a huge potential when it comes to analyzing sag potential of drilling fluids using 1D profiling. They also found correlation between T1 and T2 when varying the OWR in drilling fluids.

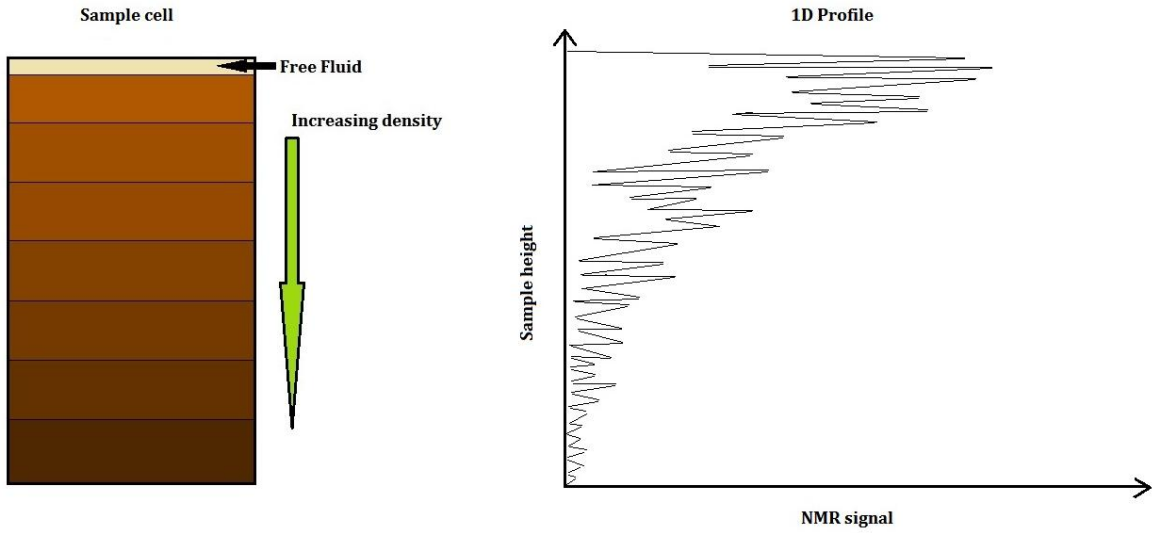

Figure 3-12: NMR 1D profiling. [F2]

The first step in making an NMR measurement is to align magnetic nuclei with a static magnetic field B_0. When the B_0 field is turned on along a direction designated as the z-axis, the energies of the nuclei are affected. The nuclear magnets are not actually lined up parallel to the +z or –z direction. Rather, the force of B_0 causes the magnetic moment to move in a circular fashion about the +z direction or about the –z direction, a motion called precession [T13, T14].

The precessional motion of the magnetic moment around B_0 occurs with angular frequency ω_0, called the Larmor frequency, and is given by [T14]:

$$\omega_0 = \gamma B_0 \tag{29}$$

Where:

ω_0 = Larmour frequency

γ = Gyromagnetic field

B_0 = External magnetic field

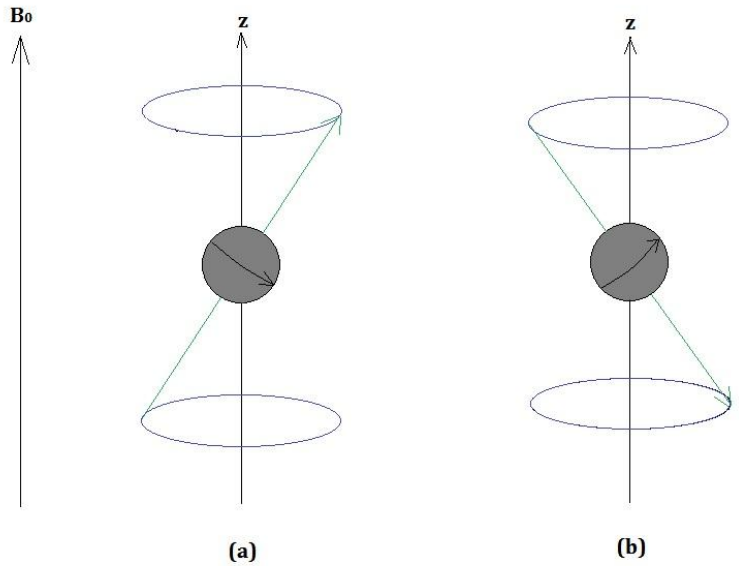

Figure 3-13: Precession of an atomic nucleus. [F3]

When a proton is subjected to an external magnetic field, the proton is forced into one of two energy states, as shown in figure 3-13. The energy state of a particular proton depends on the orientation of the precessional axis of the proton with respect to the direction of the external field. When the precessional axis is parallel to B_0, the proton is in the low-energy state (fig. 3-13 (a)), which is the preferred state. When the precessional axis is anti-parallel to B_0, the proton is in the high-energy state (fig. 3-13 (b)). The direction of B_0 is designated as the longitudinal direction [T14].

When a large number of spinning protons are precessing about B_0, more spins are precessing parallel to B_0 than anti-parallel. The difference between the number of protons aligned parallel and anti-parallel to the B_0 field forms the bulk magnetization M_0 that provides the signal measured by NMR devices, shown in figure 3-14. When the protons are polarized, they are aligned in the static magnetic field [T14].

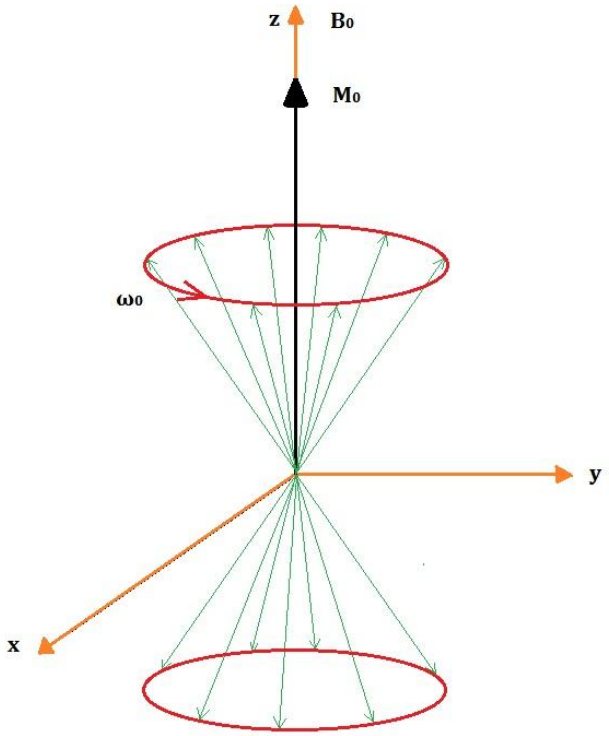

Figure 3-14: Bulk magnetization. [F3]

The second step in the NMR measurement procedure is to tip the magnetization. This tipping is accomplished by applying an oscillating magnetic field B_1. For effective tipping, the frequency of B_1 must be equal to Larmor frequency of the protons relative to B_0 [T14].

The angle the magnetization is tipped is given by [T14]:

$$\boldsymbol{\theta = \gamma B_1 t_p} \tag{30}$$

Where:

θ = Tip angle [degrees]

B_1 = Amplitude of oscillating field

t_p = Duration of the oscillating field is applied.

The B_1 field used in NMR measurements is a pulsed oscillating magnetic field. Angular-pulse terms, such as π pulse (180° pulse) and $\pi/2$ pulse (90° pulse), refer to the angle through which magnetization is tipped by B_1 [T14].

Applying a 90° pulse aligns the magnetization along the y-axis (transverse direction), as shown in figure 3-15. When the B_1 field is turned off, the proton population begins to dephase. The precessions of the protons will no longer be in phase with one another. Therefore, as dephasing progresses, the net magnetization decreases. A decaying signal in the transverse direction will be detected. This decay is usually exponential and is called free induction decay (FID). The duration of the relaxation is called transverse relaxation time, also known as T2 [T14].

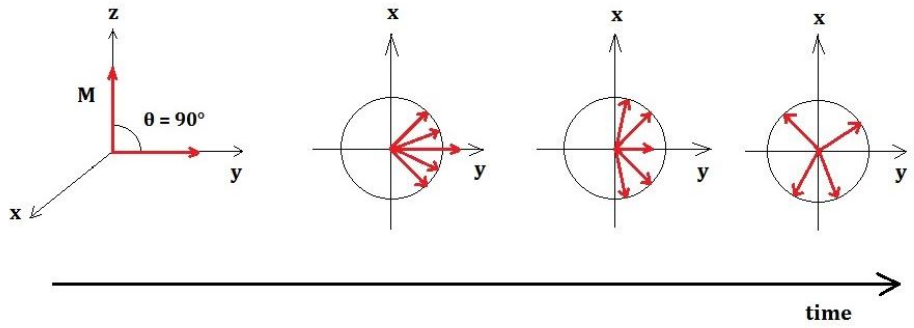

Figure 3-15: Transverse relaxation. [F3]

Applying a 180° pulse brings the magnetization along the –z direction (population inverse) as seen in figure 3-16. When the B_1 field is turned off, the magnetization will relax back to its original state in longitudinal direction. The duration of the relaxation is called longitudinal relaxation time, T1 [T14].

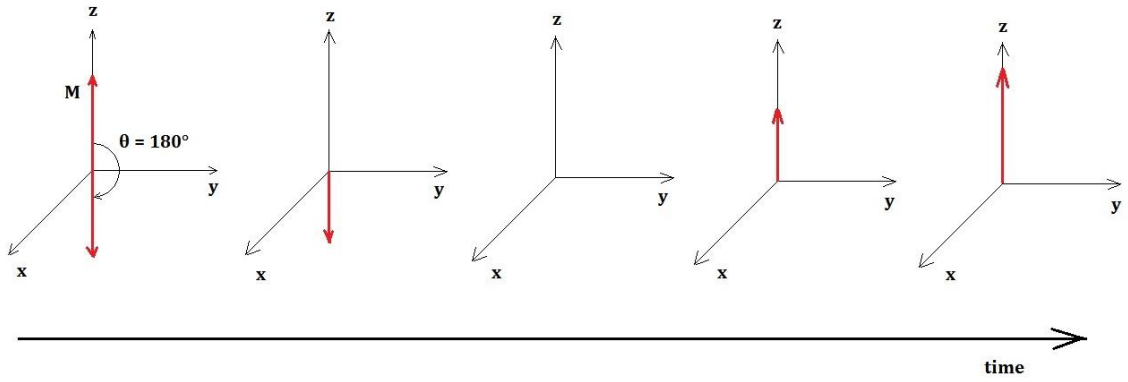

Figure 3-16: Longitudinal relaxation. [F3]

4 Experiments

[All experiments were conducted following the HSE standards of UiS and Halliburton laboratories]

In the experiment part of the thesis, the author has used his background as a laboratory technician at Halliburton to conduct the necessary tests to describe a drilling fluid system that is close to the fluid system that is likely to be used in the Brazil well (see Appendix C for more information).

The work started out with the fluid properties that Petrobras had provided. The goal with this work was not to get as close to the specifications from Petrobras as possible, but to be able to describe two systems that both can be used in the pilot hole and that performs well to describe the differences between them and their properties in relation to particle sagging. Table 4-1 presents the specifications given from Petrobras:

Table 4-1: Petrobras drilling fluid specifications. [R1]

Property	Value	Unit
Rheology		
Temp:	120 / 50	°F / °C
600	110-150	D.R
300	70-100	D.R
200	50-75	D.R
100	35-50	D.R
6	15-20	D.R
3	14-18	D.R
Gel 10 s	15-20	$lb/100ft^2$
Gel 10 min	20-26	$lb/100ft^2$
Mud weight	1.60	SG
Fluid loss HPHT	Max 9	ml
Water in filtrate	0	ml
Pm	3 to 6	ml
Salinity	Max 150.000	ppm.
Chlorides	Max 91.000	ppm.
Total solids	20-22	%
Sand content	Max 1	%
Electrical stability	Min 200	V
O/W ratio	60/40 – 65/35	

4.1 Mud systems

Reelwell AS decided to prepare two mud systems at Halliburton Baroid Fluids Laboratory. The first system is almost similar to the one suggested from Petrobras, but with some changes which also affect its properties.

4.1.1 Mix 1: Standard Oil Based Drilling Fluid (OBDF01)

Table 4-2 shows the fluid specifications.

Table 4-2: OBDF01 general specifications. [H1]

Mix Type	Mix Volume	OWR	WPS	SG
Oil Based	1400 ml	65/35	150000	1.60

Table 4-3 shows additives and concentrations along with the mix time used to prepare the mud system.

Table 4-3: OBDF01 formulation. [H1]

Product	Component	Concentration	Test Amount [g]	Mixing Time [min]
EDC 95/11	Base Oil	0.47 m3/m3	534.47	
EZ MUL NS	Emulsifier	25.7 kg/m3	35.98	10
DURATONE E	Filtration Control Agent	25.7 kg/m3	35.98	5
GELTONE II	Viscosifier	12.5 kg/m3	17.5	5
LIME	Lime	20 kg/m3	28	5
	CaCl2 Brine (SG: 1.14)			15
	- Water		358.4	
	- Salt		85.86	
BARITE	Barite	816.75 kg/m3	1143.45	15
SUM			2239.64	55

4.1.2 Mix 2: Modern Oil Based Drilling Fluid (BaraECD)

Table 4-4 shows the fluid specifications.

Table 4-4: BaraECD general specifications. [H1]

Mix Type	Mix Volume	OWR	WPS	SG
Oil Based	350 ml	80/20	150000	1.60

Table 4-5 shows additives and concentrations along with the mix time used to prepare the mud system.

Table 4-5: BaraECD formulation. [H1]

Product	Component	Concentration	Test Amount [g]	Mixing Time [min]
XP-07	Base Oil	0.53 m3/m3	142.01	
EZ MUL NS	Emulsifier 1	50 kg/m3	17.5	10
BDF-644	Emulsifier 2	9 kg/m3	3.15	5
LIME	Lime	11.4 kg/m3	3.99	5
	CaCl2 Brine (SG: 1.13)			15
	- Water		49.7	
	- Salt		11.04	
BDF-513	Filtration Control Agent	25 kg/m3	8.75	5
BARACARB 5	Bridging Material	42.9 kg/m3	15.02	5
TAU MOD	Viscosity Agent 1	14.3 kg/m3	5.01	5
BDF-568	Viscosity Agent 2	8 kg/m3	2.8	5
CIMBAR UF	Ultra Fine Barite	860.45 kg/m3	301.16	15
SUM			560.11	70

4.2 Conventional & standardized testing

The two mixes were tested in a conventional matter at the Halliburton Baroid Fluids Laboratory in Tananger, Norway. The various tests were conducted using Halliburton procedures that have been compiled from API RP 13B-2 (Recommended Practice for Field Testing Oil-Based Drilling Fluids).

The bottom hole temperature (BHT) is according to Petrobras, 51 ˚C in the Brazil well. This temperature is not high enough to make the testing valid for other wells. It was therefore decided to use 110˚C as a reference temperature when performing the ageing tests.

Table 4-6 presents the overall test program that was followed:

Table 4-6: Drilling fluid test program. [H1]

Age #0 (After mixing)	Age #0.1 (16h HR*)	Age #1 (16h S**)	Age #2 (72h S**)
Rheology @ 50°C & 20°C	Rheology @ 50°C	Rheology @ 50°C	Rheology @ 50°C
Electrical Stability	Electrical Stability	Electrical Stability	Electrical Stability
Density	-	Stability	Stability
-	-	Dynamic Sag Shoe	Dynamic Sag Shoe

*HR= Hot Roll

**S = Static

Mix 1 followed ageing #0, 1 and 2, while mix 2 followed all of them. The reason for this is that mix 2 needs to be hot rolled for the ingredients to be activated. Mix 1 on the other hand, can be set straight to static ageing after it has been mixed. See Appendix A for procedures on the conventional testing of the fluids.

After the conventional testing at Halliburton was done, the drilling fluids were brought back to the laboratory at the University of Stavanger.

4.3 Creative & non–standardized testing

This chapter presents the various creative and non-standardized tests that were performed in the laboratory at the University of Stavanger.

4.3.1 NMR

A Maran Ultra NMR spectrometer (figure 4-1) from Oxford Instruments was used to conduct the NMR measurements. This instrument has an operating permanent magnet and the proton resonance frequency is 2 MHz. The test chamber has a temperature of 35˚C.

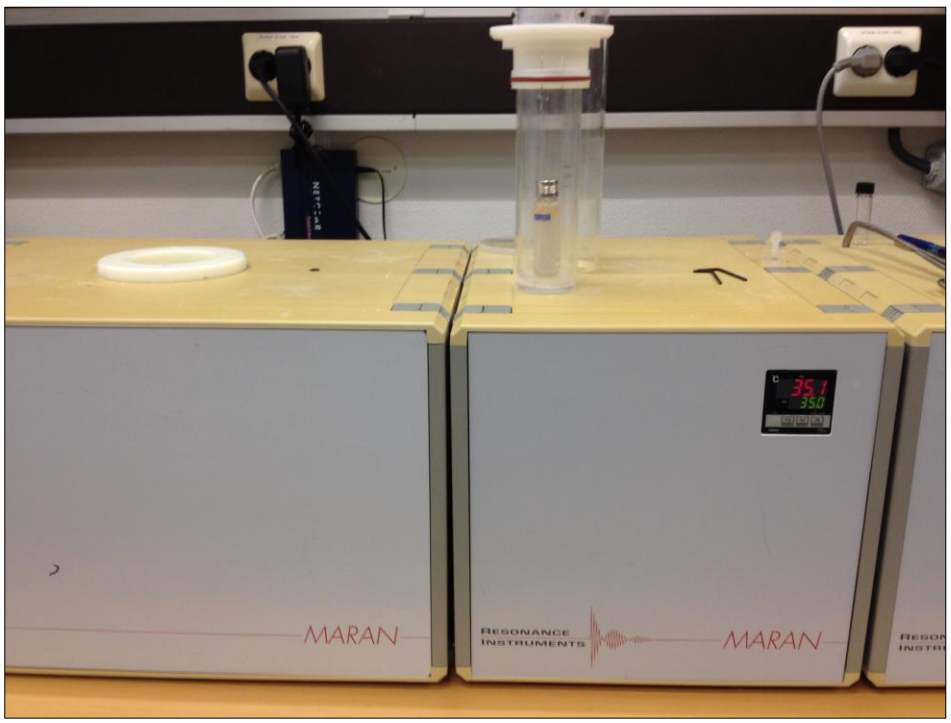

Figure 4-1: Maran Ultra NMR spectrometer (Oxford Instruments). [P1]

The test tubes (figure 4-2) were filled with the two different drilling fluids and aged for 16 and 72 hours, to make the scenario as identical to the conventional static ageing test as possible. When the samples had been aged for the defined number of hours, they were cooled down to room temperature before they were placed in the test chamber and heated up to 35 °C. The measurements were conducted using dedicated software called RINMR. The data were further analyzed using software called windxp.

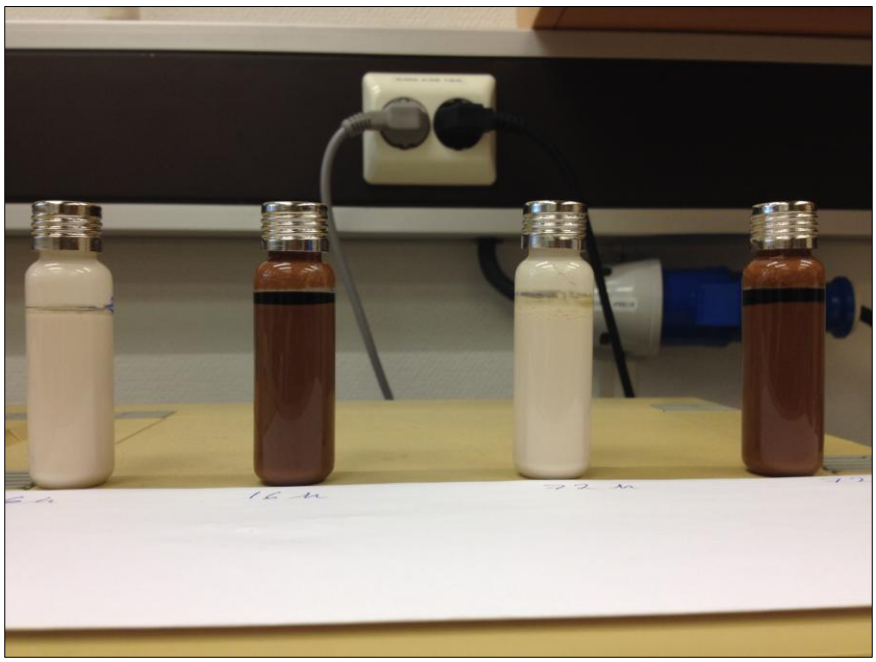

Figure 4-2: NMR test tubes. [P1]

4.3.2 Layered static sag

To get a better picture of the density profile in a static sag scenario, it is possible to use the same equipment and procedure as the conventional static sag test, but measure 7 layers instead of 3. This way, it will be easier to get a more detailed picture of the sag profile and create an analogue to a real well section (see figure 4-3).

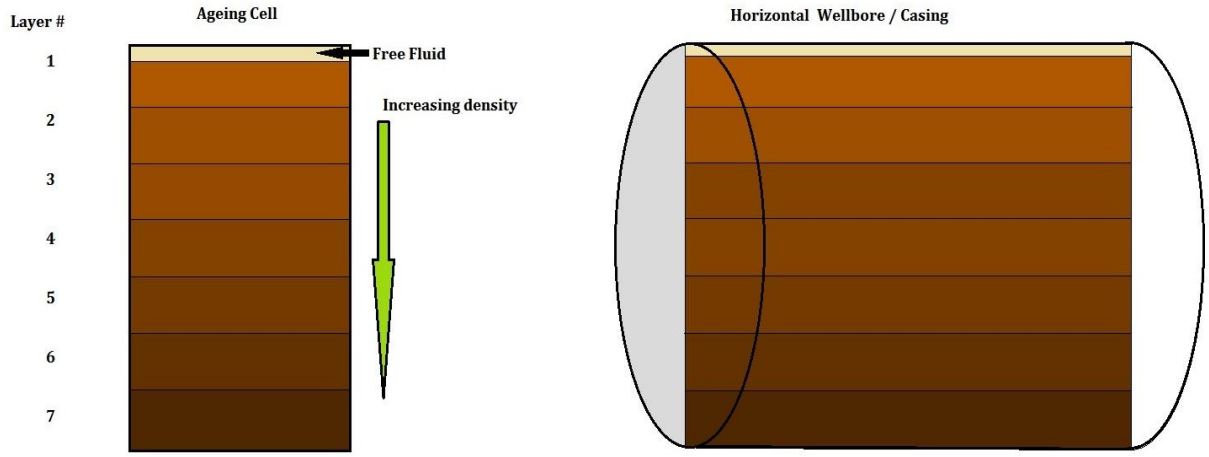

Figure 4-3: Illustration of layered static sag in cell and in a horizontal wellbore or casing. [F2]

4.3.3 Solid settling test

The solid settling test is conducted using a drilling fluid sample in a cup and an object that is connected to a scale (see figure 4-4 and 4-5). This way, the solids will start to fall out of suspension and land on the object that is standing still in the fluid and the recorded weight will increase. If the gel strength is high or the falling particles create increased buoyancy, then we will see that the weight is decreasing over time instead of increasing. This test was only conducted when the drilling fluid was at room temperature.

Equipment:

- KERN PLJ 360-3M scale
- Plastic cup
- Fishing line
- Heavy object

Figure 4-4: Solid settling test setup. [P1]

Figure 4-5: Solid settling test setup (2). [P1]

4.3.4 Viscoelasticity – Anton Paar Rheometer

The viscoelasticity measurements were carried out using the Anton Paar Modular Compact Rheometer 302 (MCR 302), see figure 4-6. There was used a parallel plate configuration with a PP50 spindle (figure 4-7). Approximately 2 ml of a drilling fluid sample was placed on the bottom test plate before the measurements were initiated. The drilling fluids were mixed for about 10 minutes on the Hamilton Beach mixer before they were placed on the plate.

The measurements were carried out in the following order using the dedicated software Rheoplus:

- Amplitude Sweep Test
  - Strain = 0.003 – 50 %
  - Angular frequency = 10 rad/s
- Frequency Sweep Test
  - Strain = 0.01 % (determined by amplitude sweep)
  - Angular frequency = 0.01 – 100 rad/s
- Time Sweep Test
  - Strain = 0.01 % (determined by amplitude sweep)
  - Angular frequency = 10 rad/s
  - Time = 0 – 60 min
- Temperature Sweep Test
  - Strain = 0.01 % (determined by amplitude sweep)
  - Angular frequency = 10 rad/s
  - Temperature = 4 – 80˚C

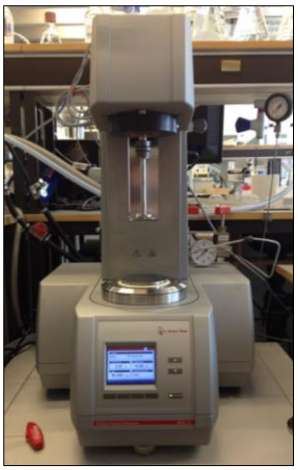

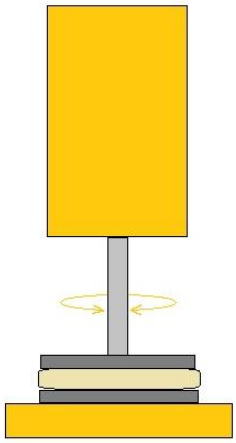

Figure 4-6: Anton Paar MCR 302. [P1] Figure 4-7: Parallel plate configuration. [F2]

4.3.5 Horizontal section sag test

To be able to simulate the fluid situation in the Reelwell drilling method, it was of great importance to create a rig that has near the same specifications as a real well (see figure 4-8). Using a 8.625“ casing and a 7.5” drill string as a reference there was acquired acrylic and plastic pipes that matched the casing/ drill string ratio. A video from the test can be found in the attachment.

Equipment:

- “Casing”: acrylic pipe with ID = 29.5 mm / L = 0.5 m
- “Drill string”: plastic rod with OD = 25.4 mm / L = 0.5 m
- “Top drive”: Drill with rotation of 100 RPM
- 10 ml syringe
- Duct tape
- Workshop stand
- KERN PLJ 360-3M scale
- GoPro Hero 3
- Digital protractor
- Foam plugs

To simulate a real scenario it is of interest to see how the drilling fluid behaves when being agitated at 100 RPM and left static for a time before being re-agitated. The following procedure was followed when executing this experiment:

1. Mix the fluid on Hamilton Beach for 10 minutes
2. Fill the pipe with fluid and make sure it is not leaking on either sides (figure 4-9)
3. Rotate the drill string for 5 minutes at 100 RPM
4. Leave static for 60 minutes (without rotation)
5. Measure the density of the fluid at the high-side and low-side of the pipe
6. Rotate the drill string for 30 seconds at 100 RPM
7. Repeat step 5

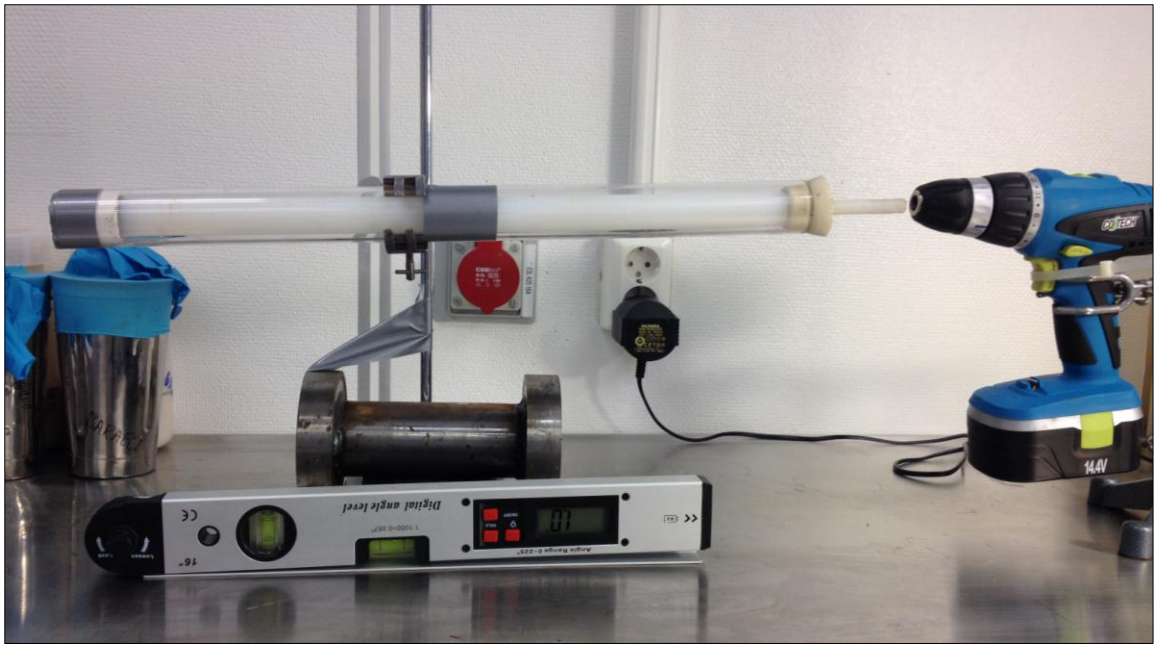

Figure 4-8: Horizontal section sag test setup. [P1]

Figure 4-9: Horizontal section sag test – filling of drilling fluid. [P1]

4.3.6 HOL vertical simulation

During the work with this thesis, the author was asked to conduct an experiment that could display the behavior of two drilling fluids with different densities. These fluids were to be placed in a pipe with a ratio between inner diameter and length of at least 1:500. This was done to make an estimate of how long the mixing zone will be during a real Heavy Over Light (HOL) drilling operation (see figure 4-10). In order to conduct these experiments, it was necessary to make one of the fluids used in the other experiments heavier. The OBDF01 fluid was weighted up from 1.60 SG to 1.84 SG using barite. Since the ODBF01 is brown and the BaraECD is white in color, they were quite easy to differentiate during the experiments. As seen from the list of equipment, the testing was done in small scale in the first experiment and in medium scale in the second experiment. Pictures from the testing can be found in Appendix B. A video from experiment 2 can be found in the attachment.

Experiment 1

Equipment:

- "Wellbore/ Casing": transparent pipe with ID = 3.00 mm / L = 2.00 m
- "Drill string": wire with OD = 1.00 mm / L = 2.00 m
- "Top drive": drill with rotation of 100 RPM
- Heavy mud, 1.84 SG (OBDF01), 25˚C
- Light mud, 1.60 SG (BaraECD), 25˚C

Procedure:

1. Fill the lower part of the pipe with light mud
2. Fill the upper part of the pipe with heavy mud
3. Observe and report any changes in the fluid interface and mixing zone
4. Insert the wire into the pipe from above and attach the drill to the top of the wire
5. Start the rotation of the "drill string" at 100 RPM
6. Observe and report any changes in the fluid interface and mixing zone

Experiment 2

Equipment:

- "Wellbore/ Casing": transparent pipe with ID = 10.00 mm / L = 4.50 m
- "Drill string": wire with OD = 3.00 mm / L = 4.50 m
- "Top drive": drill with rotation of 100 RPM
- Heavy mud, 1.84 SG (OBDF01), heated to 40 ℃
- Light mud, 1.60 SG (BaraECD), heated to 40 ℃

Procedure:

1. Fill the lower part of the pipe with light mud
2. Fill the upper part of the pipe with heavy mud
3. Observe and report any changes in the fluid interface and mixing zone
4. Insert the wire into the pipe from above and attach the drill to the top of the wire
5. Start the rotation of the "drill string" at 100 RPM
6. Observe and report any changes in the fluid interface and mixing zone

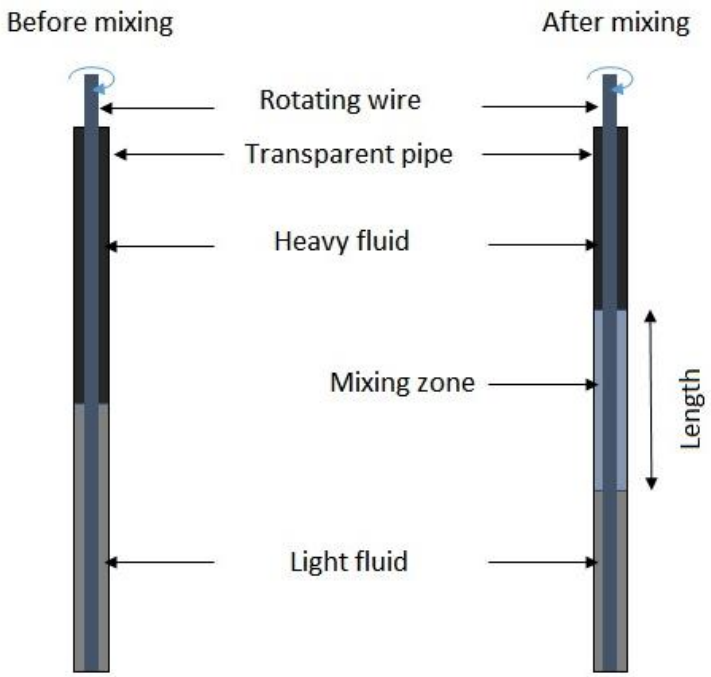

Figure 4-10: Illustration of the HOL vertical simulation setup before and after mixing. [F2]

5 Result Analysis

The following chapter presents the result analysis of the conventional and creative testing.

5.1 Results from the conventional & standardized testing

This subchapter presents the results from the conventional testing. Chapter 5.1.1 and 5.1.2 presents the results for each mix in tables before the results are compared graphically in chapter 5.1.3. Comments and analysis of the results is also included in chapter 5.1.3.

5.1.1 Mix 1 (OBDF01)

Table 5-1 – 5-4 presents the results from the conventional testing on mix 1 (OBDF01):

Rheology

Table 5-1: Rheology results, OBDF01.

Ageing	0	0	1	2
Temp. [℃]	20	50	50	50
600 rpm	185	97	97	93
300 rpm	113	60	60	57
200 rpm	87	46	47	44
100 rpm	58	31	32	29
60 rpm	45	24	25	23
30 rpm	34	19	19	17
6 rpm	20	11	11	10
3 rpm	18	9	10	8
10 s gel	19	10	11	9
10 min gel	20	13	12	11
30 min gel				
PV [cP]	72	37	37	36
YP [lb/100ft2]	41	23	23	21
YP [Pa]	19.7	11	11	10.1
LSRYP [lb/100ft2]		7	9	6

Electrical Stability (ES)

Table 5-2: ES results, OBDF01.

Ageing	0	1	2
ES [V]	420	310	225

Stability

Table 5-3: Stability results, OBDF01.

Ageing	1	2
Hours aged	16	72
Aging temperature [°C]	110	110
Free Fluid [ml]	5	12
Top SG	1.548	1.545
Bottom SG	1.606	1.679
Mud SG	1.60	1.60
Sag Factor	0.509	0.521
Sag Index	0.505	0.528

Dynamic sag shoe

Table 5-4: Dynamic sag shoe results, OBDF01.

Ageing	1	2
M_{F1} [g]	22.31	22.34
M_{F2} [g]	25.25	25.01
M_{F3} [g]	23.05	23.27
B_{VSST} [ppg]	2.46	2.23
R_{BPU} [%]	74.92	65.17

5.1.2 Mix 2 (BaraECD)

Table 5-5 – 5-8 presents the results from the conventional testing on mix 2 (BaraECD):

Rheology

Table 5-5: Rheology results, BaraECD.

Ageing	0	0	1	2
Temp. [℃]	20	50	50	50
600 rpm	115	79	51	46
300 rpm	79	54	33	29
200 rpm	67	44	25	22
100 rpm	50	31	17	14
60 rpm	42	24	13	10
30 rpm	35	18	9	8
6 rpm	31	16	6	4
3 rpm	28	14	5	4
10 s gel	44	23	8	7
10 min gel	50	25	22	17
30 min gel	51	27	23	20
PV [cP]	36	25	18	17
YP [lb/100ft2]	43	29	15	12
YP [Pa]	20.6	13.9	7.2	5.8
LSRYP [lb/100ft2]		12	4	4

Electrical Stability (ES)

Table 5-6: ES results, BaraECD.

Ageing	0	1	2
ES [V]	1530	1120	930

Stability

Table 5-7: Stability results, BaraECD.

Ageing	1	2
Hours aged	16	72
Ageing temperature [° C]	110	110
Free Fluid [ml]	5	17.6
Top SG	1.593	1.573
Bottom SG	1.651	1.768
Mud SG	1.60	1.60
Sag Factor	0.509	0.529
Sag Index	0.519	0.556

Dynamic sag shoe

Table 5-8: Dynamic sag shoe results, BaraECD.

Ageing	1	2
M_{F1} [g]	22.25	22.25
M_{F2} [g]	22.79	22.67
M_{F3} [g]	22.46	22.55
B_{VSST} [ppg]	0.45	0.35
R_{BPU} [%]	61.11	28.57

5.1.3 Graphical representation of results from conventional testing

Figure 5-1 shows the flow curves for the two different fluids at different ageings. As we can see from the graph, the OBDF01 had an overall higher viscosity than the BaraECD. The BaraECD had a higher yield point than the OBDF01 at age #0, but the shear stress became lower at higher shear rates. Note that the OBDF01 had almost the same values at age #0 and #1. The BaraECD had higher shear stress values at age #2 than age #1 on the higher shear rates. The Herschel Bulkley model was chosen to present the viscosity curves, since this model takes yield point into consideration and is the best model for presenting modern drilling fluids which often has high shear stress values on the low-end and low shear stress values on the high-end of the shear rate scale.

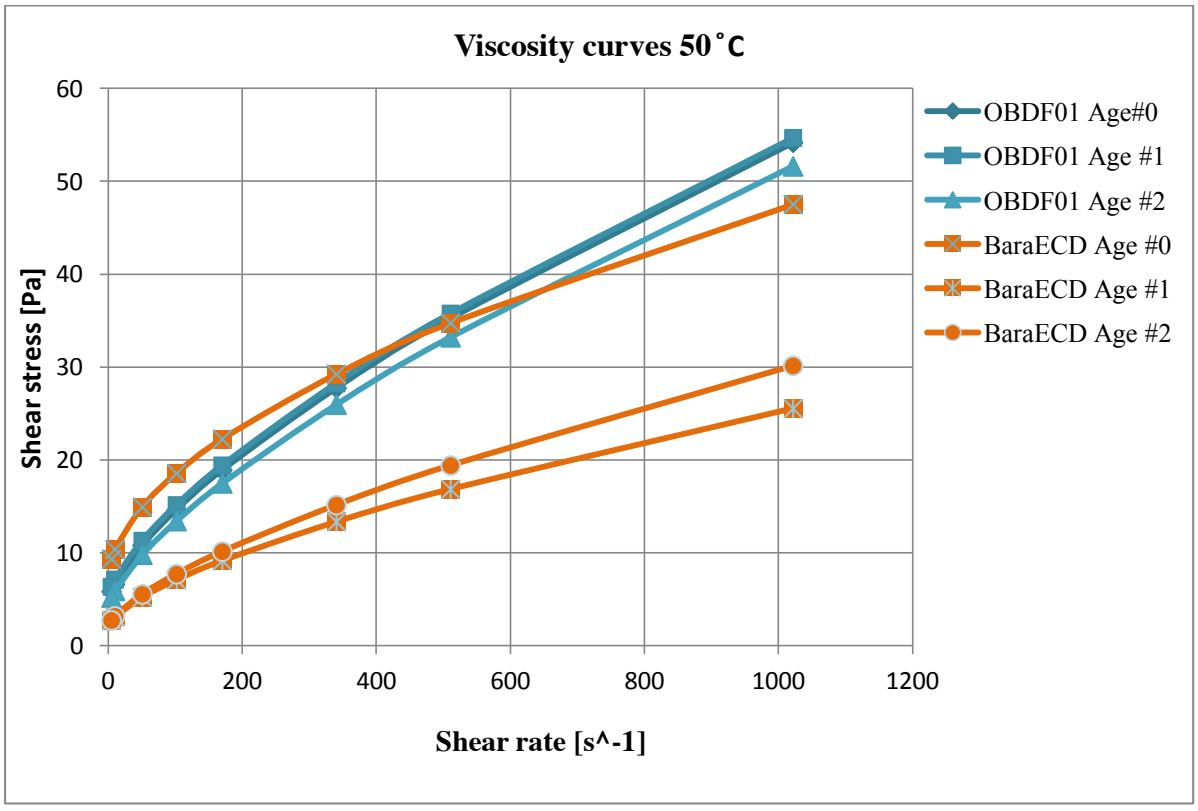

Figure 5-1: Viscosity curves for the different ageings (Herschel Bulkley model).

Figure 5-2 shows the gel strength values for the two fluids at different ageings. As seen from figure 5-1, the shear stress values are decreasing as the fluid is exposed to energy in form of heat and motion over time. The same happens to the gel strength, as we can see in the figure below. At age #0 we can see that the 10 seconds to 10 minutes (10T10) increase in gel strength is 30 % for the OBDF01 and about 9 % for the BaraECD. At age #1, the chemicals in the BaraECD have been activated and this can be clearly seen as a 10T10 increase of 143 %, while the OBDF01 has a 10T10 increase of 9 %. On the last ageing, both fluids have been affected by the temperature over time and the absolute values are lower than at age #1. The OBDF01 has a 10T10 increase of 22 %, while the BaraECD has an increase of 114 %.

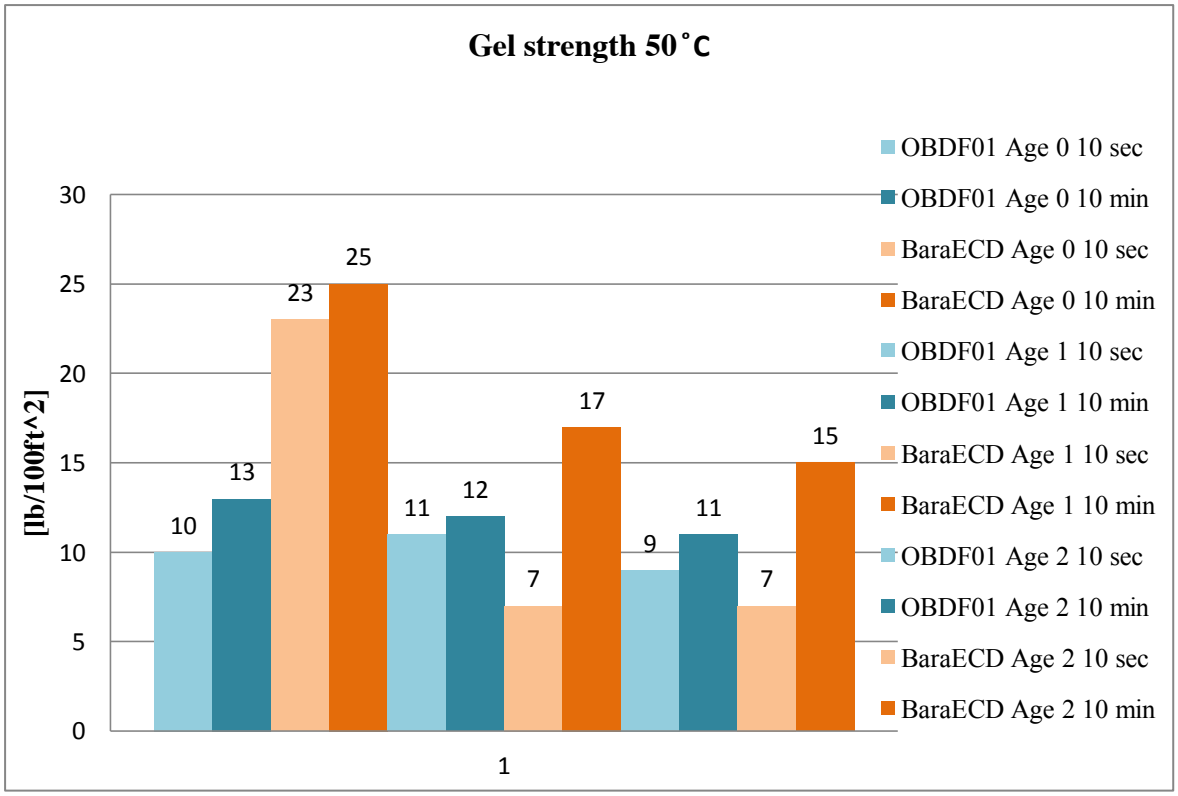

Figure 5-2: Gel strenght values at the different ageings.

Figure 5-3 shows the ES values of the fluids. As seen from the chart, the BaraECD has significant higher ES values than the OBDF01. The absolute values are reduced as the fluids are aged.

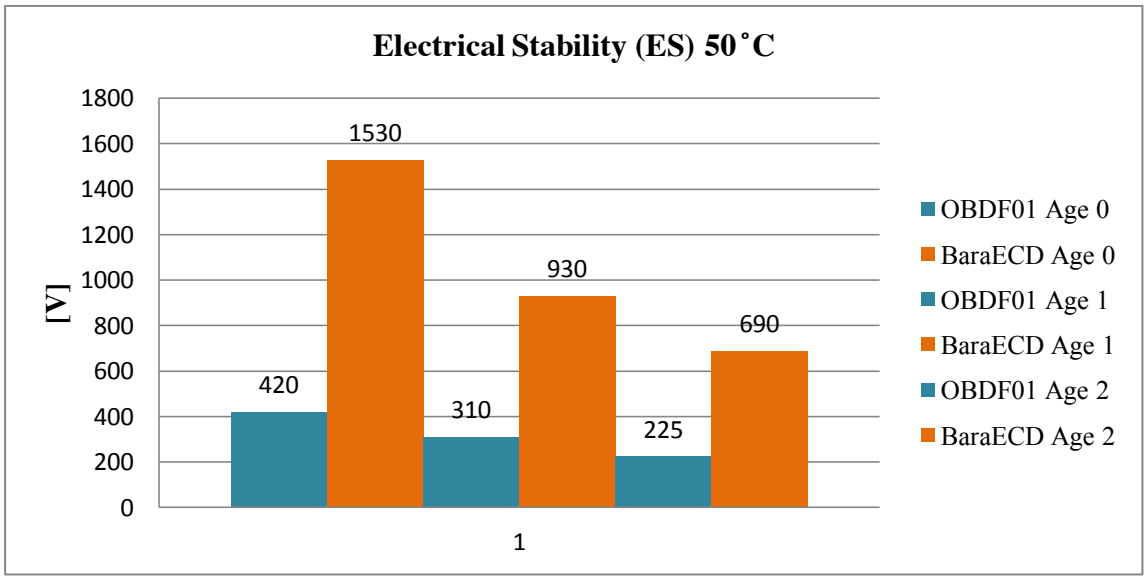

Figure 5-3: ES values at the different ageings.

Figure 5-4 shows the sag factor for the two fluids after ageing. As seen from the chart, the values are equal for the 16 hour ageing (age #1), while the value for the BaraECD is a bit higher than for the OBDF01 on the 72 hour ageing (age #2). This result shows that there has been a bit more bottom layer sag on the BaraECD than on the OBDF01.

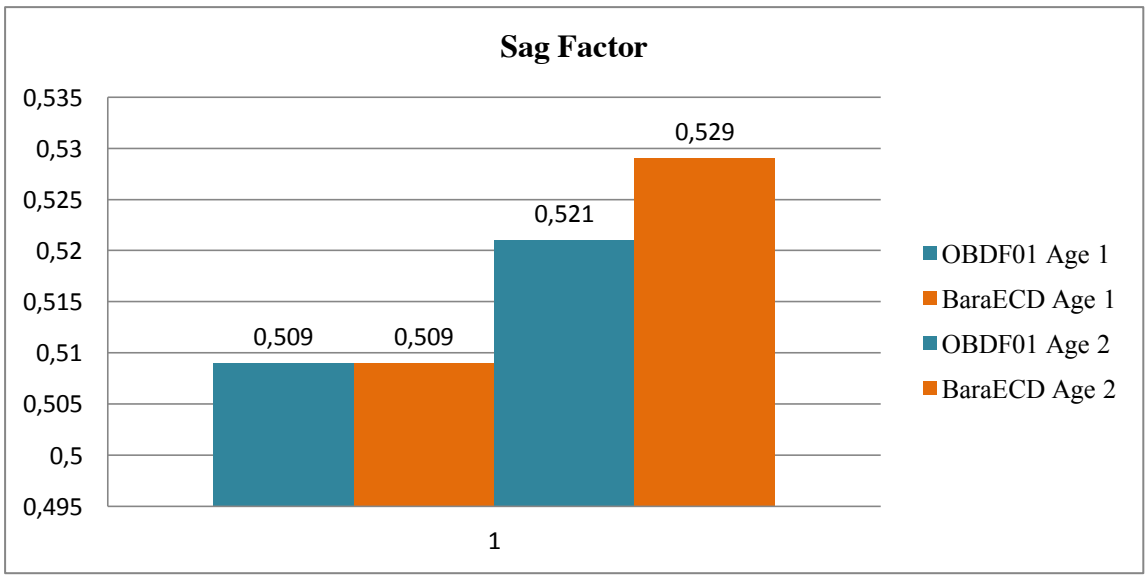

Figure 5-4: Sag factor values at the different ageings.

Figure 5-5 shows the sag index values of the fluids. As opposed to the sag factor which describes the density contrast within the main body of the fluid, the sag index relates the density of the bottom layer to the original fluid density. As we can see from the chart, we have a near linear development as the fluids are being aged.

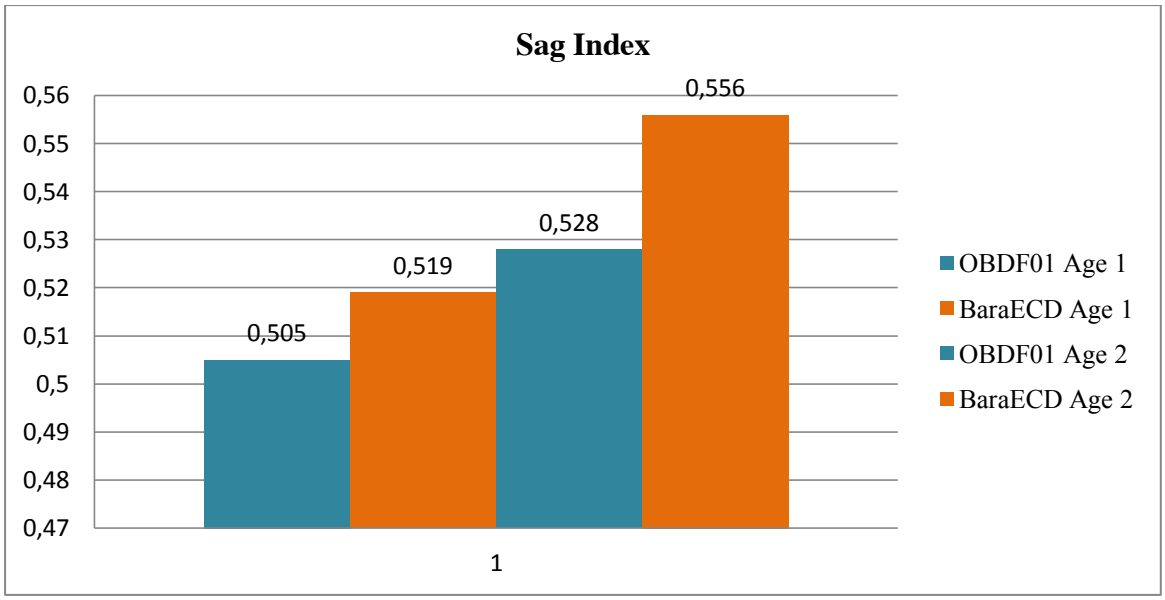

Figure 5-5: Sag index values at the different ageings.

Figure 5-6 shows the density increase during the viscometer sag shoe test (VSST). As seen from the chart, the OBDF01 has a significant higher density increase than the BaraECD.

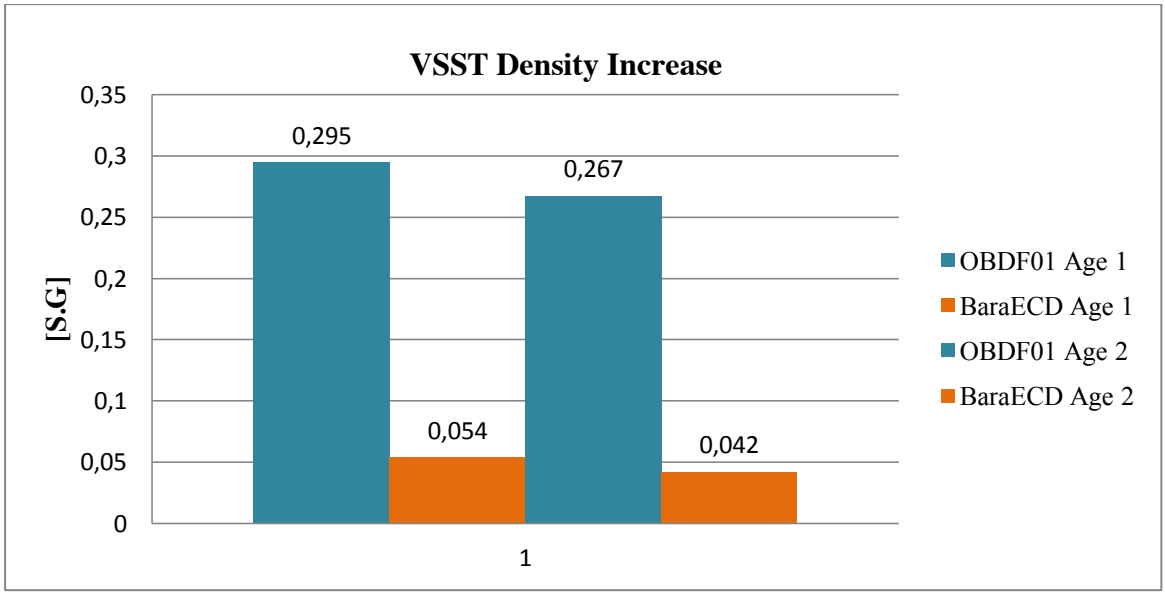

Figure 5-6: VSST density increase.

Figure 5-7 shows the bed pickup measurement ratio for the two fluids. As seen from the chart, the OBDF01 has a bit higher pickup ratio than the BaraECD. This can be due to the different amount of particles in the collection well.

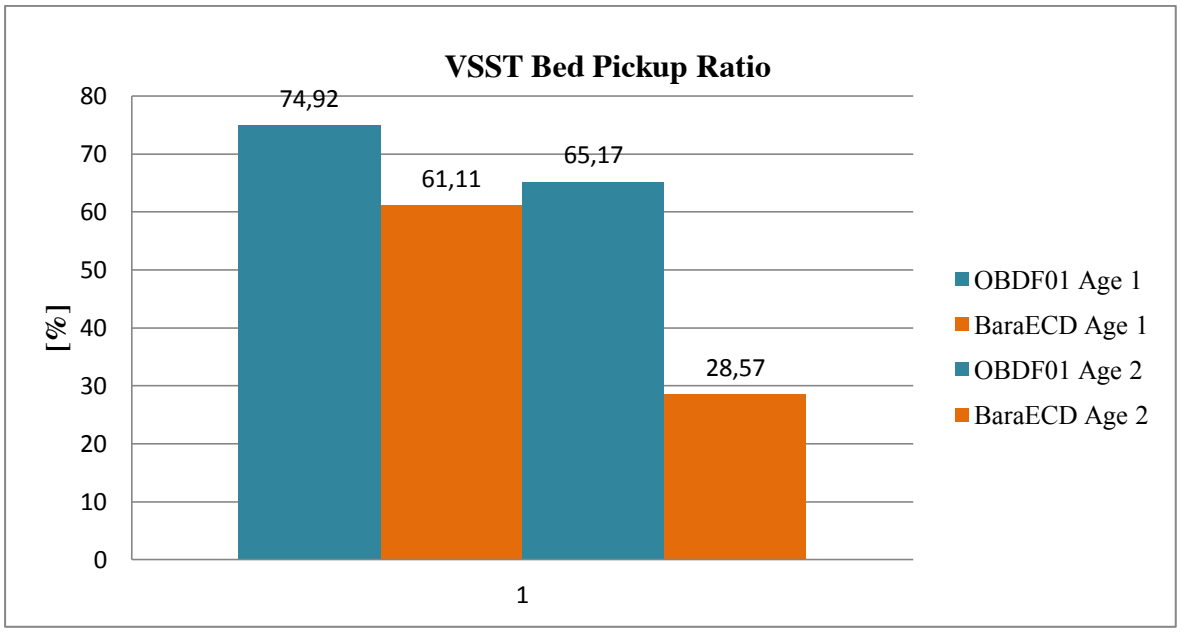

Figure 5-7: VSST bed pickup ratio.

5.2 Results from the creative & non – standardized testing

This subchapter presents the result analysis from the creative & non-standardized testing.

5.2.1 NMR

The following four plots represent the data gathered from the NMR measurements that were performed on the aged drilling fluid samples. The y axis represents the test tube height, where 0 cm is the bottom and 6 cm is the top of the tube. The test tubes were filled up to about 5.5 cm; hence there is no signal above this height.

Figure 5-8 shows the 1D profile of the OBDF01 fluid after being aged for 16 hours at 110 ˚C. As seen from the graph, we have a varying, but overall stable distribution between 3000 and 7000 in NMR signal. This can be interpreted as a stable fluid with an even distribution of weight particles.

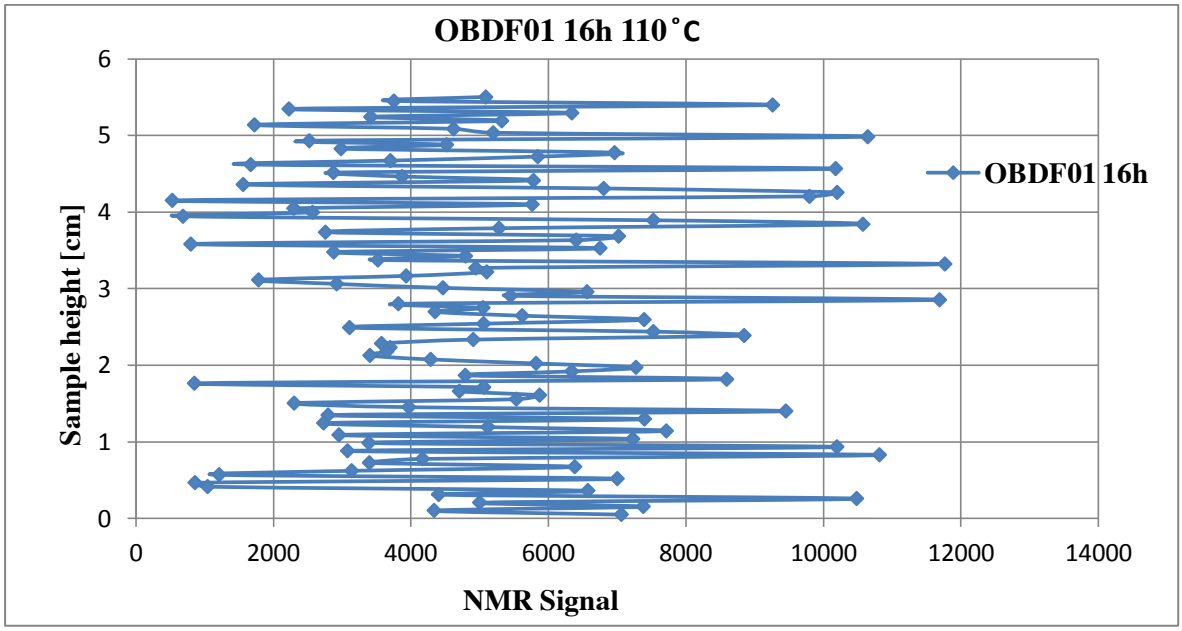

Figure 5-8: 1D profile, OBDF01 16h.

Figure 5-9 shows the OBDF01 profile after 72 hours of ageing. As opposed to the situation in figure 5-8, we see a less varying signal, but with significantly higher signal strength in the upper 3/4 of the test tube. This can be interpreted as a more unstable fluid with increasing weight material content down through the test tube. Since there is only free fluid and light mud on top of the test tube we have almost no attenuation, which can be seen as very high signal strength.

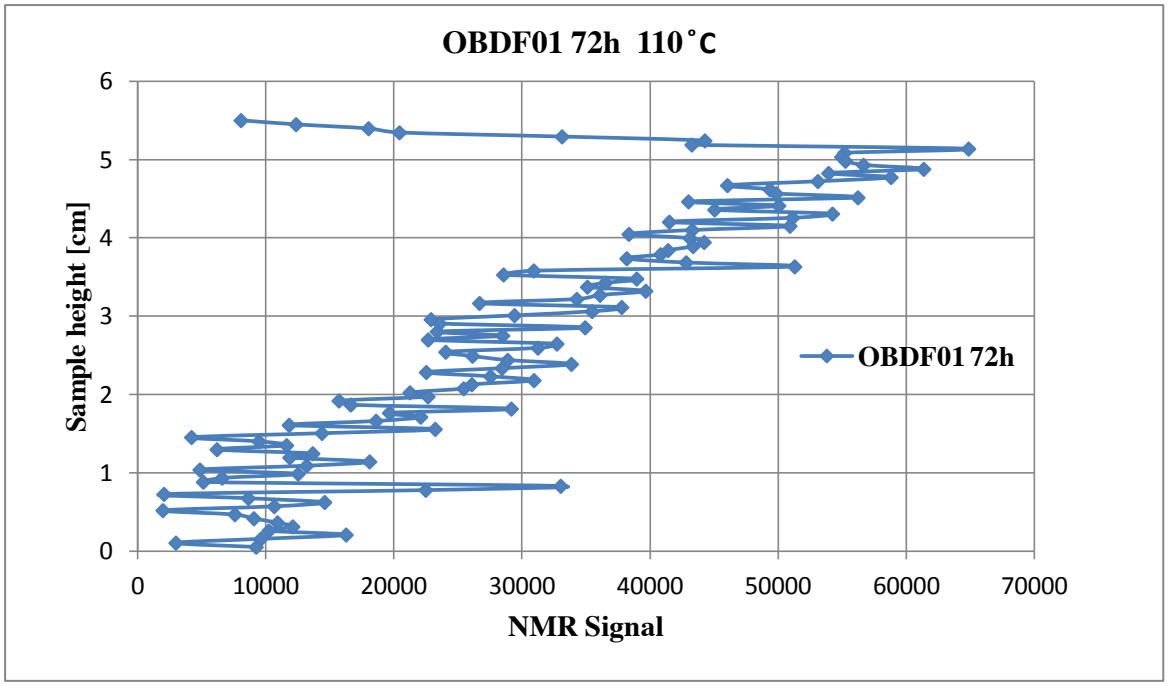

Figure 5-9: 1D profile, OBDF01 72h.

Figure 5-10 shows the BaraECD profile after 16 hours of ageing. Like the OBDF01 16h, this plot is varying, but overall stable between a signal strength of 4000 and 8000. This fluid can also be interpreted as stable with an even weight particle distribution.

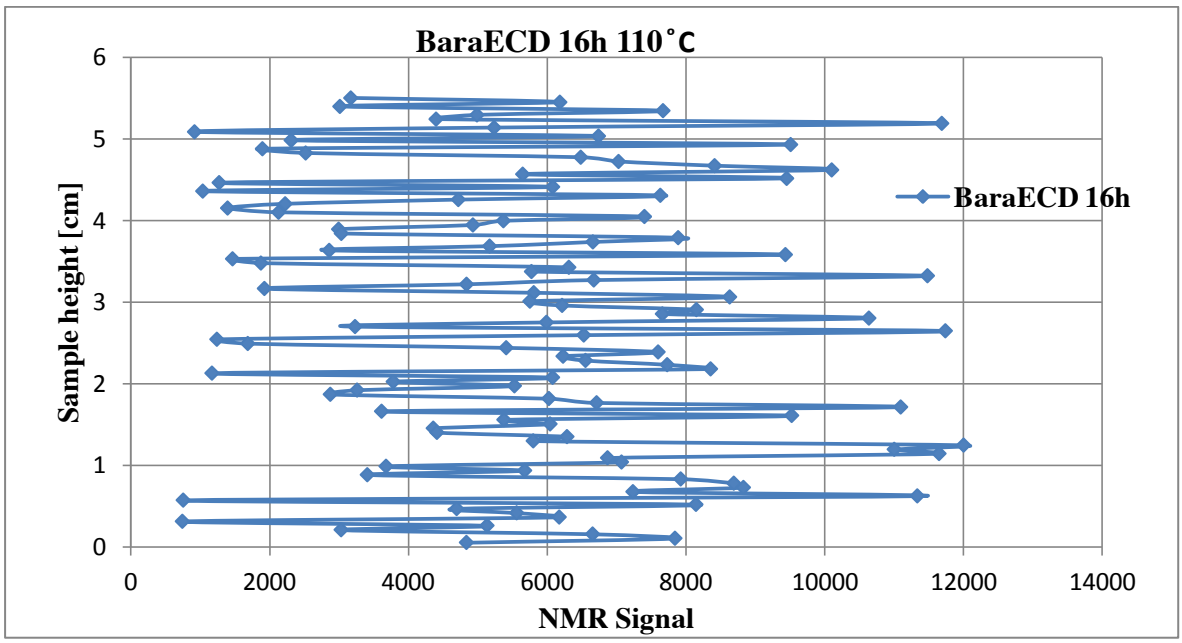

Figure 5-10: 1D profile, BaraECD 16h.

Figure 5-11 shows the 1D profile of the BaraECD fluid after 72 hours of ageing. The NMR signal is varying between 5000 and 55000 depending on the amount of weight particles, which are attenuating the signal. The fluid can be interpreted as significantly more unstable after 72 hours than what was the case after 16 hours of ageing.

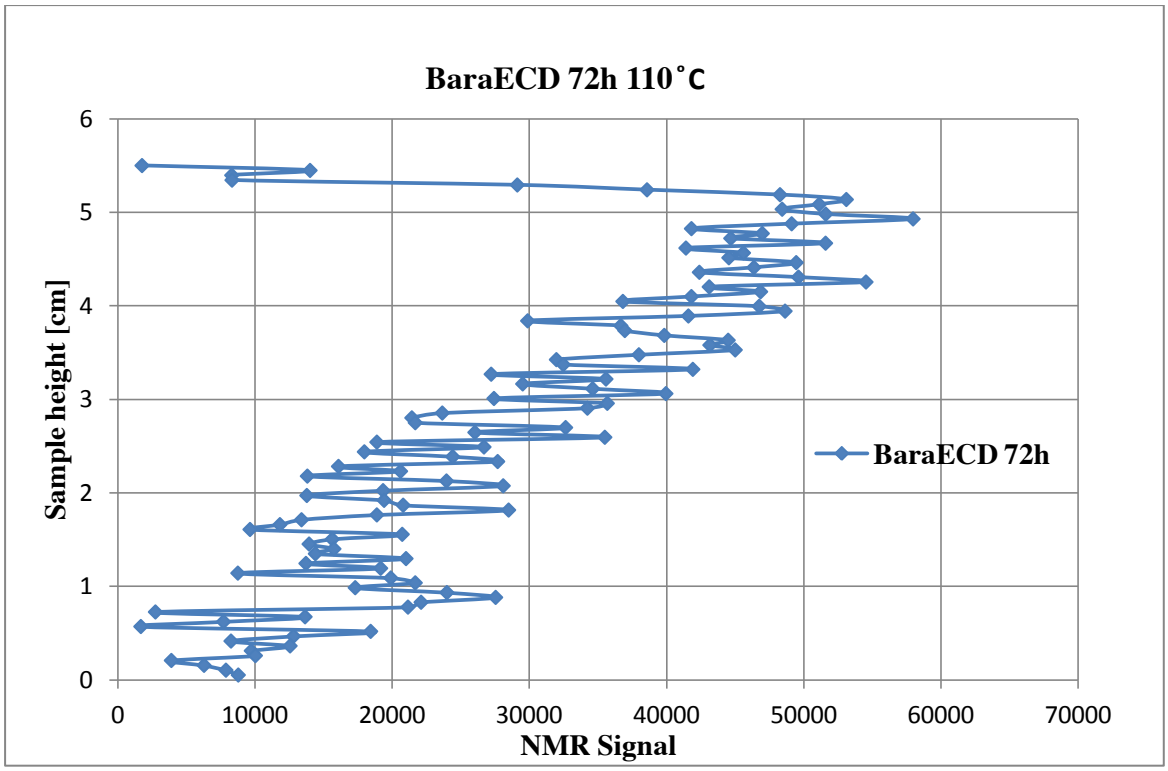

Figure 5-11: 1D profile, BaraECD 72h.

5.2.2 Layered static ageing test

The layered static ageing test was conducted according to the procedure in chapter 4 and the density values for the two fluids are presented in table 5-9 and figure 5-12. Layer 1 is the top layer of the cell (under the free fluid) and layer 7 is the bottom layer of the cell. Both fluids had an initial density of 1.60 SG, but after 72 hours of ageing at 110 ˚C there are significant differences in the density at each layer. Note that the OBDF01 has a more smooth transition in density values down the cell. Especially from layer 1 to 2 in the BaraECD, a significant increase in density is observed.

Table 5-9: Layered static ageing test results.

	OBDF01 (Mix 1)	BaraECD (Mix 2)
Free Fluid [ml]	13	18
#1 *	1.573	1.574
#2 *	1.575	1.616
#3 *	1.577	1.620
#4 *	1.579	1.625
#5 *	1.586	1.642
#6 *	1.608	1.660
#7 *	1.693	1.766

*: Specific Gravity [S.G]

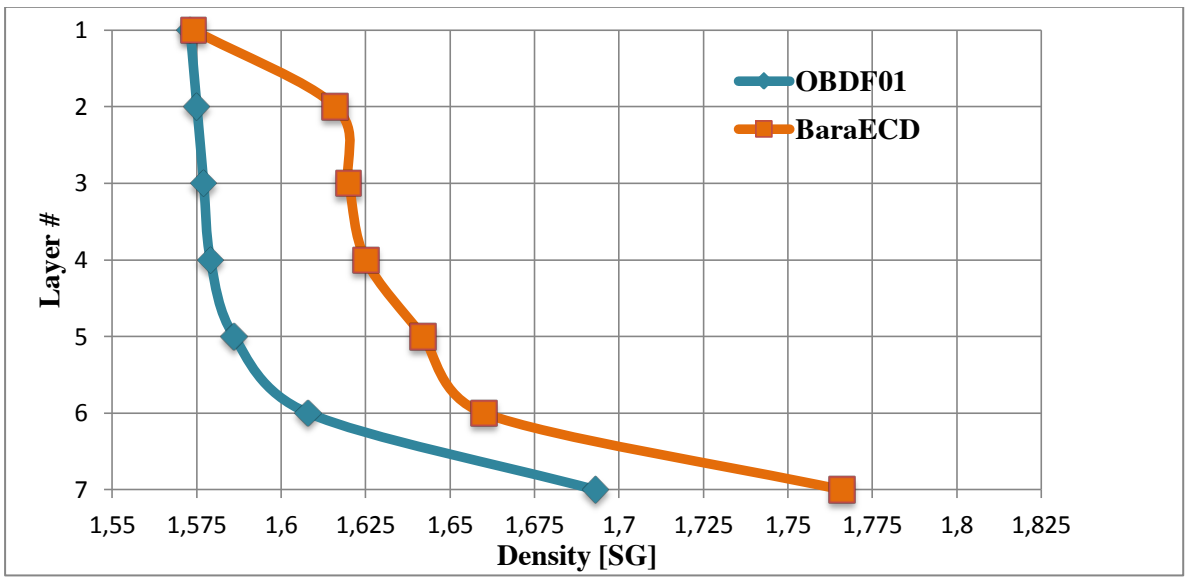

Figure 5-12 Graphs representing the layered density values.

5.2.3 Solid settling test

The solid settling test was conducted according to the procedure in chapter 4 and the results are presented in figure 5-13. The test was performed at a temperature of 20 ˚C, a factor that affects the gel strength of the fluid significantly. As we can see from the graph, the weight was increasing the first 30 minutes in the OBDF01 fluid. The fluid seemed to be in equilibrium from 30 to 60 minutes before the weight decreased a bit towards the end of the test. The values for the BaraECD were decreasing from the start of the test. The decrease in weight is almost linear the last 50 minutes.

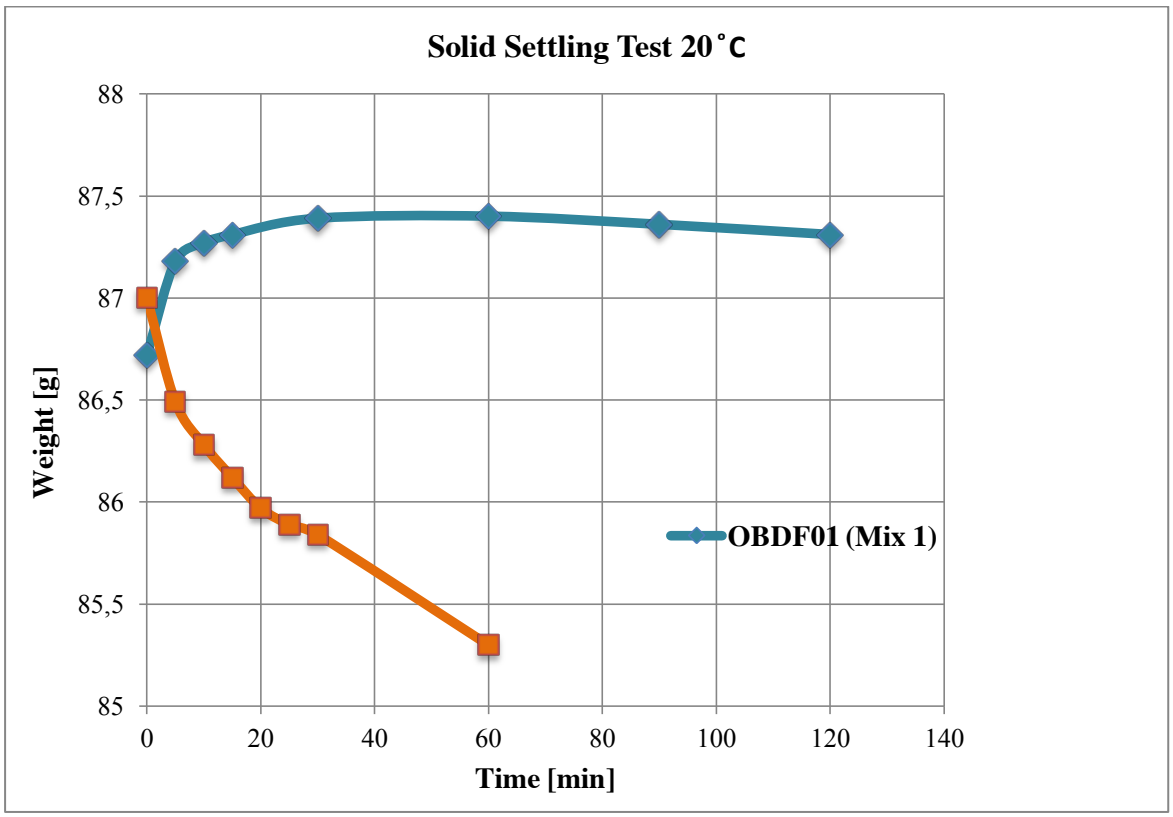

Figure 5-13: Solid settling test.

5.2.4 Viscoelasticity – Anton Paar Rheometer

The following 4 plots represent the viscoelasticity measurements that were conducted on the two samples. Figure 5-14 shows the amplitude sweep test results. The test was performed with a strain ranging from 0.003 - 50 % and at a constant angular frequency of 10 rad/s. The test temperature was set to 20 ˚C. The main purpose of this test was to define the linear viscoelastic range, which the other tests were based upon. The blue arrows points out the limit value of the linear viscoelastic (LVE) range. This point is also known as the yield point, in other words the point where the elastic modulus (G´) and viscous modulus (G´´) are in balance. As we can see from the graphs, the storage modulus is above the loss modulus in the LVE range for both fluids. This shows that the fluids have a gel like behavior in the LVE range and indicates that they have a stability or firmness in the low shear range.

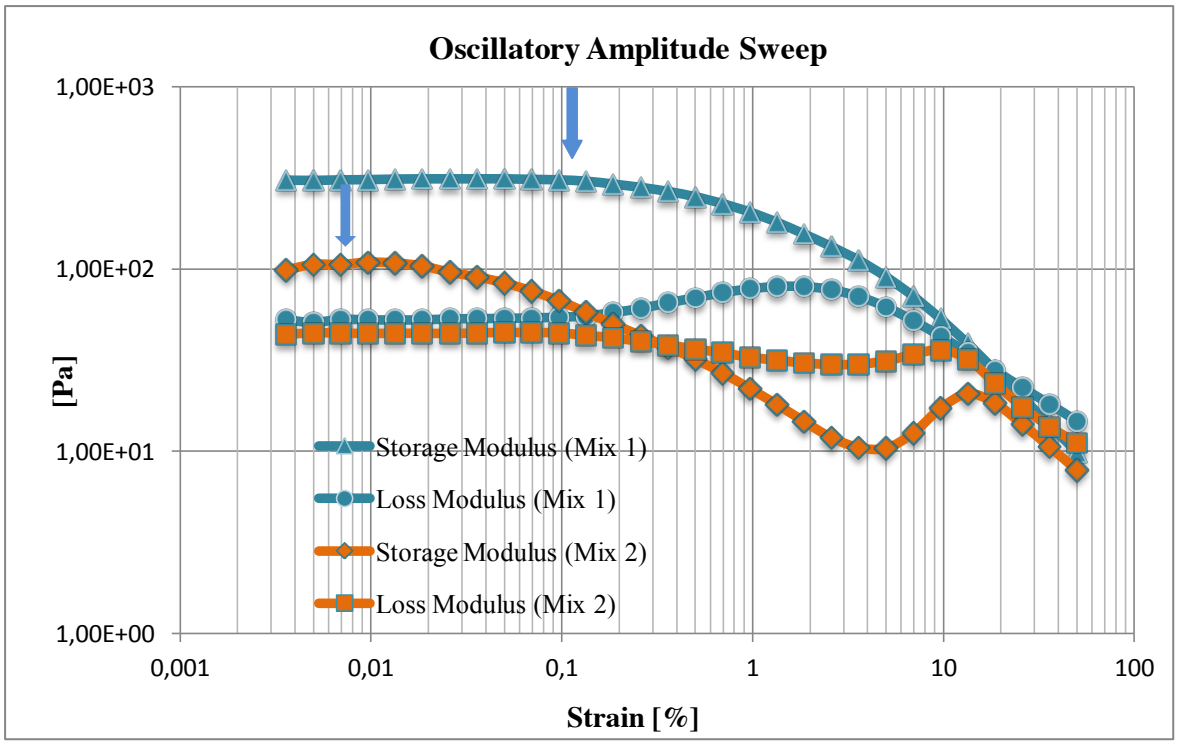

Figure 5-14: Plot showing the oscillatory amplitude sweep test. Storage modulus (G´) and loss modulus (G´´) are plotted. Blue arrows indicate the limit value of the LVE range.

Figure 5-15 shows the oscillatory frequency sweep test results. The amplitude sweep test gave the strain value that was used in this and the following two sweep tests. The strain value that was chosen was in the middle of the LVE range for both fluids; 0.01 %. Since these fluids have a sag potential, it was of great importance to set the frequency sweep from high to low. In this manner the fluids could not lose particles out of suspension before the end of the test. Since time is the inverse of frequency, frequency tests can be used to investigate deformation behavior that is time-dependent. A low frequency corresponds to a slow deformation, while a high frequency corresponds to a fast deformation. This gives an opportunity to look at frequency test data to evaluate if a samples deformation response at a certain speed is viscous or elastic. If the storage modulus (G´) is higher than the loss modulus (G´´) at a given frequency, the deformation response is dominated by an elastic behavior. This is as seen from the graph the case for both fluids. This is again an indication of a stable gel structure, which is able to keep particles in suspension.

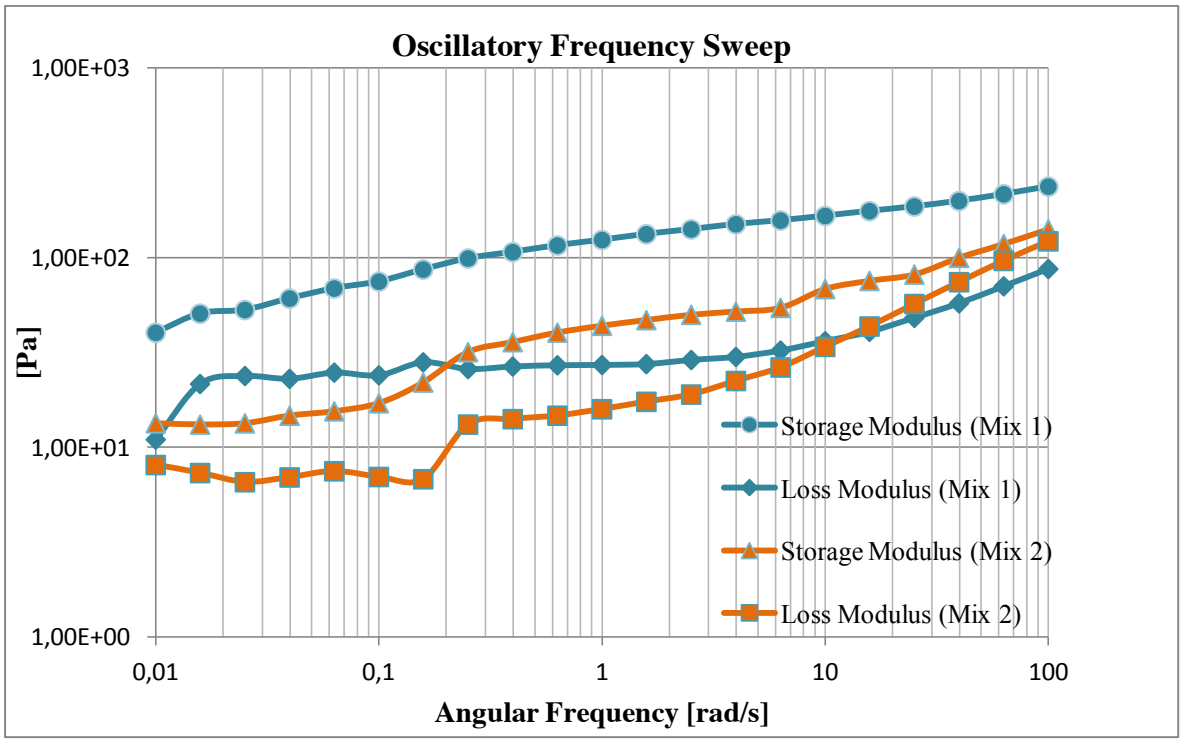

Figure 5-15: Oscillatory frequency sweep test.

Figure 5-16 shows the plot from the oscillatory time sweep test. The strain was set to 0.01 %, while the angular frequency was set to 10 rad/s. During this test, the storage and loss modulus were monitored over time till they reached a stable value. As we can see from the graph, the storage modulus reaches stable values (green arrows) at about 23 minutes for the OBDF01 and about 37 minutes for the BaraECD fluid. There can be seen a decrease in storage modulus for both fluids between 27 and 60 minutes for the OBD01 and between 40 and 60 minutes for the BaraECD. This can be due to particle settling and relaxation of gel structure.

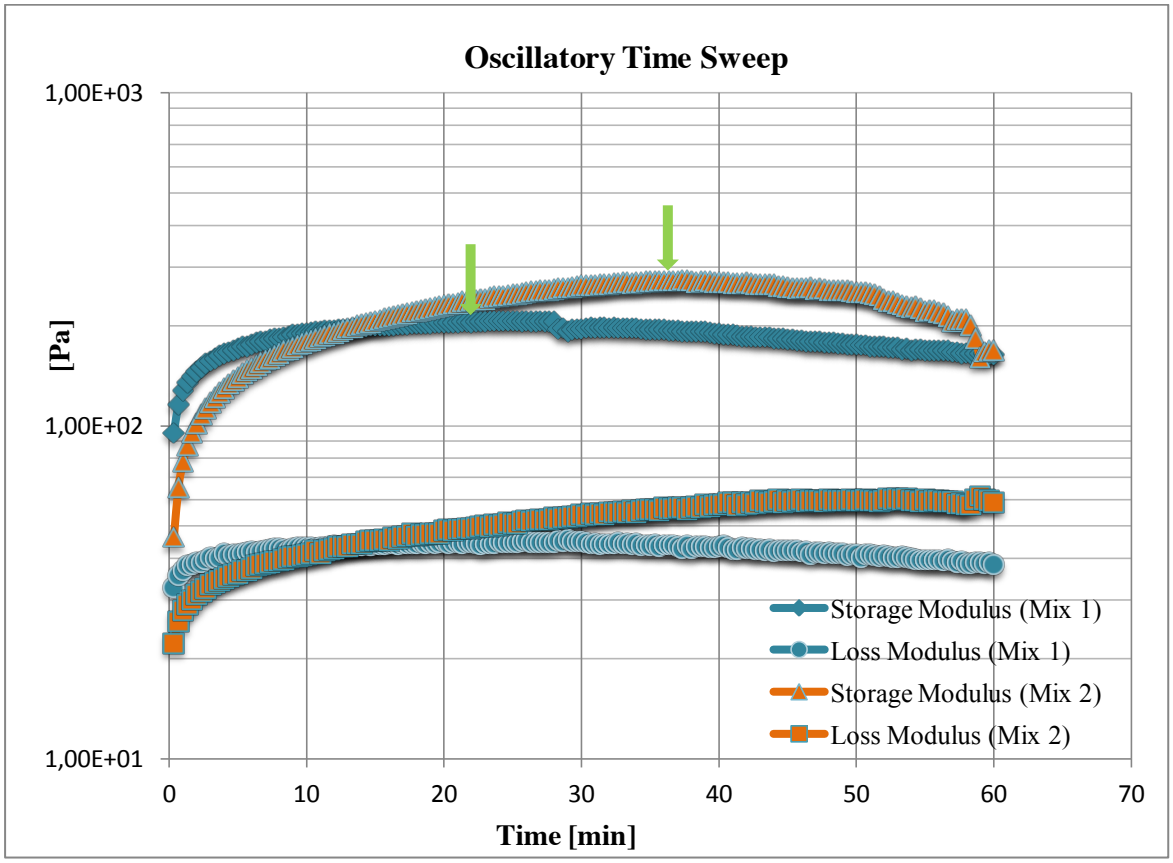

Figure 5-16: Oscillatory time sweep test. The green arrows points out the highest stable value of storage modulus.

Figure 5-17 shows the plot from the oscillatory temperature sweep test. This test was conducted by changing the temperature linearly from 4 – 80˚C. The heat rate was set to 0.009 ˚C/s. The strain and angular frequency were once again set to 0.01 % and 10 rad/s. As we can see from the graph, the OBDF01 has a higher storage modulus (G´) then loss modulus (G´´) in the intervals 4 – 35 ˚C and 48 – 80 ˚C. This can be interpreted as the fluid has an elastic property in these areas, while the response between 35 and 48 ˚C has a viscous property since the loss modulus is higher than the storage modulus in this area. The BaraECD has a similar development between 4 and 35 ˚C, but the storage modulus is higher than the loss modulus during the whole interval. A high increase in shear stress is observed for the BaraECD between 35 and 80˚C. The response between 4 and 40˚C is expected since drilling fluids tend to have high shear stress values at low temperatures and decreasing values as the temperature is increased. The response we see between 45 and 80 ˚C is unexpected for both fluids since the logic response would be a further decrease in shear stress values.

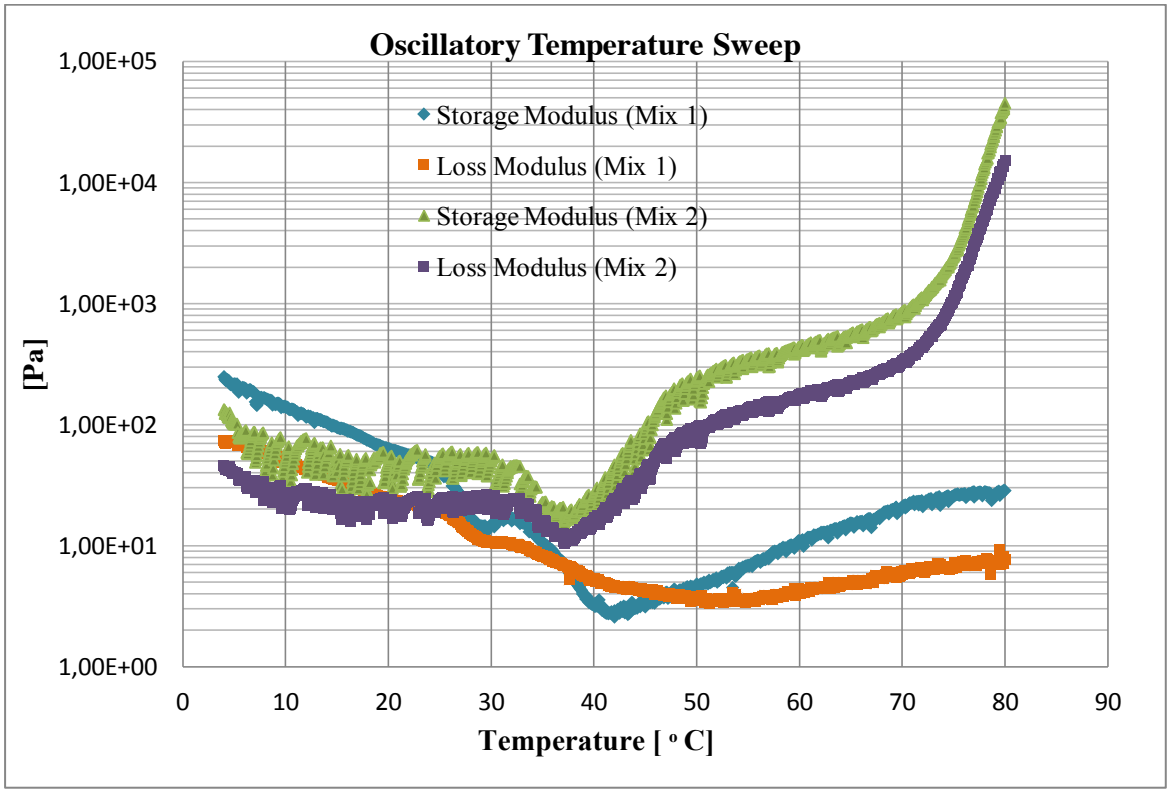

Figure 5-17: Oscillatory temperature sweep test.

5.2.5 Horizontal section sag test

The test was performed according to the procedure described in chapter 4. Due to air on the high side of the pipe it was not possible to make a density measurement here. As we can see from the results presented in table 5-10, there was a relatively small increase in density after the static time had passed. This is most likely due to the temperature which was stable at about 25˚C.

A video from the experiment can be found in the attachment.

Table 5-10: Horizontal section sag test results.

Test temperature	25˚C
Initial density of drilling fluid	1.599 S.G
Low side density after 60 min static	1.604 S.G
Low side density after applied shear	1.598 S.G

5.2.6 HOL vertical simulation

Pictures from the experiments can be found in Appendix B, and a video from experiment 2 can be found in the attachment.

Experiment 1

The inner diameter to length ration in this experiment was about 1:667, and it was therefore expected that the mixing zone would not cover the whole length of the pipe. The small ID pipes were considered to most likely be too small to freely transport the viscous drilling fluids. This was the case at some extent, but the fluids seemed to make an interface and mixed together without being too affected by the low ID and possible trapped air. The mixing zone was measured to be around 0.5 meters after a total of about 8 hours of mixing with the drill. This gives an ID to mixing zone ratio of 1:167. Because of the unknown effects from the small ID pipe, there was decided to conduct an experiment where a larger ID pipe would be used.

Experiment 2

The ID to length ratio in this experiment was 1:450. This was a bit less than in experiment #1, but should be sufficient to cover the whole mixing zone. The experiment was conducted in the same manner as experiment #1, but the drilling fluids seemed to flow much easier in this pipe due to the increased ID. As the heavy fluid flowed down the pipe and made an interface with the light fluid, some channeling could be observed. The mixing zone was more and more evenly distributed as time went by. After approximately 30 minutes, the “drill string” was inserted into the pipe and the rotation was set to 100 RPM. The interface and mixing zone was observed for about 30 minutes while the drill string rotated. The mixing zone seemed to reach a maximum after about 45 minutes from the start of the experiment. The length of the mixing zone was discussed and there was decided that the final mixing zone was around 3-4 meters long. This gives an ID to mixing zone ratio of 1:400 in a worst-case scenario.

6 Performance Simulation Study

The effect of the sag situation was further analyzed using simulations in the Landmark software Wellplan. The results from the layered static ageing test are used as basis for the simulations. This makes it possible to simulate torque and drag under different density scenarios.

6.1 Simulation arrangement

The simulations were partially based upon the horizontal section that is to be drilled in Brazil. The dimensions of the open hole section and the OD of the steel drill pipes are correct. Note that the drill string is not a DDS, and that the density is equal on the inside and outside of the drillstring. Hence, it is not possible to simulate a complete HOL scenario in Wellplan.

General Input

- Open hole section: 12 ¼”
- Drill Pipes: Conventional 6 5/8”, 25.20 lb/ft, E grade, FH connections
- Drill string elements to for a BHA
- Initial density for both OBDF01 and BaraECD: 1.60 SG
- Top, mid and bottom density values from layered static testing. See table 6-1:

Table 6-1: Table presenting the density values used in the simulation.

Fluid	Top Layer	Mid Layer	Bottom Layer
OBDF01	1.573	1.579	1.693
BaraECD	1.574	1.625	1.766

- Rheology
- WOB: 44.5 kN
- Torque at bit: 13.56 kNm
- RPM: 100 (tripping in and out)

Well Schematic

Figure 6-1 shows the well schematic of the simulated horizontal drilling operation:

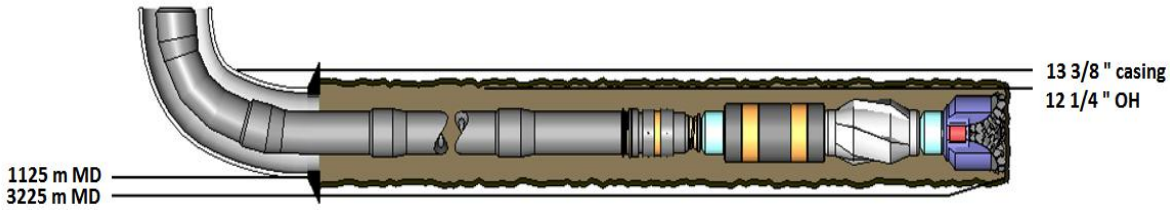

Figure 6-1: WellPlan well schematic, horizontal section.

String Editor

Table 6-2 shows the selected drill string components used in the simulations:

Table 6-2: String editor table from WellPlan software.

	Section Type	Length (ft)	Measured Depth (ft)	OD (in)	ID (in)	Weight (ppf)	Item Description
1	Drill Pipe	10022,00	10022,0	6,625	5,965	27,15	Drill Pipe 6 5/8 in, 25.20 ppf, E, FH, P
2	Heavy Weight	120,00	10142,0	6,625	4,500	70,50	Heavy Weight Drill Pipe Grant Prideco, 6 5/8 in, 70.50 ppf
3	Jar	32,00	10174,0	6,500	2,750	91,79	Hydraulic Jar Dailey Hyd., 6 1/2 in
4	Heavy Weight	305,00	10479,0	5,000	3,000	49,70	Heavy Weight Drill Pipe Grant Prideco, 5 in, 49.70 ppf
5	Sub	5,00	10484,0	6,000	2,400	79,51	Bit Sub 6, 6 x2 1/2 in
6	MWD	85,00	10569,0	8,000	2,500	154,36	MWD Tool 8 , 8 x2 1/2 in
7	Stabilizer	5,00	10574,0	6,250	2,000	93,72	Integral Blade Stabilizer 8 1/2" FG, 6 1/4 x2 in
8	Sub	5,00	10579,0	6,000	2,400	79,51	Bit Sub 6, 6 x2 1/2 in
9	Bit	1,00	10580,0	10,625		166,00	Tri-Cone Bit, 0,589 in²

Hole Section Editor

Table 6-3 shows the selected hole section parameters such as length, ID, capacity and friction:

Table 6-3: Hole section editor from WellPlan software.

	Section Type	Measured Depth (ft)	Length (ft)	Tapered?	Shoe Measured Depth (ft)	ID (in)	Drift (in)	Effective Hole Diameter (in)	Friction Factor	Linear Capacity (bbl/ft)	Excess (%)	Item Description
1	Casing	4012,5	4012,50	☐	4012,5	12,250	12,459	12,615	0,25	0,1458		13 3/8 in, 54.5 ppf, J-55,
2	Open Hole	10580,0	6567,50	☐		12,250		12,250	0,30	0,1458	0,00	

Fluid Editor

Figure 6-2 shows the WellPlan Fluid Editor, where the density and rheology values from each layer was inserted:

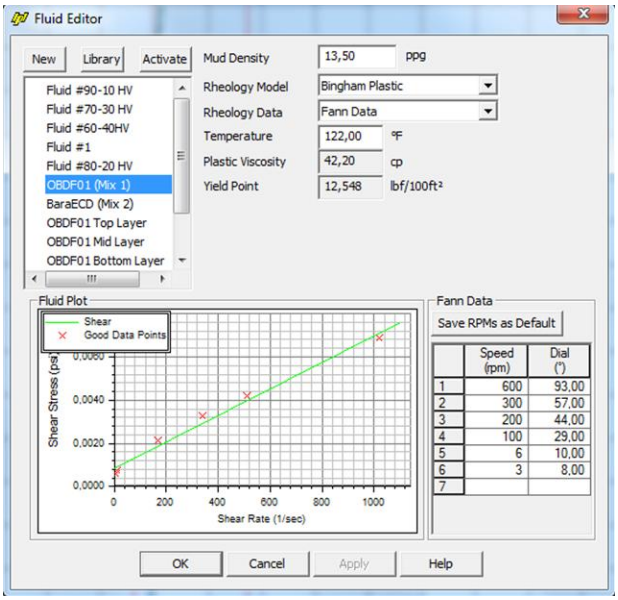

Figure 6-2: WellPlan Fluid Editor.

Mode Data – Normal Analysis

Figure 6-3 shows the Mode Data and selected drilling and tripping parameters:

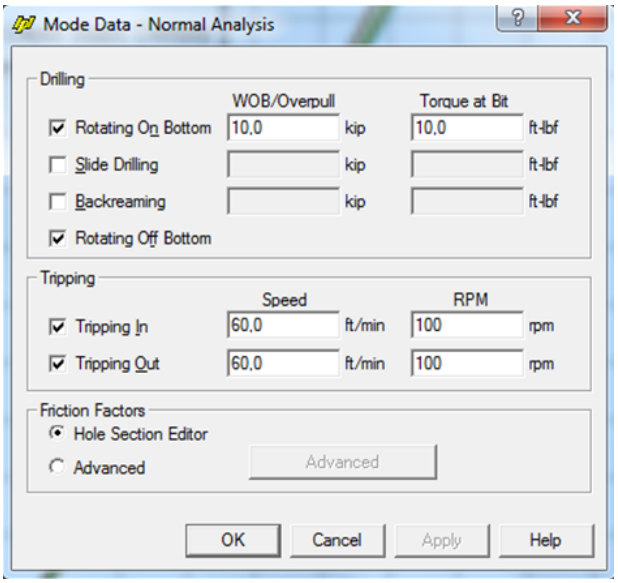

Figure 6-3: WellPlan Normal Mode Analysis.

6.2 Simulation of torque

Figure 6-4 shows that all the torque values are under the torque limit. This indicates that the given scenarios are safe.

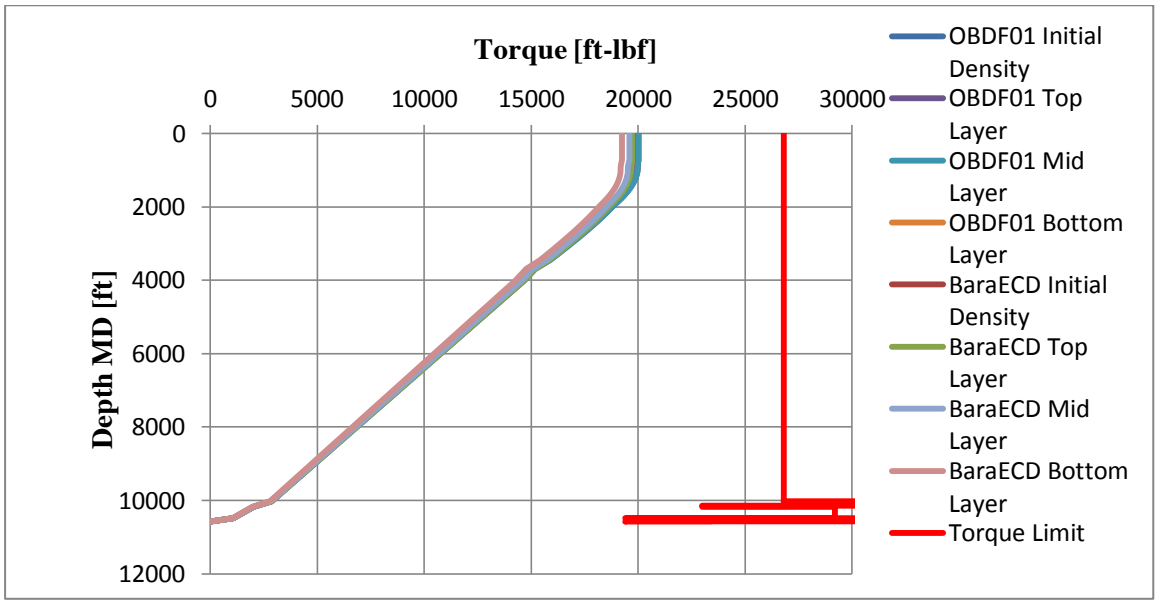

Figure 6-4: Plot of the torque effect on different drilling fluid densities.

Figure 6-5 shows a chart presenting the maximum values of torque. These were recorded at ground level (0 m MD). As we can see from the chart, the torque values are decreasing as the density is increasing, thus increasing the buoyancy force on the drill string.

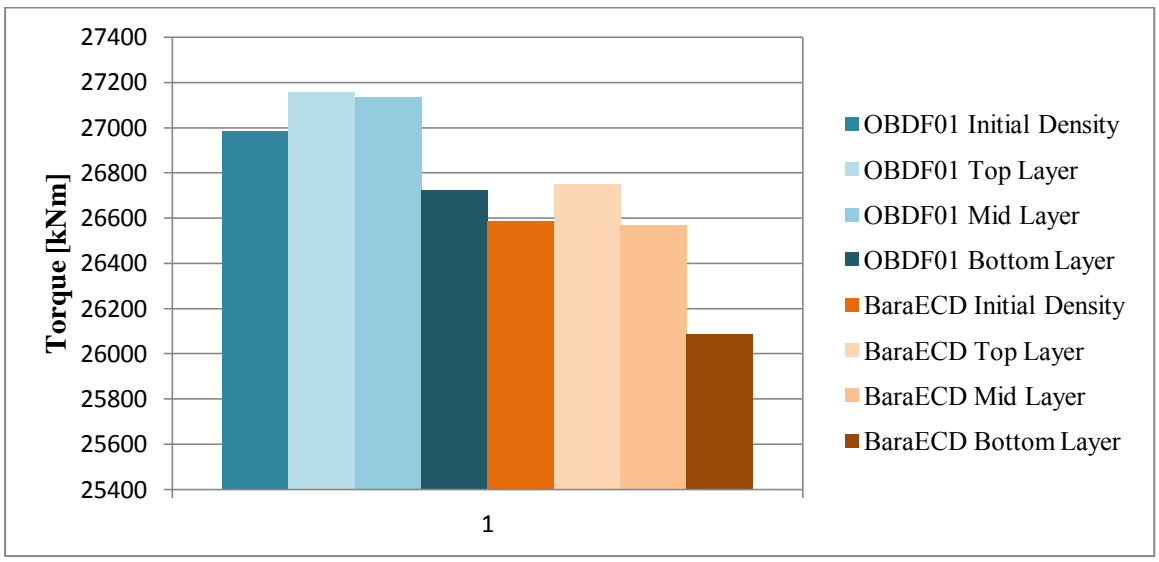

Figure 6-5: Chart presenting the maximum values of torque (taken at 0 m MD).

6.3 Simulation of drag

Figure 6-6 shows that all the tension (drag) values are between the tension and buckling limit. This indicates that the given scenarios are safe. The maximum values were recorded at ground level (0 m MD).

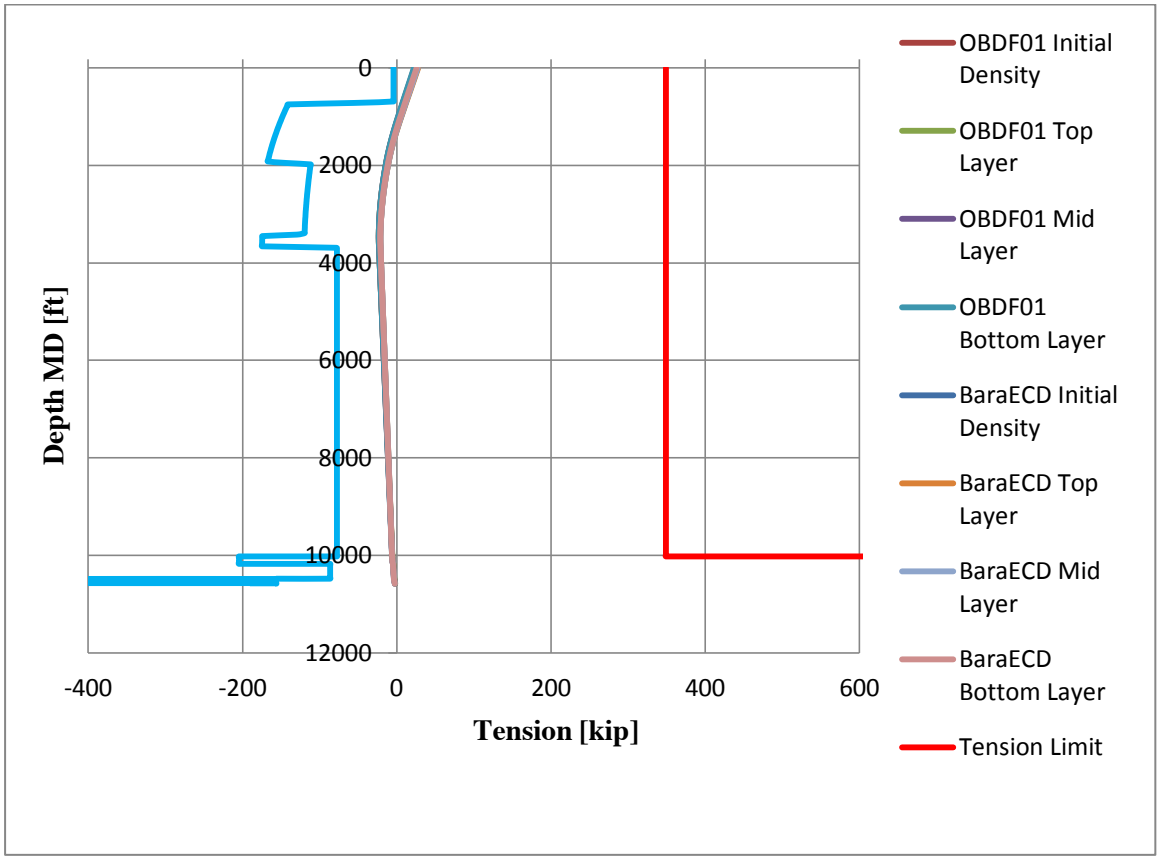

Figure 6-6: Plot of the drag effect on different drilling fluid densities.

Figure 6-7 illustrates the same development that was seen in the torque simulation. As the density is increasing down the ageing cell or height of a horizontal wellbore, the drag force is decreasing. This is again due to the increased buoyancy force on the drill string.

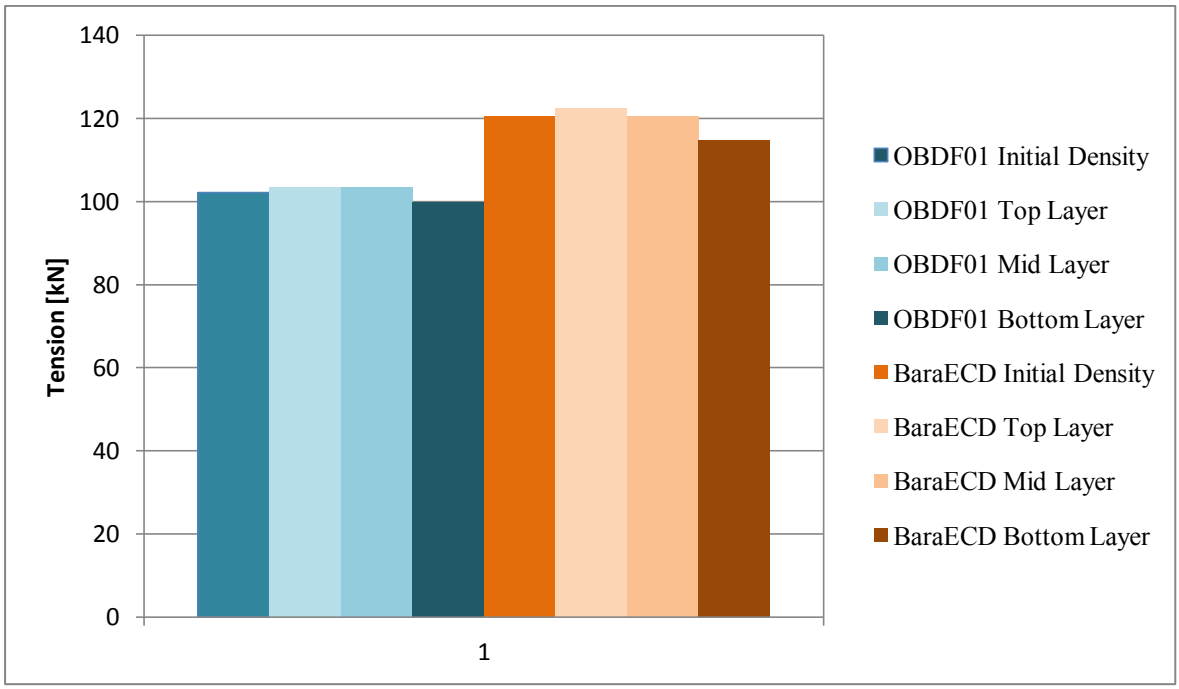

Figure 6-7: Chart presenting the maximum values of drag (taken at 0 m MD).

Given the RDM scenario, the active drilling fluid on the inside will be equal or have a lower density than the passive fluid on the outside. This will further increase the buoyancy force of the drill string and make the torque and drag values above further decrease.

7 Discussion

The conventional testing was conducted at the Halliburton Fluids Laboratory where calibrated equipment was used and standardized working methods were followed. Such an environment gives less room for error since this laboratory is working to provide correct data for real well operations. Oil-service laboratories are also having regularly audits where procedures and the overall working environment are assessed. The creative testing at the University of Stavanger was as the name states conducted in a less standardized and controlled environment. This gives room for more error, but also the opportunity to find new and interesting ways to analyze and solve challenges.

7.1 Conventional testing

The conventional testing started out with rheology measurements at 50˚C. The results showed that the OBDF01 had an overall higher viscosity than the BaraECD. This is most likely due to the difference in components and that the OWR is different in the two fluids. The OBDF01 had an almost similar viscosity at age #0 and age #1, this shows that the fluid was not particularly affected by the temperature effect during the 16 hours of static ageing. As expected, the viscosity curve was a bit lower after 72 hours, but still considered stable. The BaraECD on the other hand showed a larger difference in viscosity between age #0 and age #1. This is due to the fact that the components used in this fluid needs 16 hours of hot rolling (dynamic ageing) to be activated. Note that the BaraECD has the desired property of having high shear stress values at low shear rates and low shear stress values at high shear rates. This makes the fluid good in relation to sag where the problem often occurs at low shear rates. In addition, the fluid will be easier to pump at high velocities.

The gel strength had the same development as the rheology with decreasing values as the hours of ageing increased. At age #0 the OBDF01 had the highest increase in gel strength from 10 seconds to 10 minutes, while the BaraECD had the highest increase at the other ageings. This is again due to the components in the BaraECD not being activated before after the hot rolling. The advantage of a high and rapid increase in gel strength is to quickly make a gel structure stable and strong enough to hold the particles in suspension when the circulation stops.

As seen from the result analysis chapter, the BaraECD had much higher ES values than the OBDF01. According to the specifications provided by Petrobras, the ES values should be above 200 V. Both fluids fulfill this requirement at all ageing, but the OBDF01 fluid is considered to have relatively poor emulsion stability with ES values ranging from 225 to 420 V. The high ES values in the BaraECD is most likely due to the micronized weight particles that have both an oil-wet surface and a much lower PSD, making it possible to disperse the brine droplets into a fine structure. Another reason can be that there was used a different emulsifier in the BaraECD, which may be more effective in reducing the interfacial tension. In addition it can be noted that the OWR was different in the two mixes, making this a possible reason for the differences. Since the mechanical shearing of the fluids is of great importance for creating a stable emulsion, it can also be noted that there are used two different mixers when preparing the fluids. Hence, the geometry of the mixing head and rotational speed was different.

To evaluate the static sag potential through the standardized tests it is important to look at both free fluid, sag factor and sag index. On age #1, the free fluid and sag factor was the same for both fluids. The sag index was a bit higher on the BaraECD. This shows that this fluid has a bit more static sag relative to the initial mud density. On age #2, there was about 50 % more free fluid in the BaraECD than in the OBDF01. The sag factor and index were also a bit higher in the BaraECD. The BaraECD gave an indication of having overall higher static sag than the OBDF01.

The dynamic sag test indicated that the BaraECD has a much lower sag potential under dynamic conditions. At age #1, the BaraECD had an increase in density of about 3%, while the OBDF01 had an increase of about 18%. At age #2, the development was a little unexpected with lower values than on age #1. To give an impression of the fluids ability to remove a particle bed, the additional BPU test was run. The test showed that the OBDF01 has a higher pickup ratio than the BaraECD. This is most likely due to the significant amount of particles in the collection well that is so close to the rotating sleeve that they easily can be set in motion and back into suspension. The few BaraECD particles in the bottom of the collection well is therefore more difficult to pick up, hence making the pickup ratio lower.

7.2 Creative testing

The creative part of the testing was started by conducting NMR measurements on the two fluids. The sample tubes were statically aged for the same amount of hours and at the same temperature as the standardized static test to provide a similar base of investigation. The NMR results showed clear indications of particle sagging, displayed by strong signal attenuation where the particles had settled. This way of using NMR technology has as mentioned earlier been used under previous investigations, but is as far as the author is aware of not been implemented as a test method in the oil service industry. This way of non-invasive testing has a great potential to be further developed and to be brought offshore as a standardized field test. By combining conventional static testing with NMR measurements, it may be possible to make the NMR signal correspond directly to density values. This will require extended research to determine all the factors affecting the NMR signal.

The layered static ageing test was conducted according to the standardized work method, except that the density was measured at seven layers instead of three. This gave a much more detailed picture of the density profile in the cell, which is an analogue to how a profile can be in a horizontal section after 72 hours of static sag. The results showed that the OBDF01 had a more smooth transition in density layers down the cell, than the BaraECD.

The solid settling test was conducted to see how the particles settled vertically onto an object near the bottom of a cup. The results showed an increased weight with time in the OBDF01, while the opposite was the case for the BaraECD. The temperature plays a great role in this type of experiment by affecting the gel strength. The gel strength in the BaraECD has as seen from the other tests showed high values at low temperatures. This may be seen as the weight is decreasing during the experiment. Another reason can be that the falling particles created increased buoyancy, making the objects effective weight decrease. The same phenomenon can be seen in the OBDF01 from 60 to 120 minutes of static time.

The viscoelasticity measurements were conducted using an Anton Paar rheometer. The Anton Paar instruments is known for having a high accuracy and be the preferred company for delivering high-grade equipment to leading laboratories studying viscoelasticity. The results from the amplitude sweep test showed that both fluids had gel like behavior in the LVE range and a stability or firmness in the low shear range. The frequency sweep test showed that the fluids deformation response is dominated by an elastic behavior. This is again a strong indication of a stable gel structure and that the fluids can be considered to be viscoelastic. The time sweep test was run to see how the fluids gel structure developed over time. As seen from the results, the OBDF01 reached a stable value at about 23 minutes, while the BaraECD became stable at around 37 minutes. This indicates that the standardized test using a 30 minute gel strength measurement is not enough to fully display the gel strength potential of a fluid like the BaraECD. There is observed a decrease in storage modulus for both fluids after some time. This can be due to particles settling in the sample or a relaxation of the gel structure. The temperature sweep test was run in order to study the development of viscoelastic behavior as the temperature was increased. At low temperatures, the storage modulus was as expected high for both fluids. The reason for choosing the temperature sweep to start as low as 4 ˚C is to see how the fluid may behave in an arctic environment. The challenges around arctic drilling does definitely include drilling fluids and how to keep the viscosity low enough to keep the fluids circulating without the need for extreme pump pressures. Both fluids had as expected decreasing storage modulus as the temperature increased. This was the case until 35 ˚C was reached, then the BaraECD started to strongly increase in storage and loss modulus towards the end temperature of 80 ˚C. This was also the case for the OBDF01, starting an increase at around 40 ˚C. The reason for this can be the complex components in the fluids and that the rheological properties of each component can change differently and independently of each other.

The horizontal section sag test was conducted as an analogue to the situation found in a real well. The dimensions of the pipes were scaled equal to the real casing and drill pipe diameters. The test showed a relatively small increase in density after the static time had passed. This is most likely due to the rig being set in room temperature, hence the fluid had a temperature of about 25 ˚C. The gel strength at this temperature is as seen from the other results high enough to keep the weight particles in suspension. The rotating “drill string” made the few particles on the bottom to be set back into suspension.

The HOL vertical simulation was developed as an additional objective during the work with this thesis. The experiments were conducted in both small and medium scale. This was done to first check that the fluids behaved as expected before going over to more "correct" dimensions relative to the fluids viscosity. In experiment 1, the mixing zone was measured to be around 0.5 m after 8 hours of "drill string" rotation. This gave an ID to mixing zone ratio of 1:167. Experiment 2 showed a mixing zone of 3-4 meters. This gave an ID to mixing zone ratio of 1:400 in a worst case scenario. Since the dimensions in experiment 2 were considered to be more correct relative to the fluids viscosity, the ratio 1:400 seems like the best estimate. If this value had been applied to a well with ID = 8.5 inches, the mixing zone would have been around 90 meters. This is considered to be acceptable for the HOL principle, taking into account that very long sections are drilled using this method. A future testing method to be performed in relation to the HOL principle could be to create a rig with several pressure points along the wellbore. This is a more advanced and time consuming test method to develop, but will be very accurate in displaying the density distribution. There is also important to make a setup that can keep the fluids at a minimum of 50˚C to make it a realistic scenario. The temperatures that can be encountered in future HOL drilling operations can go into the HPHT regime, with temperatures above 150˚C.

7.3 Sag in horizontal sections

To give Reelwell an indication of the sag situation in a horizontal section, it is of great importance to make an illustration of the challenges and complexity of the matter and to present a summary of the most important results found during the investigations. Figure 7-1 presents the two effects that are considered to be most relevant. The fluid is affected by both drill string movement and rotation during drilling. In addition, the fluid movement may be both stopped and reduced. This gives the opportunity for dynamic and static sag potential. The weight particles follows the curvature of the casing or wellbore and forms a bed on the low side. The bed formation may provide an additional friction force against lateral movement of the drill pipe. Note that if the weight particles have a lower friction factor against the pipe than the friction factor between the wellbore and pipe, the torque effect may be reduced. The other effect created by the falling particles is that an uneven density distribution will be created over the diameter (height) of the casing or wellbore. The increased density of the surrounding fluid will reduce the effective weight of the immersed drill pipe. This can further reduce the torque and drag effects, as seen from the simulations in chapter 6.

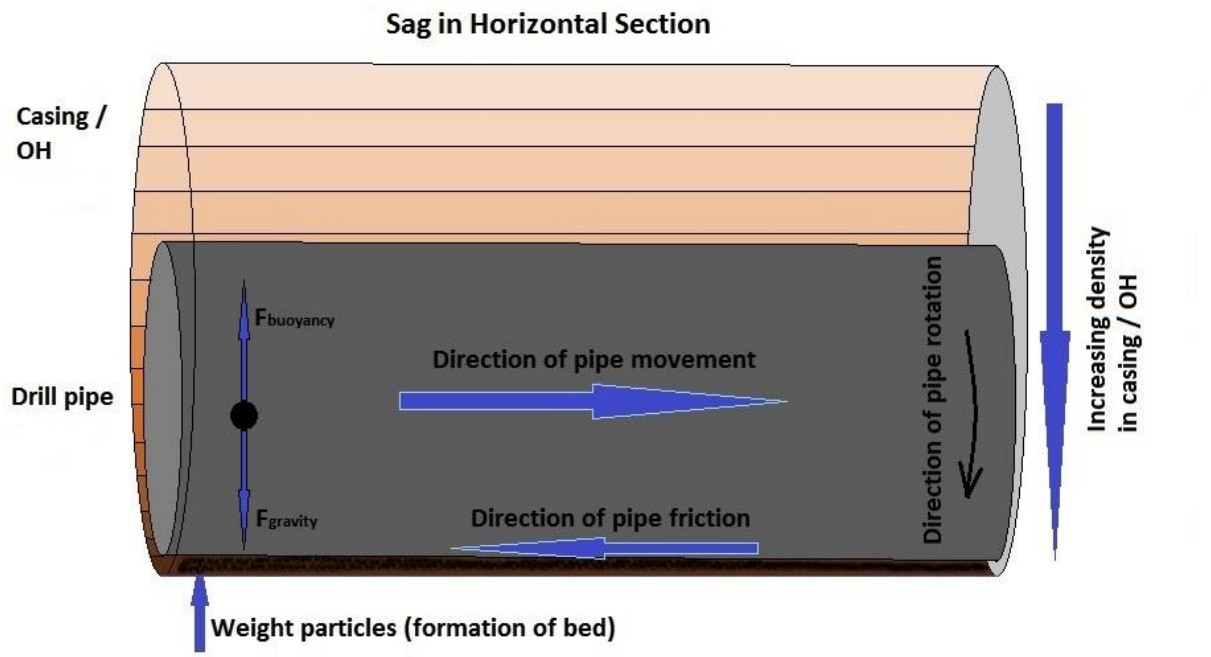

Figure 7-1: Illustration of the dynamic sag challenge in a horizontal section. [F2]

Static sag – buoyancy effect

Taking the scenario of a 72 hour operational stop, the buoyancy factor can be calculated at each level in the wellbore height using the data found in the layered static sag test. In this example, there is used a 12 ¼" open hole section as outer tubular and a 5 7/8" aluminum drill pipe as inner tubular. This is also the dimensions of the horizontal section in the Brazil well (see Appendix C). The mud density on the inside of the drill pipe is 1.10 SG.

Case data is presented in table 7-1:

Table 7-1: Buoyancy calculation data.

Open Hole	Drill Pipe	Inner OH radius	Inner DP radius	Mud density inside	Initial mud density outside	Aluminum density
12 1/4"	5 7/8"	6.125"	2.523"	1.10 SG	1.60 SG	2.70 SG

Example of calculation using equation 5 from chapter 3.6:

$$\beta = 1 - \frac{\rho_o r_o^2 - \rho_i r_i^2}{\rho_{pipe}(r_o^2 - r_i^2)} = 1 - \frac{1.60 * 6.125^2 - 1.10 * 2{,}523^2}{2.70 * (6.125^2 - 2.523^2)} = 0.370$$

By using equation 5 we have the following buoyancy factors for the two fluids in an ideal situation with an even distribution of weight material:

Table 7-2: Reference data of buoyancy calculations.

OBDF01 density	BaraECD density	Buoyancy factor OBDF01	Buoyancy factor BaraECD
1.60 SG	1.60 SG	0.370	0.370

By using the density values obtained from the 72 hour layered static test, the buoyancy factor at each layer can be calculated as shown in table 7-3. See figure figure 7-2 for an illustration of the scenario.

Table 7-3: Layered buoyancy calculations, 72 hour static situation at 110˚C.

Layer #	OBDF01 SG	BaraECD SG	Buoyancy factor OBDF01	Buoyancy factor BaraECD
1	1.573	1.574	0.382	0.381
2	1.575	1.616	0.381	0.362
3	1.577	1.62	0.380	0.361
4	1.579	1.625	0.379	0.358
5	1.586	1.642	0.376	0.351
6	1.608	1.66	0.366	0.343
7	1.693	1.766	0.328	0.296

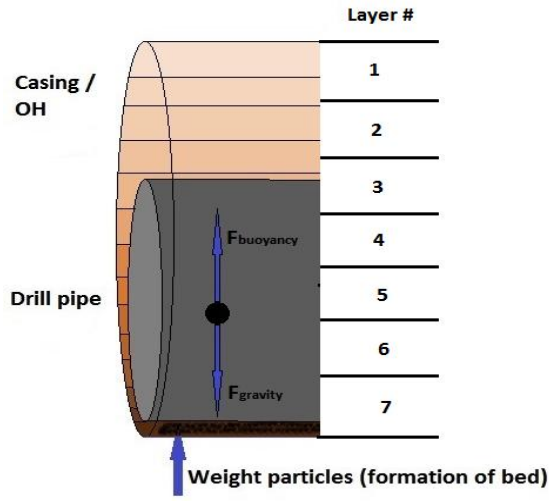

Figure 7-2: Illustration of the layers in a wellbore. [F2]

By choosing layer 6 as the layer that is at the center of the drill pipe diameter, we can compare this situation to the non-sag situation:

Table 7-4: Comparing static sag and ideal buoyancy factor.

Ideal buoyancy factor OBDF01	Ideal buoyancy factor BaraECD	Static sag buoyancy factor OBDF01	Static sag buoyancy factor BaraECD	Change in buoyancy factor OBDF01	Change in buoyancy factor BaraECD	Percentage change in buoyancy factor OBDF01	Percentage change in buoyancy factor BaraECD
0.370	0.370	0.366	0.343	0.004	0.027	1.10 %	7.30 %

As we can see from table 7-4, the BaraECD has about 6 % higher decrease in buoyancy factor (i.e. increase in buoyancy force) then the OBDF01 assuming a static sag scenario. Note that by choosing a mid layer it is assumed that the distribution is even over the drill pipe diameter (height). For simplicity, the tool joints are neglected in these calculations.

Dynamic sag – buoyancy effect

By using the results obtained from the dynamic sag shoe test, one can estimate the buoyancy effect after 30 min of rotation at 100 RPM and 50 ˚C. Note that the fluids were aged static for 72 hours at 110 ˚C prior to running the VSST test. The measured density in the collection well will correspond to the bottom layer of the layered static test. Case data is the same as in the static sag calculation.

Equation 5 gives the following buoyancy factors under dynamic conditions:

Table 7-5: Dynamic sag buoyancy calculations.

OBDF01 density	BaraECD density	OBDF01 –VSST density increase	BaraECD –VSST density increase	OBDF01 dynamic bottom layer density	BaraECD dynamic bottom layer density	Buoyancy factor OBDF01	Buoyancy factor BaraECD
1.60 SG	1.60 SG	0.267 SG	0.042	1.867	1.642	0.250	0.351

Comparing the ideal situation to the dynamic sag situation gives:

Table 7-6: Comparing of dynamic sag and ideal buoyancy factor.

Ideal buoyancy factor OBDF01	Ideal buoyancy factor BaraECD	Dynamic sag buoyancy factor OBDF01	Dynamic sag buoyancy factor BaraECD	Change in buoyancy factor OBDF01	Change in buoyancy factor BaraECD	Percentage change in buoyancy factor OBDF01	Percentage change in buoyancy factor BaraECD
0.370	0.370	0.250	0.351	0.12	0.019	32.43 %	5.14 %

As we can see from table 7-6, the OBDF01 has about 27 % higher decrease in buoyancy factor (i.e. increase in buoyancy force) than the BaraECD under dynamic conditions. Note that the fluid density is taken at the bottom layer instead of at the center of the drill pipe as in the static sag example. This gives a higher buoyancy force then what can be expected.

As we can see from the buoyancy case presented, the buoyancy factors are affected by the weight particle sagging. The Wellplan simulations showed that the torque and drag effects were affected by the different density values. The simulations showed that the torque and drag values were inside the limit envelope, indicating that the scenarios were safe. The simulations did not take into account the use of a lighter fluid inside the drill string, which would have increased the buoyancy force even more. The question is therefore if the increased buoyancy force of the drill string weighs up for the possible change in friction on the low side of the wellbore. To answer this question, there is a need for extensive investigations. An interesting experiment could be to use a down-scaled moving and rotating drill string that is connected to an instrument measuring the force of torque and drag. The test should be run in both a high and low sag-potential fluid to see the differences in friction force.

Summary

Taking into consideration the various testing performed in this thesis and the scenarios that is most likely to occur in a real drilling operation, it seems preferable to use a modern drilling fluid like the BaraECD. A situation where we have a 72 hour stop in fluid circulation is less likely than a situation where we experience dynamic sag. As the static ageing and NMR testing indicated, there is not a problem to leave the fluid static for 16 hours, but this can be considered as a maximum to ensure an even distribution of weight particles. The BaraECD has shown to be a suitable alternative for the RDM with its micronized weight particles, high low-end and low high-end viscosity. The fluid has in addition shown high ES values, making it durable in keeping good emulsion stability. The low ES values indicate that the OBDF01 fluid doesn't have a durable emulsion stability, which again makes it more unstable as it is exposed to heat over time. This can also be one of the main reasons why it showed such high dynamic sag potential. A way of treating the OBDF01 to become usable for these applications can be to increase the concentration of emulsifier, hence making the emulsion more stable.

7.4 Maintenance of HOL density profile

The author was asked to come up with ideas around how to handle the fluid which has been part of the fluid interface, thus has a density value between the light and the heavy fluid. First of all it is an advantage to use the same type of fluid as both the light and heavy fluid. The components will be the same in the two fluids, only the concentrations will be different. Having one set of components will also make the logistics a lot easier. As the light fluid is circulating, it will be in contact with the heavy fluid and increase in density with time. The heavy fluid is not circulated, but will be mixed with the light fluid in the HOL interface when the drill string rotates. This gives an overall reduction in density over time. This does not need to be a problem in relation to maintaining the well pressure. Since the two fluids are compatible and miscible, there will be a smooth and even transition of hydrostatic pressure. When there is a need for reducing the mud weight, this can be done by diluting the fluid with base oil and/or brine. In the opposite situation, more weighting agent is added to increase the density. This shows once again that it is a great benefit having only one set of components. In such an operation, there is also a need for having enough backup of components. In order to make this type of operation as effective as possible, there could have been developed an automatic density controller. Such an instrument could have measured the density of the fluid and either sent the fluid further into another circulation or sent it to a modifier-tank where either diluting agent or weighting agent can be added and mixed. See figure 7-3 for how a possible setup can look like. Note that the returning drilling fluid must be sent through treatment such as shale shakers etc. before entering the “density control unit”. A key point when adjusting a drilling fluids density is to keep the emulsion stability high. This is possible by adding the agents regularly in small portions instead of now and then in big portions. This way, the fluid density will be kept seamlessly stable during the drilling operation.

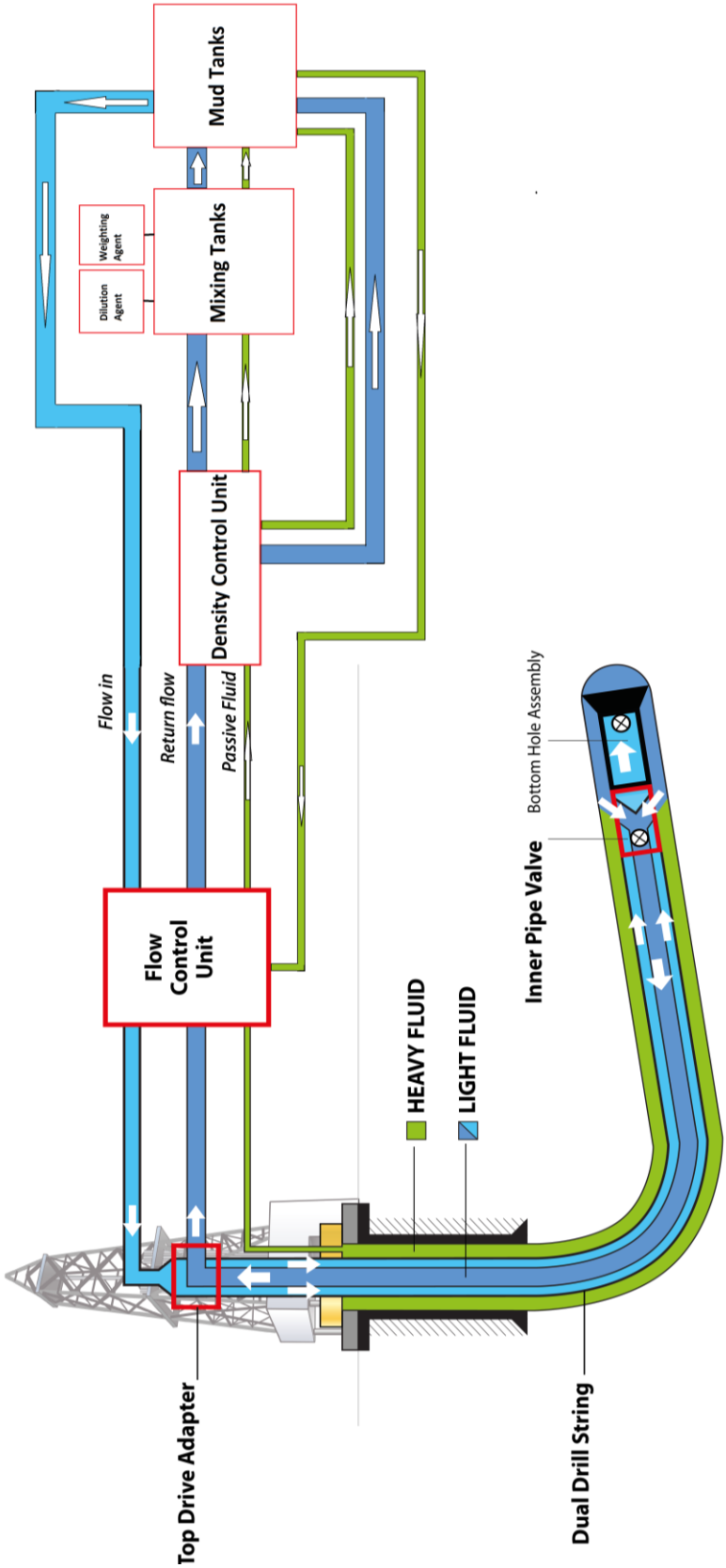

Figure 7-3: A modified HOL rig setup. [F1, F2]

8 Conclusion

The conventional testing provided the following main discoveries:

- The BaraECD (Mix 2) showed a high and rapid increase in gel strength in addition to a high low-end and low high-end viscosity
- The static sag was 6 % higher in the BaraECD (Mix 2) than in the OBDF01 (Mix 1), considering the bottom layer density after 72 hour static ageing
- The dynamic sag was 14 % higher in OBDF01 (Mix 1) than in the BaraECD (Mix 2), considering the VSST after 72 hour static ageing

The creative testing provided the following main discoveries:

- The NMR testing showed that the 1D profiling can be used to determine fluid sag
- The viscoelasticity testing indicated that the drilling fluids have viscoelastic behavior
- The time sweep test showed that the OBDF01 (Mix 1) reached a stable gel strength after 23 minutes, while the BaraECD became stable at about 37 minutes. This indicates that the conventional 30 minute gel strength measurement is not sufficient to fully display such a fluids gel strength potential
- Both fluids showed a radical increase in both storage and loss modulus, when the temperature was increased from 35 to 80˚C
- The HOL vertical simulation experiments indicated that the length of the mixing zone stabilize below 400 x ID of the well for the small scale test arrangement

The testing showed that sag creates a changed density distribution over the height (diameter) of a wellbore or casing in a horizontal section. The Wellplan simulations and buoyancy calculations showed that sag can be beneficial by increasing drill string buoyancy and thereby reduce torque and drag.

The conventional OBDF01 fluid showed lower ES values and larger variations in dynamic sag, than the modern BaraECD fluid. The modern fluid may therefore be preferred for these applications.

Monitoring the density of the light and heavy fluid will be of great importance during a HOL operation. The rig equipment can be developed to contain a density control unit and a density adjustment unit to make sure that the density of the fluids is seamlessly controlled and adjusted.

9 References

[Citation style: IEEE]

Theory

[T1] T. Omland, ”Particles Settling in Non-Newtonian Drilling Fluids,” Ph.D. dissertation, UiS, Stavanger, Norway, 2009.

[T2] P. Scott, M. Zamora and C. Aldea, “Barite-Sag Management: Challenges, Strategies, Opportunities,” SPE 87136, SPE/IADC, Dallas, Texas, U.S.A, 2004.

[T3] P. Bern, M. Slater and K. Hearn, “The Influence of Drilling Variables on Barite Sag,” SPE 36670, SPE, Denver, Colorado, U.S.A, 1996.

[T4] M. Zamora, “Mechanisms, Measurement and Mitigation of Barite Sag,” OMC-2009-105, Ravenna, Italy, 2009.

[T5] Encyclopedia Britannica, “Stokes's law | physics”, 2014. [Online]. Available: http://global.britannica.com/EBchecked/topic/567002/Stokess-law. [Accessed: 20- Apr- 2015].

[T6] Sam-marsh.staff.shef.ac.uk, “Newton`s Laws, 2015. [Online]. Available: http://sam-marsh.staff.shef.ac.uk/mas115/docs/week10lab.html. [Accessed: 10- Mar- 2015].

[T7] B. Aadnøy, I. Cooper, S. Miska, R. Mitchell and M. Payne, *Advanced Drilling and Well Technology*. Richardson, TX: Society of Petroleum Engineers, 2009.

[T8] R. Clark, “Understanding Rheology,” CP Kelco presentation, San Diego R&D, 2011.

[T9] H. Hodne, *Forelesningsnotater i Bore- og Brønnvæsker*, UiS, Stavanger, Norway, 2013.

[T10] P. Skalle, *Drilling Fluid Engineering*, Trondheim: Ventus Publishing ApS, 2012.

[T11] B. Bui, ”Viscoelastic Properties of Oil Based Drilling Fluids,” Annual Transactions of the Nordic Rheology Society, 20, 2012.

[T12] I. Sandvold, ”Gel Evolution in Oil Based Drilling Fluids,” M.S. thesis, NTNU, Trondheim, Norway, 2012.

[T13] R. Rismanto, ”Explorative Study of NMR Drilling Fluids Measurement,” M.S. thesis, UiS, Stavanger, Norway, 2006.

[T14] G. Coates, L. Xiao and M. Prammer, "NMR Physics," in *NMR Logging Principles & Applications*, Houston, TX: Halliburton Energy Services Publication, 1999, pp. 33-43.

[T15] T. Mezger, *The Rheology Handbook*, Hanover: European Coating Tech Files, 2011.

[T16] T. Hemphill, "Yield-Power Law Model More Accurately Predicts Mud Rheology," Oil & Gas Journal 91, no. 34, 1993.

[T17] E. Kaarstad, "Theory and Application of Buoyancy in Wells," Modern Applied Science 5, no. 3, 2011.

Reelwell

[R1] Reelwell, Internal documents, Feb 2015.

[R2] e. Systems, "Description / Technology / Home – www.reelwell.no", Reelwell.com, 2015. [Online]. Available: http://reelwell.com/Technology/Description. [Accessed: 28-Apr- 2015].

Halliburton

[H1] Halliburton, Internal documents, Mar 2015.

Figures

[F1] Reelwell, Internal figures, May 2015.
[F2] Magne Hurum, Drawn figures, Mar – May 2015.
[F3] Magne Hurum, Drawn figures based on figures from [T14], Apr 2015.
[F4] Magne Hurum, Drawn figures based on figures from [T15], May 2015.

Pictures

[P1] Magne Hurum, Personal pictures, Feb – May 2015.

Appendix A Work Methods

Halliburton OBDF01 mixing

Equipment:

- Silverson L4RT-A laboratory mixer
- Analytical balance
- Mixing jug
- Spoon
- Spatula
- Water bath
- Thermometer

The rotation was set to 6000 RPM. The mixing jug was placed in a water bath to keep the temperature between 50 and 62˚C in order to prevent the fluid agents from degenerating.

Procedure:

1. Place the mixing jug on the analytical balance and weigh up the correct amount of mineral oil.
2. Weigh up emulsifier, filtration control agent and viscosifier. Add them to the mixing jug in the correct order and let them mix for the predefined number of minutes.
3. Weigh up lime. Add it to the mixing jug and mix for 5 minutes.
4. Place the mixing jug in a water bath to control the mixing temperature.
5. Weigh up $CaCl_2$ brine. Add it to the mixing jug and mix for 15 minutes.
6. Weigh up the weighting material. Add it to the mixing jug and mix for 15 minutes.

Picture 1: Mixing of OBDF01. [P1]

Halliburton BaraECD mixing

Equipment:

- Fann Multi-Mixer Model 9B
- Mixing cups
- Analytical balance
- Spoon
- Spatula
- Thermometer

Procedure:

1. Weigh up base oil in the mixing cup, using the analytical balance.
2. Weigh up emulsifiers, lime and $CaCl_2$ brine. Add them to the mixing cup while it is agitated on the multi-mixer. Make sure to add them in the right order and for the pre defined number of minutes.
3. Weigh up viscosifiers, bridging agent and filtration control agent. Add them to the mixing cup in the right order and mix for 5 minutes each.
4. Weigh up weighting material. Add it to the mixing cup and mix for 15 minutes.

Picture 2: Mixing of BaraECD. [P1

Picture 3: BaraECD chemicals. [P1]

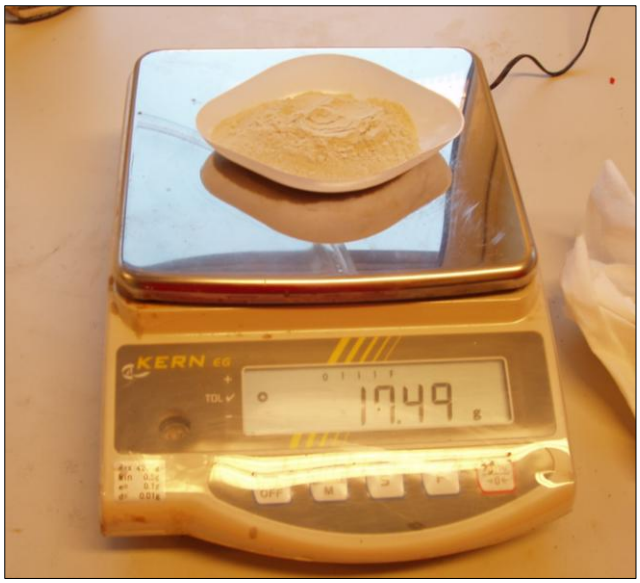

Picture 4: Kern analytical balance. [P1]

Rheology

Equipment:

- Fann Viscometer Model 35 SA
- Fann Thermo cup
- Timer
- Thermometer

Procedure:

1. Place a sample of drilling fluid in a thermo cup and immerse the viscometer sleeve to the scribed line. The test should be conducted at the standard 50 ± 1 °C (120 ± 1 °F) or other specified temperatures.
2. Heat or cool the sample to the correct temperature while the sleeve is rotating at 600 RPM. Record the temperature of the sample.
3. While the sleeve is rotating at 600 RPM, wait for the dial reading to reach a steady value. Record the dial reading for 600 RPM.
4. Do the same as in step 3 for 300, 200, 100, 60, 30, 6, and 3 RPM. The RPM is changed using the gear and top knob.

Picture 5: Fann Viscometer Model 35 SA. [P1]

Gel Strength Determination

Procedure:

1. After recording the value for 3 RPM in the rheology measurement, set the sleeve rotation to 600 RPM and let it run for 30 seconds.
2. Set the timer to 10 seconds and start it, while you stop the rotating sleeve. After the 10 seconds has passed, start the viscometer at 3 RPM and record the maximum dial reading value. This is the 10 s gel strength value in $lb/100ft^2$.
3. Set the rotation to 600 RPM again and let it run for 10 seconds and then stop it while starting the timer set to 10 minutes. After the 10 minutes has passed, start the viscometer at 3 RPM and record the maximum dial reading value. This is the 10 min gel strength value in $lb/100ft^2$.
4. If the value of the gel strength after 10 minutes is at least twice the value after 10 seconds (10 min gel $\geq$ 2 * 10 s gel), it is necessary to run the gel strength for 30 minutes. Set the rotation to 600 RPM and let it run for 10 seconds and then stop it while starting the timer set to 30 minutes. After the 30 minutes has passed, start the viscometer at 3 RPM and record the maximum dial reading value. This is the 30 min gel strength value in $lb/100ft^2$.

Electrical Stability (ES)

Equipment:

- Fann Electrical Stability tester

Procedure:

1. Heat or cool the sample to 50 ± 1 ℃ (120 ± 1 ℉). Record the temperature.
2. Turn on the instrument by pressing the “on” button and then calibrate the instrument by pushing the “test” button without having the electrode connected.
3. Inspect the cleanliness of the electrode, connect it to the instrument and immerse the electrode into the drilling fluid. Stir the sample with the electrode for approximately 10 seconds. Hold the electrode motionless in the sample and do not let the electrode touch the sides or the bottom of the thermo cup.
4. While holding the electrode still, push the “test” button and let the value on the screen stabilize. Record the value.
5. Repeat step 3 and 4 two more times before taking the average of the three values. This value is the electrical stability of the sample, expressed in volts.

Picture 6: Fann ES tester. [P1]

Stability test

Equipment:

- Ageing Cell
- Allen key
- Wrench
- 10 ml syringe
- Measuring cylinder
- Spoon
- 2 Measuring cups
- Analytical balance
- Hamilton Beach mixing cup

Procedure:

1. Statically age a 350 ml mud sample for a certain number of hours and cool down to room temperature.
2. Carefully bleed off the pressure prior to disassembling the cell.
3. Measure amount of liquid separated on top of drilling fluid using a syringe and a measuring cylinder. Report this as free fluid (ml).
4. Use a syringe or a spoon to transfer 50 ml of top layer of the drilling fluid to a measuring cup.
5. Use a syringe or a spoon to transfer the mid layer of the drilling fluid to a Hamilton Beach mixing cup.
6. Pour the bottom layer (50 ml) into another measuring cup. Record the mobility of the mud. If you must dig out the bottom layer, the mud is immobile.
7. Determine the density of the top and bottom layer using a 10 ml syringe. Fill the tip of syringe with drilling fluid and place it on the balance to zero. Fill the syringe with drilling fluid. Remove any trapped air from the syringe. Compress the fluid to the 10 ml marking. Place the syringe on the balance and note the weight in grams. SG = weight[g]/10.

Picture 7: Freshly opened ageing cell with free fluid on top. [P1]

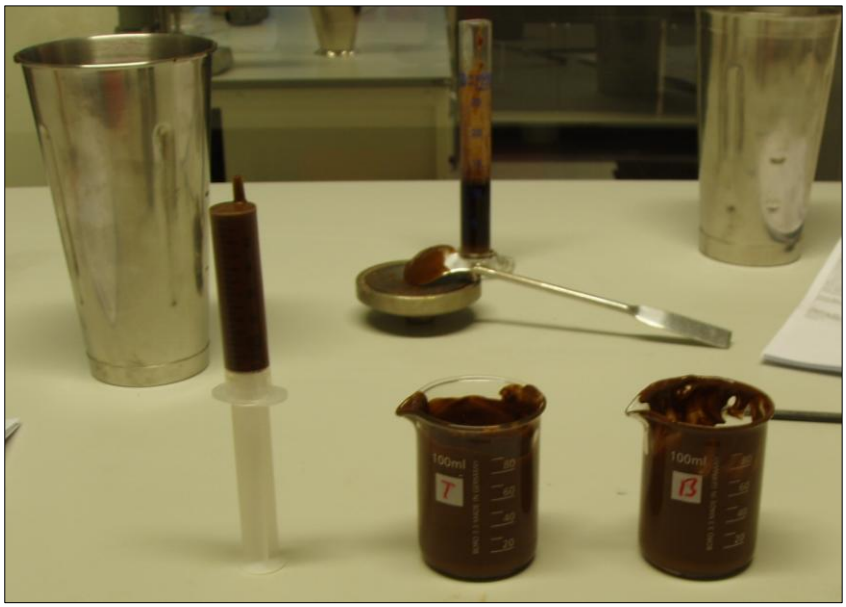

Picture 8: Picture taken during stability sag test. [P1]

Dynamic sag shoe test

Equipment:

- Fann Viscometer Model 35 SA
- Thermo cup
- VSST Sag Shoe
- Timer
- 10 ml syringe
- Pipetting needle
- Analytical balance
- Spatula

Procedure:

Equipment Setup

1. Insert the Sag Shoe into the thermo cup and place both on the viscometer plate. Make sure the outside diameter of the sag shoe is just smaller than the inside diameter of the thermo cup such that it fits snug.
2. Raise the plate until the top of the Sag Shoe touches the bottom of the viscometer sleeve, and mark the support leg at the upper edge of the locking mechanism.
3. Lower the plate and thermo cup to the base, and mark the support leg 7 mm below the first mark.

Sag Measurement

1. Insert the Sag Shoe into the thermo cup with the collection well positioned for easy access by the syringe, e.g. 60˚ to 90˚ either side of the viscometer centerline.
2. Collect a 350 ml drilling fluid sample in a container, mix appropriately, and pour approximately 140 ml into the thermo cup. Heat the drilling fluid to 50 ˚C while stirring at 600 RPM.
3. Position and lock the upper edge of the viscometer locking mechanism to coincide with the lower mark on the support leg. The top of the Sag Shoe should be 7 mm below the viscometer sleeve.
4. Set the viscometer to 100 RPM and start the 30 min timer.

5. Using the syringe with blunt-end pipetting needle attached and cleared of air, draw slightly over 10 ml from the drilling fluid remaining in the container. Carefully clear the syringe and pipetting needle of residual air and push the plunger to the 10 ml calibration mark. Wipe the pipetting needle and syringe surfaces until clean and dry.
6. Weigh the fluid-filled syringe and record the mass as m_{F1}, expressed in grams.
7. Stop viscometer rotation at the end of the 30 min test period.
8. Repeat step 5, this time taking the sample from the collection well of the Sag Shoe. Use the pipetting needle tip to find the collection well.
9. Weigh the fluid-filled syringe and record the total mass as m_{F2}, expressed in grams.

Bed Pickup Measurement (m_{F3})

1. Gently return the 10 ml test sample from the fluid-filled syringe obtained in relation to m_{F2} to the Sag Shoe collection well.
2. Run the viscometer at 600 RPM for 20 minutes.
3. Collect a sample from the Sag Shoe collection well as described earlier and weigh the fluid-filled syringe and record the total mass as m_{F3}, expressed in grams.

Appendix B HOL Vertical Simulation

Pictures from experiment 1:

Picture 9: Picture taken after the light fluid has been inserted into the pipe. [P1]

Picture 10: Heavy over light fluid interface (HOL). [P1]

Pictures from experiment 2:

Picture 11: Heavy over light fluid interface (HOL). [P1]

Picture 12: Displaying the fluid interface length using a folding rule. [P1]

Picture 13: Fluid interface. [P1]

Picture 14: Fluid interface (2). [P1]

Picture 15: Lower fluid interface compared to a pure light fluid (right). [P1]

Appendix C Brazil Well (Petrobras)

This appendix includes the well data for the pilot hole that will be drilled in Brazil.

Well trajectory

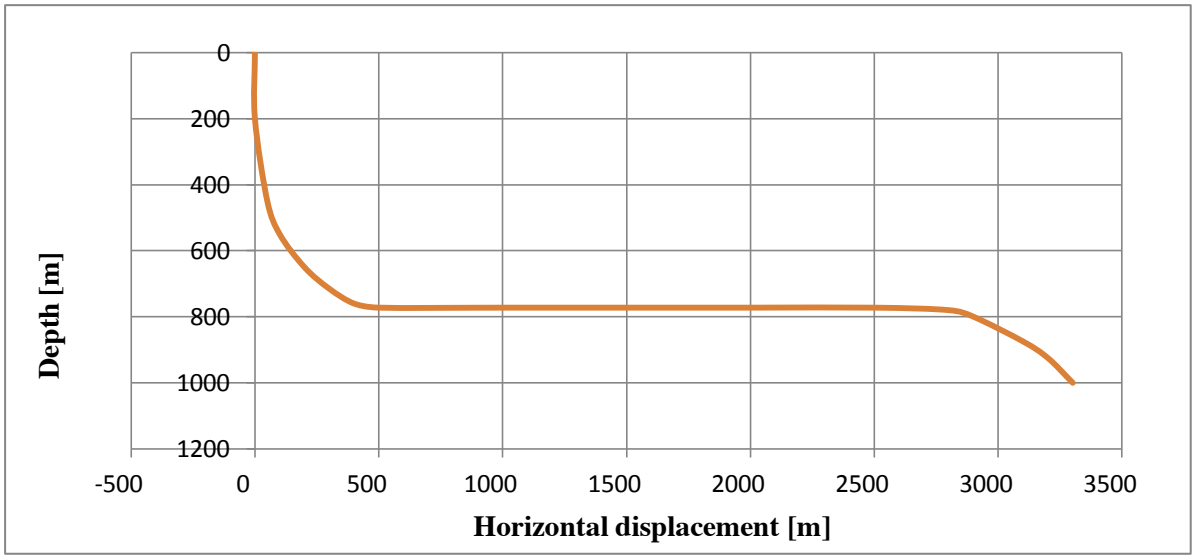

Appendix figure 1: Well trajectory.

Drilling program

Appendix Table 1: Drilling Program.

Well Section	Scope
Top hole section (0 – 1125 m MD)	- Entry in a pre-installed and cemented 20” conductor, shoe depth at 370 m. - Conventional drilling of 17 ½” hole, build to horizontal by 1088 m MD. - Continue drilling horizontal section to 1125 m MD. - Run and cement 13 3/8” casing inside the 17 ½” hole. - Drill out casing shoe and FIT using 12 ¼“ bit.

Horizontal section (1125 – 3225 m MD)	- Use RDM HOL solution to drill 12 ¼" hole to depth of 3225 m MD. - Run and cement 9 5/8" casing inside the 12 ¼" hole. - Drill out casing shoe and FIT using 8 ¾" bit.
Reservoir section (3225 – 3915 m MD)	- Use RDM HOL solution to drill 8 ¾" hole to target depth of 3915 m MD.

Pressure and temperature gradient prognosis

- Pore pressure gradient: 8.3 ppg
- Fracture pressure gradient: 16.5 ppg
- Temperature at 772 m TVD; 124˚F / 51˚C

Drilling fluid densities

HOL solution;

- Light fluid: 9.00 ppg / 1.10 SG
- Heavy fluid: 13.50 ppg / 1.60 SG

Appendix D NMR System and Application Parameters

System parameters

Appendix Table 2: NMR system parameters. [P1]

ID	Value
P90	9.8
P180	13.55
DEAD1	60.0
DEAD2	3.0
SF	1.809000
O1	12117.16

Application parameters

Appendix Table 3: NMR application parameters. [P1]

ID	Value
FW	100000.0
DW	15.6
SW	64102.6
SI	128
NS	64
RG	100.00
RD	10000000.0
D1	100.0
D2	2000.0
D3	1055.0
TAU	3300.0
G1	1000
G2	1000
GX	0
GY	32767
GZ	0
PH1	02
PH2	02
PH3	11
DS	0
RFA0	100.0

Attachment – 1 experimental DVD

The attached DVD contains videos from the following experiments:

- HOL vertical simulation (02:41)
- Horizontal section sag test (04:58)

Format: MP4

Quality: 1920x1080P